

**A Comparative Morphological and Morphometric Study of the
Musculi bulbi oculi and *Apparatus lacrimalis* in the Ostrich
(*Struthio camelus*) and Emu (*Dromaius novaehollandiae*).**



By

ELLENÉ KLEYN

BSc (Vet Biol) BVSc

Submitted in fulfilment of the requirements for the degree MSc Veterinary Science.

DEPARTMENT OF ANATOMY AND PHYSIOLOGY

FACULTY OF VETERINARY SCIENCE

UNIVERSITY OF PRETORIA

2017



UNIVERSITY OF PRETORIA
FACULTY OF VETERINARY SCIENCE
DECLARATION OF ORIGINALITY


**This document must be signed and submitted with every
essay, report, project, assignment, mini-dissertation, dissertation and/or thesis**

Full names of student:Dr Ellené Kleyn.....

Student number:04388968.....

Declaration:

1. I understand what plagiarism is and am aware of the University's policy in this regard.
2. I declare that this dissertation is my own original work. Where other people's work has been used (either from a printed source, Internet or any other source), this has been properly acknowledged and referenced in accordance with departmental requirements.
3. I have not used work previously produced by another student or any other person to hand in as my own.
4. I have not allowed, and will not allow, anyone to copy my work with the intention of passing it off as his or her own work.

Signature of student: 

Signature of supervisor: 

Supervisor: Professor Herman. B. Groenewald
Department of Anatomy and Physiology
Faculty of Veterinary Science
University of Pretoria

DEDICATION

To my dearest dad and mom, Pieter and Elzari Kleyn, thank you for always having lovingly supported and encouraged me, in wisdom and grace. Mom, your steadfast faith and love, will remain my greatest inspiration. Thank you for teaching me to see true beauty in every God-given moment. Dad, your sincerity and the zeal you had for life, will always motivate me to reach my goals and to enrich the lives of others.

ACKNOWLEDGEMENTS

Prof. Herman Groenewald, for his consistent and thorough guidance and support as supervisor of this thesis.

Prof. John Soley and Dr. Martina Crole for their advice and guidance in the histology and morphometry chapters.

To Lizette du Plessis and Antoinette Lensink, at the Electron Microscopy Unit, my sincere thanks for assisting me with the microscope work that was done during this study.

Prof. Peter Thompson for his contribution, enthusiasm and advice regarding the morphometric calculations and statistics pertaining to this study.

Prof. Andre Ganswindt for his understanding and support during the completion of this dissertation.

The staff at the Onderstepoort Pathology Laboratory for their assistance in preparing the histological material used during this study.

My sincere thanks to all the staff at the Department of Anatomy and Physiology, Onderstepoort, for their assistance and support.

My sincere thanks to the South African Veterinary Foundation for sponsoring the projects pertaining to this thesis.

CONTENTS

DECLARATION	ii
DEDICATION	iii
ACKNOWLEDGEMENTS	iv
CONTENTS	v
SUMMARY	vi
CHAPTER 1: General Introduction.	1
CHAPTER 2: Gross Morphology and Innervation of the <i>M. bulbi oculi</i> in the in the ostrich (<i>Struthio camelus</i>) and emu (<i>Dromaius novaehollandiae</i>).	16
CHAPTER 3: Morphometric characteristics of the <i>M. bulbi oculi</i> in the in the ostrich (<i>Struthio camelus</i>) and emu (<i>Dromaius novaehollandiae</i>).	54
CHAPTER 4: Gross Morphology and Innervation of the <i>Apparatus lacrimalis</i> in the in the ostrich (<i>Struthio camelus</i>) and emu (<i>Dromaius novaehollandiae</i>).	78
CHAPTER 5: Histological Structure of the <i>Apparatus lacrimalis</i> in the in the ostrich (<i>Struthio camelus</i>) and emu (<i>Dromaius novaehollandiae</i>).	97
CHAPTER 6: General conclusions	134
APPENDICES	137

SUMMARY

A Comparative Morphological and Morphometric Study of the *Musculi bulbi oculi* and *Apparatus lacrimalis* in the Ostrich (*Struthio camelus*) and Emu (*Dromaius novaehollandiae*).

by

ELLENÉ KLEYN

SUPERVISOR: Professor Herman. B. Groenewald

DEPARTMENT: Department of Anatomy and Physiology, Faculty of Veterinary Science, University of Pretoria, Private Bag X 04, Onderstepoort, 0110, Republic of South Africa.

DEGREE: MSc (Veterinary Science)

The unique adaptation of the avian eye is reflected in its ocular anatomy. The ostrich and emu are commercially important species and a comparative study of the *M. bulbi*, lacrimal apparatus and their innervation would provide important ophthalmological data. Both species have large eye globes to which four recti, two oblique and two nictitating membrane muscles insert. Greater similarities in the origins of these muscles are evident between the two species, compared to their respective insertions. Branches of cranial nerves II to VII course within the orbit of both species, with cranial nerves II to VI innervating the eye and *M. bulbi*. The route of CN VI differs from that of other avian species whereas that of CN V and VII differs between the ostrich and emu. The *M. bulbi* in both species differ in mass, volume, isometric force and power generation, indicating possible variations in the dynamics of ocular motility.

Each eye has an associated Harderian and lacrimal gland which empty at the inner margin of the nictitating membrane and lower eye lid, respectively. Morphological variation is evident, with the ostrich lacrimal apparatus being more robust, distinctly lobulated and pigmented. In both species, the lacrimal apparatus is compound in nature. A single large secretory duct extends into the body of both glands in the ostrich and emu, before branching into two to three smaller ducts into which the simple branched tubular units constituting the glands open. The

secretory epithelium is simple columnar in nature. Concentrations of lymphocytes are observed in both glands confirming the general observation that the Harderian gland in particular plays an important role in local ocular immunity.

The morphology and innervation of the ostrich and emu *M. bulbi* and *Apparatus lacrimalis* follow the general avian pattern. However, the small interspecies variations noted should be considered during diagnostic or surgical procedures on the eye or associated structures.

CHAPTER 1

General Introduction.

1.1 An introduction to ratites

The nine to ten thousand extant avian species (Pimm et al., 2014) are categorised into two super-orders, namely, *Palaeognathae* and *Neognathae* (Krabichler et al., 2015). Six of the numerous extant avian families are classified as *Palaeognathae* (Wright & Bowmaker, 2001) due to the unique palatal structure evident in these species (Mitchell et al., 2014). Extant families include; *Struthionidae* (Ostrich), *Dromaiidae* (Emu), *Casuariidae* (Cassowary sp.), *Apterygidae* (Kiwi sp.), *Rheidae* (Rhea sp.) and *Tinamidae* (Tinamous sp.). All extant families of palaeognathous species are flightless except for the South American Tinamous (*Tinamidae*) (Wright & Bowmaker, 2001). Merrem first used the term *Ratitae* in 1813, in reference to flightless avian species (Webb, 1957).

The ostrich (*Struthio camelus*) and emu (*Dromaius novaehollandiae*) are the largest extant ratites and are native to Africa (Deeming, 1999) and Australia (Sales, 2007), respectively. There are four extant ostrich sub-species, namely *Struthio camelus* (North African or Red-necked Ostrich), *S.c molybdophanes* (Somali Ostrich), *S.c massaicus* (Masai Ostrich) and *S.c australis* (Southern African Ostrich) (Deeming, 1999). *D. novaehollandiae* is the only extant emu species, of which there are three subspecies; *D. n novaehollandiae*, *D. n woodwardi*, *D. n rothschildi* (Sales, 2007).

1.2 Commercial uses of ostrich and emu

The ostrich and emu are commercially important ratites, the products of which have been of great benefit to the medicinal, fashion, culinary and cosmetic industries (Deeming, 1999; Goonewardene et al., 2003; Wilson et al., 2004; Sales, 2007; Nadhanan et al., 2012; Jeengar et al., 2015). Native inhabitants utilized ostrich hides, meat, feathers, fat and eggs for centuries (Deeming, 1999). Thus, intensive ostrich farming and artificial incubation of eggs was initiated in South Africa's Karoo and Eastern Cape regions in 1860 (Deeming, 1999). Ostriches are farmed on an intensive scale for meat and feathers which are utilized in the culinary and fashion industries respectively (Deeming, 1999). The species of ostrich farmed on an intensive scale is described as *S. c. var. domesticus* (Deeming, 1999). Success has likewise been achieved in the commercial emu industry (Goonewardene et al., 2003; Sales, 2007).

The commercial emu industry started in approximately 1990, with primary focus on oil production from emu fat (Sales, 2007). Emus are slaughtered at 15 to 18 months of age, the sub-cutaneous and retroperitoneal fat deposits removed, processed and oil finally extracted (Sales, 2007). The oil holds various medicinal and cosmetic benefits such as treating inflammation, hypercholesterolemia, arthritis, hypopigmentation, alopecia, xerosis, burn wounds and osteoporosis (Wilson et al., 2004; Nadhanan et al., 2012; Jeengar et al., 2015).

The variety of commercially viable products obtained from the emu and ostrich make these ratites valuable production animals. These highly adaptable ratites have the potential of producing high quality, healthy meat and leather as well as various products which benefit human health and wellness.

1.3 The Avian *Organum visum* and associated structures

Eyesight in avian species plays an important role in nesting, foraging, mating behaviour and detecting predators. The ostrich and emu relies on eyesight to feed on shrubs, seeds, grasses (Deeming, 1999; Calvino-Cancela et al., 2006; Sales, 2007; Miller & Fowler, 2015) and some insects. Accurate pecking is directed by a binocular field of vision that do not differ markedly in dimension and shape compared to other avian species, despite ratites having different phylogenies and habitats (Martin et al, 2001). The eyes of avian species are arranged laterally in the cranium, thus binocular vision is limited and rotation of the globe is necessary to alter this field of vision when foraging (King & McLelland, 1985).

Form and function in avian species have been extensively studied in neognathous species, such as *Passeriformes*, *Anseriformes*, *Galliformes* and *Psittaciformes* (King & McLelland, 1985; Baumel et al., 1993). The avian eye is similar to mammals but displays certain unique characteristics. A large proportion of the cranial space is occupied by the osseous orbit (Baumel et al., 1993). In avian species, the osseous orbit is comprised of cranial bones, however the ventrum of the orbit consists only of jaw muscles (Baumel et al., 1993). The interorbital septum (*Septum interorbitale*) or posterior portion of the avian orbit is particularly thin, compressed by the particularly large eye globe (King & McLelland, 1985; Baumel et al., 1993). The orbit in avian species is composed of the *Os laterosphenoidale/pleurosphenoidale* caudally, a *Septum interorbitale* posteriorly, an *Os ectethmoidale* rostrally and an *Os frontale* dorsally (Baumel et al., 1993).

Each orbit contains a globe, associated extrinsic muscles as well as the lacrimal apparatus (Baumel et al., 1993). Coursing through the orbit are nerves and blood vessels, some of which supply the *Organum visum* and lacrimal apparatus (Baumel et al., 1993). Remaining nerves and blood vessels within the orbit, are associated with cranial structures such as the muscles of mastication, as well as the organs of olfaction and hearing (Baumel et al., 1993). Innervation to the extrinsic ocular muscles or *M. bulbi*, enables rotation of the globe (King & McLelland, 1985; Slonaker, 1918).

The gross morphology of the *M. bulbi*, have been described in the homing pigeon (Chard & Gundlach, 1938), the Tinamous (Elzanowski, 1987) and the English or house sparrow (*Passer domesticus*) (King & McLelland, 1985; Slonaker, 1918). The Tinamous is the most extensively described of the palaeognathous species. The following intrinsic and extrinsic ocular features are common to avian species: *Musculi bulbi oculi* (*M. bulbi*) consists of six extrinsic ocular muscles (four *Mm. recti*, two *M. obliquus*) and two *M. membranae nictitantis* (Chard & Gundlach, 1938; King & McLelland, 1985; Baumel et al., 1993; Ritchie et. al., 1994).

The straight extrinsic muscles include the dorsal, ventral, medial and lateral recti, whereas the *Mm. obliquus* is composed of the dorsal and ventral oblique muscles (King & McLelland, 1985; Baumel et al., 1993; Ritchie et. al., 1994). Movement of the nictitating membrane across the eye is initiated by the contractions of *M. quadratus membranae nictitantis* (quadratus muscle) and *M. pyramidalis membranae nictitantis* (pyramidal muscle) (Chard & Gundlach, 1938; King & McLelland, 1985; Baumel et al., 1993; Ritchie et. al., 1994).

Function and topography of the avian cranial nerves have been thoroughly described (Baumel et al., 1993; Harrison & Lightfoot, 2005; Jones, 2007; Orosz & Bradshaw, 2007). The innervation of the *M. bulbi*, lacrimal apparatus and orbit in the domestic fowl (*Gallus gallus*) have been documented (Baumel et al., 1993; Orosz & Bradshaw, 2007). In the English sparrow (*Passer domesticus*) the innervation to the *M. bulbi* has previously been described (Slonaker, 1918), as well as in other neognathous avian species (Harrison & Lightfoot, 2005). The globe is innervated by CN II to VI (Slonaker, 1918; Baumel et al., 1993; Harrison & Lightfoot, 2005) of which CN III, IV and VI innervates the muscles responsible for rotation of the globe and movement of the nictitating membrane (Slonaker, 1918; Jones, 2007). The optic nerve or *N. opticus* (CN II) is particularly well developed in *Falconiformes* (Jones, 2007) in comparison to other avian species.

N. oculomotorius (CN III) has a dorsal branch innervating the dorsal rectus muscle (Slonaker, 1918; Baumel et al., 1993; Jones, 2007) and *M. levator palpebrae superioris* (Jones, 2007)

and a ventral ramus to the ventral and medial recti and ventral oblique muscles (Slonaker, 1918; Baumel et al., 1993; Jones, 2007). *N. trochlearis* (CN IV) innervates the dorsal oblique muscle (Slonaker, 1918; Baumel et al., 1993; Jones, 2007).

Detailed descriptions of the trigeminal nerve and its branches in the domestic fowl are available (Baumel et al., 1993). The *N. trigeminus* (CN V) has unnamed rami innervating the conjunctiva, whereas the ophthalmic nerve branches innervate the choroid, ciliary muscles (Slonaker, 1918), *M. obicularis oculi* and *M. depressor palpebrae ventralis* (Jones, 2007). The *N. oculomotorius* and *N. trigeminus* have an unnamed communicating ramus in the sparrow (Slonaker, 1918). The communicating ramus between two nerves in avian species is referred to as a *connexus* (Baumel et al., 1993). In *Gallus gallus*, there is a *connexus* between the *N. trochlearis* and the ophthalmic branch (*N. ophthalmicus*) of the *N. trigeminus* (Baumel et al., 1993). The *N. abducens* (CN VI) has branches innervating the lateral rectus and both muscles of the nictitating membrane (Slonaker, 1918; Jones, 2007). It is thus evident that information on the morphology and innervation of the *M. bulbi* in avian species are numerous. It appears that no information is available on the morphometric properties of these muscles in avian species.

Morphometry refers to the dimensions of an object or the measurements of curvatures and the angles pertaining to it (Pearsall, 2002). The volume, mass, length, cross-sectional area and density of a muscle are morphometric properties of muscle (Biewener, 2003; Payne et al., 2005; Hill et al., 2008). The latter are used to deduce the maximum contractile velocity and maximum isometric force exerted by a muscle (Biewener, 2003; Payne et al., 2005; Hill et al., 2008). Contractile velocity and isometric force exerted by a muscle are used to determine the power it generates (Biewener, 2003; Payne et al., 2005; Hill et al., 2008). Such data is useful in interpreting the functional properties of that muscle (Biewener, 2003; Payne et al., 2005; Hill et al., 2008).

The function of locomotory muscles has been explored in several neognathous species (Bennett, 1996; Tobalske, 2007; Meyers & McFarland, 2016). The contractile velocity, power as well as force generated by flight muscles have been documented in the cockatiel (*Nymphicus hollandicus*) (Biewener, 2003; Morris & Askew, 2010), golden eagle (*Aquila chrysaetos*) (Meyers & McFarland, 2016), bald eagle (*Haliaeetus leucocephalus*) (Meyers & McFarland, 2016), ring-neck dove (*Streptopelia risoria*) (Biewener, 2003), domestic pigeon (*Columba livia*) (Biewener, 2003), and mallard duck (*Anas platyrhynchos*) (Biewener, 2003). It seems evident that emphasis has been placed on the morphometry of avian locomotory muscles compared to avian extrinsic ocular muscles.

The extrinsic ocular muscles allow for drifts, flicks, oscillations and tremors of the eye globe which ensure accurate focus of an image onto the retina when an object is viewed at close proximity, for example during foraging (King & McLelland, 1985). Extrinsic ocular muscles are thin and allow limited rotation of the large globe, as it is fitted tightly in the orbit of avian species (King & McLelland, 1985). The mean bulbar axial length of the ostrich is 38mm (Martin et al., 2001) and is notably large, however it resembles the axial lengths recorded in albatross species (*Diomedea melanophris* and *Diomedea chrysostoma*) and the wedge-tailed eagle (*Aquila audax*) (Martin et al., 2001). Avian species do not primarily rely on rotation of the globe when observing their environment, grooming, foraging or flying. Instead, a light weight skull and flexible neck, allow for rapid, full range movement of the head (King & McLelland, 1985).

The lacrimal apparatus are accessory ocular structures which play a vital role in maintaining ocular health in avian species (King & McLelland, 1985; Montgomery & Maslin, 1992; Schat et al., 2014). The following features are common to avian species: *Membrana nictitans* or nictitating membrane is responsible for protecting the eye against the elements, as well as keeping the cornea moist by spreading the secretions from the lacrimal apparatus across the eye (King & McLelland, 1985). In avian species, the nictitating membrane is located within the dorso-nasal region of the conjunctival pouch (Baumel et al., 1993).

The *Apparatus lacrimalis* is comprised of a *Glandula membranae nictitantis* or Harderian gland as well as a *Glandula lacrimalis* or lacrimal gland (King & McLelland, 1985). The Harderian gland is common to most avian species, reptiles, rodents, amphibians (Rothwell et al., 1972; Shirama et al., 1982; Chieffi et al., 1996; Altunay & Kozlu, 2004) and some mammalian species (Sakai & van Lennep, 1984). The *Gl. lacrimalis* is present in mammals, amphibians, reptiles and avian species (Shirama & Hokano, 1992). The gland of the nictitating membrane or Harderian gland is positioned near the *Septum interorbitale*, within the ventro-rostral compartment of orbit (Baumel et al., 1993). Secretions from the Harderian gland empty via the *Ductus gl. membranae nictitantis* into the conjunctival region between the cornea and nictitating membrane (Baumel et al., 1993). Antimicrobial products present in the Harderian gland secretion are vital for clear vision (Klećkowska-Nawrot et al., 2015).

The avian lacrimal gland is positioned in the ventro-temporal region of the orbit (Baumel et al., 1993). In the fowl, it is noted that numerous *Ductus gl. lacrimalis* carry the lacrimal secretion to the conjunctival space beneath the lower eye lid (Baumel et al., 1993). The serous to mucoid secretion of the lacrimal gland contributes to the tear film (King & McLelland, 1985). The tear film which moistens, cleans and protects the cornea against environmental insult (King & McLelland, 1985).

The innervation to the lacrimal apparatus has previously been described in neognathous species (Slonaker, 1918; Baumel et al., 1993; Jones, 2007; Orosz and Bradshaw, 2007). The gland of the nictitating membrane is innervated by *Rr. glandulae membranae nictitantis* which is situated between the *Ganglion ethmoidale* and *Ganglion sphenopalatinum*, with contributions from the ventral and dorsal rami of *N. palatinus* originating from CN VII (Baumel et al., 1993). In birds of prey, the lacrimal gland is innervated by the maxillary branch of the *N. trigeminus* (CN V) (Jones, 2007). Jones described an unnamed branch of the *N. facialis* (CN VII) providing sympathetic innervation to the same glands in birds of prey (Jones, 2007). In the sparrow, the *N. trigeminus* has been described innervating the lacrimal gland (Slonaker, 1918).

The histological and gross morphological structure of the para-ocular glands have been extensively studied in numerous neognathous avian species such as the domestic fowl (Mueller et al., 1971; Burns & Maxwell, 1979; Maxwell & Burns, 1979; Schat et al., 2014), pigeon and house sparrow (Aitken & Survashe, 1977), turkey (*Meleagris gallopavo*) (Burns & Maxwell, 1979; Maxwell et al., 1986), rook (*Corvus frugilegus*) (Burns, 1975), duck (*Anas platyrhynchos*) (Oliveira et al., 2006) and *Anas sterilis* (Dimitrov & Nikiforov, 2005). The avian Harderian gland is histologically described as varying from compound tubular to compound tubulo-acinar and the excretory product being primarily mucoid (Aitken & Survashe, 1977). The avian lacrimal gland is described as compound tubulo-acinar in nature (Aitken & Survashe, 1977). The gross and histological structure of lacrimal apparatus in the ostrich has been described in detail (Klećkowska-Nawrot et al., 2015). Comparatively, information on the emu lacrimal apparatus is scant and is confined to basic classification of these glands and the characteristics of immune cells evident in the emu lacrimal apparatus (Aitken & Survashe, 1977).

The avian lacrimal and Harderian glands form part of the head associated lymphoid tissue (Montgomery & Maslin, 1992; Schat et al., 2014; Klećkowska-Nawrot et al., 2015). The Harderian gland however, plays a vital role in local humoral immunity of the ocular structures and upper airways (Mueller et al., 1971; Fix, 1990; Burns, 1992). A high density of plasma cells is found within the Harderian gland interstitium (Bang & Bang, 1968; Wight et al., 1971; Burns & Maxwell, 1979). Bursa dependent lymphocytes and plasma cells are concentrated in the body of the gland and interspersed macrophage and T-cell dependent inter-follicular regions are evident in some avian species (Schat et al., 2014). Immunoglobulins are synthesised after viral exposure in fowl (Parry & Aitken, 1977) and removal of the Harderian gland in fowl results in decreased protective immunity against certain viruses after vaccination

(Davelaar & Kouwenhoven, 1980). Increased disease prevalence has been documented in decreased local immunity (Malkison & Small, 1977).

Vision in avian species is influenced by conditions such as periorbital abscesses or neoplasia, which may involve the lacrimal apparatus, extrinsic muscles, fascia, vessels, nerves as well as the upper air ways and sinuses (Ritchie et al., 1994). Certain ocular inflammatory conditions have been described in the ostrich such as conjunctivitis caused by flukes (*Philophthalmus* sp.) (Ritchie et al., 1994; Tully & Shane, 1996), *Staphylococcus aureus* (Sahinduran, 2004), *Escherichia coli* (Ghaffari et al., 2010), Pox virus and Avian Influenza virus (Allwright et al., 1993; Monfared & Bakhteyari, 2013). Other pathologies affecting the ostrich eye, include fungal keratopathy and corneal ulceration (Ritchie et al., 1994; Monfared & Bakhteyari, 2013). Ocular haemorrhage, exophthalmos and hyphema may result due to cranial trauma or trauma to the eye globe. Enucleation may be required when the globe has been irreparably damaged through trauma, non-responsive inflammation or neoplasia (Bayon et al., 2007; Ritchie et al., 1994). The procedure is similar to that in mammals, however certain anatomical features in avian species have to be considered when removing an eye globe. Important extra-ocular structures can only be visualized once the large globe is collapsed by incising the cornea and expressing the ocular content (Ritchie et al., 1994). If excessive traction is placed on the short optic nerve, trauma to the adjacent structures and brain may result (Ritchie et al., 1994).

Increased attention has been given to ratite form and function due to their economic importance and their flightless nature making them a fascinating order to study. Numerous studies have been conducted on ostrich ocular anatomy (Mac Alister, 1864; Webb, 1957; Deeming, 1999; Monfared & Bakhteyari, 2013) as well as the visual field of the ostrich (Martin & Katzir, 1995; Martin et al., 2001). In comparison, scant information is available on ocular anatomy in the emu, except the structure of retinal photoreceptors and *Pecten oculi* in the emu (Braekevelt, 1998). In both ostrich and emu cranial osteology has been described (Parker, 1866; Kestevens, 1942; Webb, 1957; Predoi et al., 2007; Crole & Soley; 2016).

The *M. bulbi* in the ostrich follow the basic avian pattern, however scant morphological data is available compared to neognathous species. To my knowledge, data on the morphology of the *M. bulbi* in the emu is not available and is assumed to follow the general avian pattern. It appears that no information is available on the morphometry of the *M. bulbi* in the ostrich and emu. The morphology and histology of lacrimal apparatus in neognathous avian species have been extensively described. The lacrimal apparatus in the emu are scantily described,

compared to the ostrich. The innervation to the lacrimal apparatus in both ratites, warrants further investigation.

1.4 Aims and Benefits

The ostrich and emu are commercially important and a thorough description of the *M. bulbi* and *Apparatus lacrimalis* would aid in diagnostics and surgery, as ocular disease adversely affect the welfare and productivity of these ratites. The para-ocular glands play a vital role in ensuring local immunity as well as ocular health and thus optimal vision and functionality. This study aims to determine the morphometric and morphological qualities of the *M. bulbi* and *Apparatus lacrimalis*, and their respective innervation as to ascertain whether there are unique anatomical differences with respect to these structures and their innervation, in the ostrich and emu. This study will aim to prove the hypothesis that the morphology and morphometry of the *M. bulbi* and *Apparatus lacrimalis* and the innervation to these structures in the emu are comparable to the ostrich, with possible minor differences noted.

A thorough understanding of the extrinsic ocular and glandular anatomy of the emu and ostrich eye, would better equip veterinarians to accurately and successfully perform surgery and diagnostic procedures on the periorbital structures and glandular apparatus of the eye in these ratites.

1.5 References

AITKEN, I. D. & SURVASHE, B. D. (1977) Lymphoid cells in avian paraocular glands and paranasal tissues. *Comparative Biochemistry and Physiology Part A: Physiology*, 58, 3, 235-244.

ALTUNAY, H. & KOZLU, T. (2004) The fine structure of the Harderian gland in the ostrich (*Struthio camelus*). *Anatomia histologia embryologia*, 33, 3, 141-145.

ALLWRIGHT, D. M., BURGER, W. P., GEYER, A. & TERBLANCHE, A.W. (1993) Isolation of an Influenza A virus from ostriches (*Struthio camelus*). *Avian Pathology*, 22, 59-65.

BAUMEL, J. J., KING, A. S., BREAZILE, A. E., EVANS, H. E. & VAN DEN BERGE, J. C. (1993) *Handbook of Avian Anatomy: Nomina Anatomica Avium*. 2nd ed. Cambridge, Massachusetts: Nuttall Ornithological Club.

BANG, B. G. & BANG, F. B. (1968) Localized lymphoid tissues and plasma cells in paraocular and paranasal organ systems in chickens. *The American journal of pathology*. 53, 5, 735.

BAYÓN, A., ALMELA, R. M. & TALAVERA, J. (2007) Avian ophthalmology. *European Journal of Companion Animal Practice*. 17, 3.

BENNETT, M. B., (1996) Allometry of the leg muscles of birds. *The Zoological Society of London*, 238, 435–443.

BIEWENER, A. A., (2003) *Animal Locomotion*, UK: Oxford University Press.

BRAEKEVELT, C. R. (1998) Fine structure of the pecten oculi of the emu (*Dromaius novaehollandiae*). *Tissue and Cell*, 30, 2, 157-165.

BRAEKEVELT, C. R. (1998) Fine structure of the retinal photoreceptors of the emu (*Dromaius novaehollandiae*). *Tissue and cell*, 30, 2, 137-148.

BURNS, R. B. (1975) Plasma cells in the avian Harderian gland and the morphology of the gland in the rook. *Canadian journal of zoology*, 53, 9, 1258-1269.

BURNS, R. B. (1992) *Harderian Glands: Porphyrin Metabolism, Behavioral and Endocrine Effects*. The Harderian gland in birds, histology and immunology. Berlin Heidelberg: Springer.155-163.

BURNS, R. B. & MAXWELL, M. H. (1979) The structure of the Harderian and lacrimal gland ducts of the turkey, fowl and duck. A light microscope study. *Journal of anatomy*, 128, 2, 285.

CALVINO-CANCELA, M., DUNN, R. R., VAN ETTEN, E. J. B. & LAMONT, L. L. (2006) Emus as non-standard seed dispersers and their potential for long-distance dispersal. *Ecography*, 29, 632-640.

CHARD, R. D. & GUNDLACH, R. H. (1938) The structure of the eye of the homing pigeon. *Journal of comparative psychology*, 25, 2, 249–272.

CHIEFFI, G., BACCARI, G. C., DI MATTEO, L., D'ISTRIA, M., MINUCCI, S. & VARRIALE, B. (1996) Cell biology of the Harderian gland. *International review of cytology*, 168, 1-80.

CROLE, M.R. & SOLEY, J.T. (2016) Comparative morphology, morphometry and distribution pattern of the trigeminal nerve branches supplying the bill tip in the ostrich (*Struthio camelus*) and emu (*Dromaius novaehollandiae*). *Acta Zoologica*, 97, 1, 49-59.

DAVELAAR, F. G. & KOUWENHOVEN, B. (1980) Effect of the removal of the Harderian gland in 1-day-old chicks on immunity following IB vaccination. *Avian Pathology*, 9, 4, 489-497.

DEEMING, D.C. (ed.) (1999) *The ostrich: Biology, Production and health*. London: CAB International.

DIMITROV, D. S. & NIKIFOROV, I. P. (2005) Histological and histochemical studies of Harderian gland, lacrimal gland and bursa of Fabricius in mulard ducks (*Anas sterilis*) with chlamydial infection. *Bulgarian Journal of Veterinary Medicine*, 8, 2, 119-27.

ELZANOWSKI, A. (1987) Cranial and eyelid muscles of the Tinamous (Aves: *Tinamiformes*). *Zoologische Jahrbucher. Abteilung fur Anatomie und Ontogenie der Tiere*, 116, 63-118.

FIX, A. S. (1990) The structure and function of conjunctiva-associated lymphoid tissue in chickens and turkeys. *Retrospective Theses and Dissertations*. Paper 9496.

GHAFFARI, M. S., SABZAVARI, A. & KHORAMI, N. (2010) Successful treatment of severe conjunctivitis and blepharitis caused by *Escherichia coli* in an ostrich (*Struthio camelus*). *Comparative clinical pathology*, 19, 1, 121-123.

GOONEWARDENE, L. A., WANG, Z., OKINE, E., ZUIDHOF, M. J., DUNK, E. & ONDERKA, D. (2003) Comparative Growth Characteristics of Emus (*Dromaius novaehollandiae*). *The Journal of Applied Poultry Research*, 12, 1, 27-31.

HARRISON. G. J. & LIGHTFOOT. T. (2005) *Clinical Avian Medicine, Evaluating and treating the nervous system. Volume 2*. USA: Spix publishing.

HILL, A. W., WYSE G. A. & ANDERSON, M. (2008) *Animal Physiology*, 2nd ed. Sunderland, Massachusetts: Sinauer Associates Inc.

JEENGAR, M. K., P. KUMAR, P. S. & THUMMURI, D. (2015) Review on emu products for use as complementary and alternative medicine. *Nutrition Journal*, 31, 21–27.

JONES, M. P, PIERCE, K. E. & WARD, D. (2007) Avian Vision: A Review of Form and Function with Special Consideration to Birds of Prey. *Journal of Exotic Pet Medicine*, 16, 2, 69-68.

KESTEVEN, H. L. (1942) The ossification of the avian chondrocranium, with special reference to that of the emu. *Proceedings of the Linnean Society of New South Wales*, 67, 213 – 237.

KING, A. S. & MCLELLAND, J. (eds.) (1985) *Form and Function in Birds*. Volume 3. London: Academic Press.

KLECKOWSKA-NAWROT, J., GOŹDZIEWSA-HARLAJCZUK, K., BARSZCZ, K. & KOWALCZYK, A. (2015a) Morphological Studies on the Harderian Gland in the Ostrich (*Struthio camelus domesticus*) on the Embryonic and Post-natal Period. *Anatomia histologia embryologia*, 44, 2, 146-156.

KLECKOWSKA-NAWROT, J., GOŹDZIEWSA-HARLAJCZUK, K., NOWACZYK, R. & KRASUCKI, K. (2015b) Functional anatomy of the lacrimal gland in African black ostrich *Struthio camelus domesticus* in the embryonic and postnatal period. *Onderstepoort Journal of Veterinary Research*. 82, 1, 1-12.

KRABICHLER, Q., VEGA-ZUNIGA, T., MORALES, C., LUKSCH, H. & MARIN, G. J. (2015) The Visual System of a Palaeognathous Bird: Visual Field, Retinal Topography and Retino-Central Connections in the Chilean Tinamou (*Nothoprocta perdicaria*). *Journal of Comparative Neurology*. 523, 2, 226-250.

MAC ALISTER, A. (1864) On the Anatomy of the Ostrich (*Struthio camelus*). *Proceedings of the Royal Irish Academy*, 1-24.

MALIKSON, M. & SMALL, P. A. (1977) Local Immunity Against Newcastle Disease Virus in the Newly Hatched Chicken's Respiratory Tract. *American Society for Microbiology*, 16, 2. *Infection and Immunity*, 587-592.

MARTIN, G. R., ASHASH, U. & KATZIR, G. (2001) Ostrich ocular optics. *Brain Behavior and Evolution*. 58, 2, 115-120.

MARTIN, G. R. & KATZIR, G. (1995) Visual fields in ostriches. *Nature*, 2 March, 374.

MAXWELL, M. H. & BURNS, R. B. (1979) The ultrastructure of the epithelium of the ducts of the Harderian and lacrimal glands of the turkey, fowl and duck. *Journal of anatomy*, 128, 3, 445-459.

MAXWELL, M. H., ROTHWELL, B. & BURNS, R. B. (1986) A fine structural study of the turkey harderian gland. *Journal of anatomy*, 148, 147-157.

MEYERS, R. A. & MCFARLAND J.C. (2016) Anatomy and histochemistry of spread - wing posture in birds. Eagles soar with fast, not slow muscle fibres. *Acta Zoologica*, 97, July, 319–324.

MILLER, R. E. & FOWLER, M. E. (eds.) (2015) *Fowler's Zoo and Wild Animal Medicine*. Volume 8. Missouri, USA: Elsevier. 77

MITCHELL, K. J., LLAMAS, B., SOUBRIER, J., RAWLENCE, N. J., WORTHY, T. H., WOOD, J., LEE, M. S. Y. & COOPER, A. (2014) Ancient DNA reveals elephant birds and kiwi are sister taxa and clarifies ratite bird evolution. *Science*, 344, 6186, 898–900.

MONFARED, A. L & BAKHTEYARI, Z. (2013). Some Gross Anatomical Features on Ostriches' Eye and its Application for Clinical Treatment of Ocular Abnormalities. *Global Veterinaria*, 11, 1, 76-79.

MONTGOMERY, R. D. & MASLIN, W. R. (1992) A comparison of the gland of Harder response and head-associated lymphoid tissue (HALT) morphology in chickens and turkeys. *Avian diseases*, 1, 755-759

MORRIS, C. R. & ASKEW, G. N. (2010) The mechanical power output of the pectoralis muscle of cockatiel (*Nymphicus hollandicus*): the in vivo muscle length trajectory and activity patterns and their implications for power modulation. *Journal of Experimental Biology*, 213. 2770–2780.

MUELLER, A. P., SATO, K. & GLICK, B. (1971) The chicken lacrimal gland, gland of Harder, caecal tonsil, and accessory spleens as sources of antibody-producing cells. *Cellular immunology*, 2, 2, 140-152.

NADHANAN, R. R., ABIMOSLEH, S. M., SU, Y., SCHERER, M. A., HOWARTH, G. S. & XIAN, C. J. (2012) Dietary emu oil supplementation suppresses 5-fluorouracil chemotherapy-induced inflammation, osteoclast formation, and bone loss. *American Journal of Physiology-Endocrinology and Metabolism*, 302, 11, E1440-E1449.

OLIVEIRA, C. A., TELLES, L. F., OLIVEIRA, A. G., KALAPOTHAKIS, E, GONCALVES-DORNELAS, H. & MAHECHA, G. A. (2006) Expression of different classes of immunoglobulin in intraepithelial plasma cells of the Harderian gland of domestic ducks *Anas platyrhynchos*. *Veterinary immunology and immunopathology*, 113, 3-4, 257-266.

OROSZ, S. E. & BRADSHAW, G. A. (2007) Avian Neuroanatomy Revisited: From Clinical Principles to Avian Cognition. *Veterinary Clinics of North America Exotic Animal Practice*, 10, 775-802.

PARKER, W. K. (1866) On the Structure and Development of the Skull in the Ostrich Tribe. *Philosophical Transactions of the Royal Society of London*, 156, 113-183.

PARRY, S. H. & AITKEN, I. D. (1977) Local immunity in the respiratory tract of the chicken. II. The secretory immune response to Newcastle disease virus and the role of IgA. *Veterinary Microbiology*, 2, 2, 143-65.

PAYNE, R. C., HUTCHINSON, J. R., ROBILLIARD, J.J., Smith, N. C. & Wilson, A. M. (2005) Functional specialisation of the pelvic limb anatomy in horses (*Equus caballus*). *Journal of Anatomy*, 206, 557 – 574.

PEARSALL, J. (ed.) (2002) *Concise Oxford English Dictionary*, 10th ed. Oxford, UK: Oxford University Press.

PIMM, S. L., JENKINS, C. N., ABELL, R., BROOKS, T. M., GITTLEMAN, J. L., JOPPA, L. N., RAVEN, P. H., ROBERTS, C. M. & SEXTON, J. O. (2014) The biodiversity of species and their rates of extinction, distribution, and protection. *Science*, 344, 6187, 987.

PREDOI, G., BELU, C., DUMITRESCU, I., GEORGESCU, B. & ROSU, P. (2007) Comparative aspects regarding the skull bones in nandu (*Rhea Americana*) and ostrich (*Struthio camelus*). *LUCRĂRI ȘTIINȚIFICE MEDICINĂ VETERINARĂ*, 135, 7, 750-753.

RITCHIE, B. W., HARRISON, G. J. & HARRISON, L. R. (1994) *Avian Medicine: Principles and Application*. Florida, USA: Wingers Publishing, Inc.

ROTHWELL, B., WIGHT, P. A. L., BURNS, R. B. & MACKENZIE G. M. (1972) Harderian Glands of Domestic Fowl .3. Ultrastructure. *Journal of anatomy*, 112, 233.

SAHINDURAN, S. (2004) Isolation of *Escherichia coli* and *Staphylococcus aureus* from ostriches with conjunctivitis and respiratory disease. *Revue de médecine vétérinaire*, 155, 3, 167-169.

SAKAI, T. & VAN LEPPEN, E. W. (1984) The Harderian Gland in Australian Marsupials. *Journal of Mammalogy*, 65, 1, 4p, 159.

SALES, J. (2007) The emu (*Dromaius novaehollandiae*): a review of its biology and commercial products. *Avian and Poultry Biology Reviews*, 18, 1, 1-20.

SCHAT, K. A., KASPERS, B. & KAISER, P. (2014) *Avian Immunology*. 2nd ed. Academic Press.

SHIRAMA, K., KIKUYAMA, S., TAKEO, Y., SHIMIZU, K. & MAEKAWA, K. (1982) Development of Harderian gland during metamorphosis in anurans. *The Anatomical Record*, 202, 3, 371-378.

SHIRAMA, K. & HOKANO, M. (1992) *Harderian Glands: Porphyrin Metabolism, Behavioral and Endocrine Effects: Harderian glands and their development in laboratory rats and mice*. Berlin Heidelberg: Springer. 25 - 51.

SLONAKER, J. R. (1918) Physiological study of the anatomy of the eye and its accessory parts of the English sparrow (*Passer domesticus*). *Journal of morphology*, 31, 351-459.

TOBALSKE, B. W. (2007) Biomechanics of bird flight. *Journal of Experimental Biology*, 210, 3135–3146.

TULLY, T. N. & SHANE, S. M. (1996) *Ratite management, medicine and surgery*. Florida: Krieger Publishing Company.

WEBB, M. (1957) The Ontogeny of the cranial bones, cranial peripheral and cranial parasympathetic nerves together with a study of the visceral muscles of *Struthio*. *Acta Zoologica*, 81-201

WIGHT, P. A. L., BURNS, R. B., ROTHWELL, B. & MACKENZIE, G. M. (1971) Harderian Gland of Domestic Fowl .1. Histology, with Reference to Genesis of Plasma Cells and Russell Bodies. *Journal of anatomy*. 110, NOV, 307.

WILSON, T. A., NICOLOSIA, R. J., HANDELMANA, G., YOGANATHANA, S., KOTYLAA, T., ORTHOEFERB, F. & BINFORD, P. (2004) Comparative effects of emu and olive oil on aortic early atherosclerosis and associated risk factors in hypercholesterolemic hamsters. *Nutrition Research*, 24, 395–406.

WRIGHT, M. W., & BOWMAKER, J. K. (2001) Retinal photoreceptors of palaeognathous birds: the ostrich (*Struthio camelus*) and rhea (*Rhea americana*). *Vision Research*, 41, 1–12.

CHAPTER 2

Gross morphology and innervation of the *M. bulbi* in the ostrich (*Struthio camelus*) and emu (*Dromaius novaehollandiae*).

2.1 Introduction

Form and function in avian species have been studied extensively, with emphasis being placed on neognathous species such as *Passeriformes*, *Anseriformes*, *Galliformes* and *Psittaciformes* (King & McLelland, 1985; Baumel et al., 1993). The ostrich (Deeming, 1999) and emu (Sales, 2007) are commercially important ratites, thus more emphasis has been placed on ratite medicine and surgery.

Vision plays an essential role in nesting, foraging and mating behaviour in the ostrich and emu (Deeming, 1999; Calvino-Cancela et al., 2006; Sales, 2007; Cooper et al., 2010; Miller & Fowler, 2015). Ostrich and emu rely on eyesight to feed on shrubs, seeds, grasses (Deeming, 1999; Calvino-Cancela et al., 2006; Sales, 2007; Cooper et al., 2010; Miller & Fowler, 2015) and insects. Accurate pecking in these ratites is directed by a binocular field of vision that do not differ markedly in dimension and shape compared to many other avian species, despite the ostrich and emu having different phylogenies and habitats (Martin et al., 2001). Binocular vision in the ostrich is limited (Martin & Katzir, 1995) and thus rotation of the globe is required to alter the field of vision during foraging.

Rotation of the globe in the ostrich is initiated by the extrinsic ocular muscles, which allow an image to be focussed on the retina (Martin et al., 2001). The force exerted by the extrinsic ocular muscles (recti and oblique muscles) on the globe, results in rotatory motion of the globe (Ansons & Davis, 2014). Morphology of the *M. bulbi* or extrinsic ocular muscles, such as the attachments of these muscles, affects rotatory motion of the globe (Ansons & Davis, 2014).

The morphology of the *M. bulbi* in the ostrich has previously been described (Mac Alister, 1864; Webb, 1957; Deeming, 1999; Monfared & Bakhteyari, 2013; Crole & Soley, 2016). Scant information exists on the morphology of *M. bulbi* in the emu (Crole & Soley, 2016). Six extrinsic ocular (*Mm. recti superior/ inferior/ posterior/ anterior* and *Mm. obliquus inferior/ superior*) and two nictitating membrane (*M. pyramidalis membranae nictitantis*, *M. quadratus membranae nictitantis*) muscles have been described in the ostrich (Webb, 1957) and more recently, with

reference to updated nomenclature (Monfared & Bakhteyari, 2013). In the ostrich, two muscle groups attach the globe to the orbit, namely rectus and oblique muscles (Mac Alister, 1864; Monfared & Bakhteyari, 2013; Crole & Soley, 2016).

The extrinsic ocular muscles (recti and oblique muscles) in the ostrich arise from the border of the optic foramen (Mac Alister, 1864). In the ostrich, the extrinsic ocular muscles (recti and oblique muscles) are united at the respective origins by a ligament of Zinn (Mac Alister, 1864). In the ostrich, the recti and oblique muscles attach to the sclera, behind the scleral ossicles (Deeming, 1999). In comparison to the nictitating membrane muscles, morphological descriptions of the recti and oblique muscles in the ostrich are scant (Mac Alister, 1864; Webb, 1957; Deeming, 1999).

The *M. quadratus membranae nictitantis* and *M. pyramidalis membranae nictitantis* in the ostrich are robust (Mac Alister, 1864). The tendon of the pyramidal muscle or *tendo m. pyramidalis*, is common to avian species (King & McLelland, 1985; Baumel et al., 1993) and has been described in the ostrich (Mac Alister, 1864; Webb, 1957). The tendon of the pyramidal muscle attaches to the ventral margin of the nictitating membrane after passing through a loop in the distal part of the quadrate muscle (Webb, 1957). The loop of the quadrate muscle, termed the *vagina tendinis* (Baumel et al., 1993), *vagina fibrosa tendinis* (King & McLelland, 1985) or the *vagina fibrosa tendinis m. pyramidalis* (Elzanowski, 1987), is likewise the insertion of the quadrate muscle. In the ostrich, the insertion of the quadrate muscle is thickened and chondrified (Webb, 1957).

The voluminous globes in the ostrich, fit tightly into the osseous orbits, thus compressing the interorbital septum (Deeming, 1999). Rotation of the large globe in the ostrich is restricted due to it being located in a comparatively small orbit (Martin & Katzir, 1995; Martin et al., 2001). The osteology of the orbit in the ostrich (Parker, 1866; Webb, 1957; Bock, 1963; Predoi et al., 2007; Maxwell, 2009) and emu (Parker, 1866; Kesteven, 1942; Maxwell, 2009) have been described. The cranium of the ostrich and emu are typically palaeognathous in structure due to a unique palatine structure compared to neognathous species (Parker, 1866; Maxwell, 2009), however the remainder of the cranial osteology is similar to neognathous species (Baumel et al., 1993). The *foraminae* facilitating the passage of the cranial nerves into the orbit, are located within the *Septum interorbitale* (Baumel et al., 1993).

Cranial nerves II to VII are associated with the orbit, certain cranial nerves innervate the globe, associated muscles and lacrimal apparatus (Baumel et al., 1993). In reference to the ostrich

orbit, cranial nerves II to VII have been described (Mac Alister, 1864; Webb, 1957; Crole & Soley, 2016) and follow the basic avian pattern (Baumel et al, 1993). Reference has been made to the extrinsic ocular muscles in the ostrich being innervated by the trochlear and abducent nerves (Webb, 1957; Deeming, 1999). Scant information is however available on the cranial nerve morphology of the emu (Parker, 1866; Kesteven, 1942; Crole & Soley, 2016). Previous studies appear to indicate that the branches of facial (Kesteven, 1942) and trigeminal (Parker, 1866, Crole & Soley, 2016) nerves in the emu, are similar to that in the domestic fowl (Baumel et al., 1993). It appears that no information is available on the innervation to the *M. bulbi* in the emu.

The optic nerve (CN II) in the ostrich (Webb, 1957; Parker, 1866; Monfared & Bakhteyari, 2013; Crole & Soley, 2016) and emu (Parker, 1866; Crole & Soley, 2016) have previously been described. It has been documented that both optic nerves join the *Chiasma opticum* before passing through the *For. n. optici* and finally supplying the retina as it enters the sclera, ventro-rostrally (Deeming, 1999). The optic nerves and the associated chiasm are in markedly close proximity (King & McLelland, 1985). In the ostrich, the optic nerve is on average 4.5 cm in length (Monfared & Bakhteyari, 2013). The optic nerve in the ostrich is surrounded by *Dura mater* which partly extends unto the sclera (Deeming, 1999; Monfared & Bakhteyari, 2013).

The oculomotor, trochlear and abducent nerves innervate the extrinsic ocular muscles in avian species (Baumel et al., 1993; Ritchie et al., 1994; Jones et al., 2007; Orosz & Bradshaw, 2007). The trochlear nerve (CN IV) innervates the dorsal oblique muscle in the ostrich (Webb, 1957; Deeming, 1999) and enters the orbit via the *For. n. trochlearis* in both ratites (Crole & Soley, 2016).

In the ostrich, the topography of the trigeminal nerve (CN V) and associated branches have been described (Parker, 1866; Webb, 1957; Crole & Soley, 2016). The course of the *N. ophthalmicus* in the ostrich and emu, from its entry into the orbit via the *For. n. ophthalmici*, up to its termination at the beak tip (Crole & Soley, 2016), have previously been described. The ophthalmic foramen is notably larger in the ostrich compared to the emu and is often merged to the *For. n. optici* (Crole & Soley, 2016). The topography of the ophthalmic branch of the trigeminal nerve, with reference to the orbit has been described in the ostrich (Deeming, 1999).

The muscles of the nictitating membrane and lateral rectus muscle in the ostrich are innervated by the *N. abducens* (CN VI) (Webb, 1957; Deeming, 1999). In the same species, the dorsal ramus of this abducent nerve innervates the quadratus and pyramidal muscles

(Webb, 1957). In the ostrich, the lateral rectus muscle is innervated by the ventral ramus of the abducent nerve (Webb, 1957).

Scant information is available on the innervation to the *M. bulbi* in the ostrich. According to literature, it appears that the ostrich follows the basic avian pattern. Information on the innervation to the *M. bulbi* in the emu does not appear to be available and it is assumed to follow a pattern similar to that in the ostrich. The innervation of each extrinsic ocular muscle in the ostrich and emu warrants further investigation. In both species, thorough descriptions of the passage of the nerves innervating the *M. bulbi* in relation to adjacent structures are necessitated.

The morphology of the *M. bulbi* in the ostrich follows a basic avian pattern (Deeming, 1999; Monfared & Bakhteyari, 2013), however thorough descriptions of these muscles are scant compared to other avian species. It appears that no information is available on the morphology of the *M. bulbi* in the emu and it is assumed to follow the general avian pattern.

Ocular disease has a marked effect on the welfare and productivity of breeding birds. The ostrich and emu are commercially important and a thorough description of the *M. bulbi* and its innervation, would aid in performing successful diagnostics and surgery on these ratites.

2.2 Materials and Methods

The heads of eleven sub-adult ostriches (approximately 14 months old) and eleven sub-adult emus, of either sex, were collected from Klein Karoo Ostrich abattoir (Oudtshoorn, Western Cape, South Africa) and Oryx Abattoir (Krugersdorp, Gauteng, South Africa), respectively (protocol V 066 / 11; V 023 / 06), immediately after slaughter of birds for commercial use. Ethical clearance for this study was obtained through the University of Pretoria, Animal Ethics Committee (Project number: V 051 / 16).

These were thoroughly rinsed in running tap water to remove blood and other contaminants, immersion fixed in 10% buffered formalin and stored in fixative until further processing. For each species, a scalpel blade was used to make a circum-orbital incision and the eyelids removed as to expose the eye globe. The conjunctiva and connective tissue within the orbit was carefully dissected as to expose each nerve within the orbit. The tendon of the pyramidal muscle (*tendo m. pyramidalis*) and its insertion was described. Conjunctiva was transected and its insertion on the bony orbit, reflected. Each nerve was dissected and described from its entry point into the orbit to the structure it innervated.

The lacrimal apparatus was left intact. The dorsum of the cranium was removed and thereafter the entire cerebrum as to expose the optic chiasm ventrally. The optic foramen and the surrounding *foraminae* were preserved. A digital calliper (Workzone GT - DC - 02, Germany) was used to measure the distance from optic foramen to centre of the optic chiasm. The distance between the centre of the left and the centre of the right optic foramen was measured by using a digital calliper (Workzone GT - DC - 02, Germany). In this study *Foramen n. optici* or optic foramen, was used when referring to the *Foramen opticum*. Cranial nerves III to VII were further dissected and described after the dorsal cranium was removed. The eye globe was thereafter collapsed by puncturing the cornea and removing excess aqueous and vitreous fluid.

In one ostrich and one emu, each extrinsic ocular muscle was transected at its respective insertion, as to only remove the globe. In the remaining specimens, the extrinsic ocular muscles were each transected at its respective origin. Thus the portion of bony orbit around the *Foramen n. optici* was incised and the entire globe (as well as the straight ocular muscles at the respective origins) were removed and the *foraminae* surrounding the optic foramen were preserved. A dissection microscope (Zeiss GmbH, Stemi DV4) was used to dissect the *rami* of the *N. abducens* and *N. oculomotorius* and was thereafter described in relation to the remaining ocular nerves. Annotated drawings were made of each nerve's topographical orientation. The excess connective tissue surrounding each extraocular muscle was removed to clearly expose the insertion of each muscle. Each muscle was morphologically described and compared and annotated drawings were made.

The Harderian and lacrimal glands were morphologically described (see Chapter 4) and then excised by transecting the connective tissue attachment to the eye globe. The glands were immersion fixed in fresh 10% buffered formalin and stored in labelled bottles until further processing for light microscopy.

The imaginary line encompassing the globe, midway between the anterior and posterior poles, was identified as the equator. The quadrate muscle in three ostriches and three emus was transected transversely, proximal to the *vagina tendinis*. The tendon of the pyramidal muscle was then transected caudal and rostral to the *vagina tendinis*. Therefore, the insertion of the quadrate muscle as well as the portion of *tendo m. pyramidalis* attached to it, was preserved. This portion of quadrate muscle was immersion fixed in fresh 10 % buffered formalin and stored in labelled bottles until further processing for light microscopy. The samples were subsequently cut, dried by means of a graded ethanol series (70 %, 80 %, 96 %, and 2 x 100 % ethanol) and further processed through 50:50 ethanol: xylol, 2x xylol and 2 x paraffin wax

(60 - 120 minutes per step) using a Shandon model 2LE Automatic Tissue Processor (Shandon, Pittsburgh, PA). After which the samples were manually imbedded into paraffin wax within plastic moulds. Sections were cut at 4 - 6 μm and stained with Masson Trichrome to differentiate between muscle and collagenous tissue. An Olympus BX 63 light microscope equipped with a DP 72 camera and Olympus cell Sens imaging software (Olympus Corporation, Tokyo, Japan), were used to view the histological sections and record features of interest.

All anatomical nomenclature used in this study was taken from *Nomina Anatomica Avium* (Baumel et al., 1993).

2.3 Results

2.3.1 *Musculi bulbi oculi*

In each species, four recti, two oblique and two nictitating membrane muscles were identified and described (Figures 2.1, 2.2). The recti and oblique muscles were thin and sheet-like and originated from the bony orbit. Each muscle had a tendon which inserted on the sclera and was intimately merged with the scleral tissue. The oblique and recti muscles inserted unto the globe, near the equator in both species. The *M. bulbi* were further differentiated as to inserting posterior, unto or anterior to the equator (Table 2.1). Clarification as to the orientation of the ocular structures in relation to the orbit, was provided via a schematic drawing. For the purpose of this study, the terms caudal, rostral, anterior, posterior, dorsal and ventral were used when describing the morphology of the *M. bulbi* and associated structures (Figures 2.1.1, 2.1.2).

In the ostrich and emu, the nictitating membrane muscles, namely the quadrate and pyramidal muscles, had their origin on the posterior sclera (Figures 2.1, 2.2). The pyramidal muscle in both species inserted on the nictitating membrane via a robust, tube-like tendon, the *tendo m. pyramidalis* (Figures 2.1, 2.2). The quadrate muscle in the ostrich and emu inserted on the *tendo m. pyramidalis* via a *vagina tendinis* (Figures 2.1, 2.2). The nictitating membrane in both species was located rostrally and attached to the anterior orbit and posterior surface of the eyelids, distal to the eyelid margin. The nictitating membrane was comprised of two membranous walls and an opening or pouch was evident between these. In both species, the walls of the membrane joined to form a robust margin. In both species, the margin of the membrane was in contact with the corneal surface.

2.3.1.1 *M. rectus dorsalis*

In the ostrich and emu this muscle originated from the caudo-dorsal margin of the *Foramen n. optici* (Table 2.1; Figure 2.5) and inserted dorsally on the sclera (Figures 2.1, 2.2), posterior to the equator (Table 2.1), partly covering the insertion and caudal margin of the dorsal oblique muscle (Figures 2.3 to 2.4).

2.3.1.2 *M. rectus ventralis*

The ventral rectus muscle originated from the ventral margin of the *Foramen n. optici* (Table 2.1; Figure 2.5) and inserted ventro-rostrally in relation to the equator (Table 2.1), deep to the *M. obliquus ventralis* in both species. This muscle originated further rostrally and inserted on the equator in the emu, compared to the ostrich where this muscle inserted anteriorly in relation to the equator (Table 2.1). The Harderian gland was positioned against its rostral margin in both species (Figures 2.3, 2.4).

2.3.1.3 *M. rectus lateralis*

In both species, the muscle originated at the caudo-ventral margin of the *Foramen n. optici* (Table 2.1; Figure 2.5) and inserted caudally on the equator (Table 2.1). Variation in the insertion of the lateral rectus muscle was evident within species as well as between species. In the emu, the insertion of the muscle was not obliquely as was apparent in the ostrich (Table 2.1). This muscle covered a portion of the *tendo m. pyramidalis* in both species. The prominent lacrimal gland in the ostrich (see Chapter 4), was positioned proximal to the insertion of the lateral rectus muscle.

2.3.1.4 *M. rectus medialis*

In the ostrich and emu, the muscle originated from the *Septum interorbitale*, dorso-rostrally to the *Foramen n. optici* (Table 2.1; Figure 2.5). The muscle inserted rostrally, posterior to the equator, in the ostrich and emu (Table 2.1). In both species, the proximal part of the Harderian gland was adjacent to ventral margin of this muscle (Figures 2.3, 2.4).

2.3.1.5 *M. obliquus dorsalis*

In the ostrich and emu, the muscle originated from the *Os ectethmoidale*, caudo-ventrally to the *For. orbitonasale* (Table 2.1; Figure 2.5). The muscle inserted obliquely on the dorsal

sclera (Figures 2.1, 2.2), posterior to the equator (Table 2.1). This muscle was positioned deep to the *M. rectus dorsalis*, and covered the dorsal part of the *M. quadratus membranae nictitantis* (Figure 2.2).

2.3.1.6 *M. obliquus ventralis*

In the ostrich and emu, this muscle originated from the *Os ectethmoidale* (Table 2.1; Figure 2.5). The origin of the ventral oblique muscle in the ostrich was dorsal to the impression made by the Harderian gland in the osseous orbit and was partly covered by the Harderian gland neck and secretory duct. The muscle inserted obliquely on the ventral sclera (Figures 2.1, 2.2), anterior to the equator in both species (Table 2.1). This muscle inserted superficially to the insertion of the *M. rectus ventralis* in the ostrich and emu (Figures 2.1, 2.2). In both species, the ventral oblique muscle partly covered the pyramidal muscle (Figure 2.2).

2.3.1.7 *M. quadratus membranae nictitantis*

In both ostrich and emu, the muscle originated dorsally (Figures 2.1, 2.2), posterior to the equator on the posterior sclera (Table 2.1). The quadratus muscle inserted on the proximal portion of the *tendo m. pyramidalis* via a *vagina tendinis* (Table 2.1; Figure 2.1; Figure 2.2). In both ostrich and emu, the *vagina tendinis* is collagenous in nature (Figure 2.6). The *vagina tendinis* was positioned dorsal to the optic nerve forming an arch, the *Arcus tendineus nervi optici* (Figures 2.1, 2.2). The origin of the quadratus muscle was partly covered by the dorsal oblique and rectus muscles in the emu (Figure 2.2). In the ostrich, a greater portion of the proximal quadratus muscle was covered by the dorsal oblique and rectus muscles (Figure 2.2).

2.3.1.8 *M. pyramidalis membranae nictitantis*

In the ostrich and emu this muscle originated ventro-rostrally, on the posterior sclera (Table 2.1; Figures 2.1, Figure 2.2). The most proximal part of the *tendo m. pyramidalis* was located dorso-rostrally to the optic nerve (Figures 2.1, 2.2). In the ostrich, the pyramidal muscle originated further anterior on the sclera compared to the emu, in that this muscle originated on the equator in the ostrich (Table 2.1). The tendon of the pyramidal muscle coursed through the *vagina tendinis* of the quadratus muscle, located dorsal to the optic nerve (Figures 2.1, 2.2). Then the tendon of the pyramidal muscle proceeded ventro-caudally over the posterior sclera, where it was covered partly by the lateral rectus muscle. Before inserting ventrally on the free margin of the nictitating membrane, the tendon passed ventral to the insertion of the lateral

rectus muscle. In the ostrich and emu, the ventral rectus muscle and the ventral oblique muscle partly covered the caudal margin and origin of the pyramidal muscle (Figure 2.2).

2.3.2 Cranial nerves

2.3.2.1 *N. opticus*

In the ostrich and emu CN II exited the orbit via the *Foramen n. optici* which was located caudoventrally in the orbit (Figures 2.5, 2.8), at the caudal margin of the *Septum interorbitale*. It was evident that *Dura mater* covered this nerve distally and seemed to extend unto the sclera in both species. Ligamentous tissue surrounded the base of the optic nerve and the border of the optic foramen in the ostrich and emu. The optic nerve exited the posterior sclera, ventro-caudally in both species (Figures 2.1, 2.2, 2.9, 2.10).

The distance between the right and left optic *foraminae* in the ostrich averaged 14 mm and 8.5 mm in the emu. The distance from optic foramen to chiasm averaged 5.7 mm in the ostrich and 3.8 mm in the emu.

2.3.2.2 *N. oculomotorius*

In the ostrich and emu CN III, entered the orbit via the *Foramen n. oculomotorii*, caudally to the optic foramen (Figure 2.8). In the ostrich and emu, the oculomotor foramen was located ventro-caudally to the ophthalmic foramen (Figure 2.8). In both species, the *Ramus dorsalis* of the oculomotor nerve innervated the dorsal rectus muscle at its origin as the nerve exited the foramen (Figures 2.9, 2.10). After innervating the dorsal rectus muscle, the *N. oculomotorius ramus ventralis* and *Ganglion ciliare* communicated via a *connexus cum n. oculomotorius*, which entered the sclera dorso-caudally to the optic nerve in both species (Figures 2.9, 2.10).

In both species, the ventral ramus of the oculomotor nerve proceeded rostrally, adjacent to and ventral to the optic nerve, where it innervated the following extrinsic muscles in the following order: *M. rectus ventralis*, *M. obliquus ventralis* and *M. rectus medialis* (Figures 2.9, 2.10). The branch of the oculomotor nerve innervating the ventral oblique on its anterior surface, did not proceed under the Harderian gland before entering the muscle at its caudal margin, in the emu (Figure 2.10). Comparatively, the oculomotor nerve proceeded under the Harderian gland before innervating the ventral oblique muscle in the ostrich (Figure 2.9).

2.3.2.3 *N. trochlearis*

In both species CN IV entered the orbit via the *Foramen n. trochlearis* (Figure 2.8), positioned dorsally to the optic foramen in the ostrich and dorso-rostrally to the same foramen in the emu. The trochlear nerve proceeded over the ophthalmic nerve before innervating the dorsal oblique muscle in both the ostrich and emu as it entered the muscle's caudal margin midway between its origin and insertion (Figures 2.9, 2.10).

2.3.2.4 *N. trigeminus*

In both the ostrich and emu, branches of CN V coursed through the orbit (Figure 2.7). The branches of the trigeminal nerve which are associated with the orbit were described in the present study: *N. ophthalmicus* as well as the *N. maxillaris* which branches into the *N. supraorbitalis*, *N. nasopalatinus* and *N. infraorbitalis* (Figure 2.7).

In both species, the ophthalmic nerve entered the orbit via the *Foramen n. ophthalmici* which was located caudally and adjacent to the optic foramen (Figure 2.8). The ophthalmic nerve contributed to the ciliary ganglion located caudally to the optic nerve, before proceeding dorsal to the optic nerve (Figures 2.9, 2.10). After proceeding dorsal to the optic nerve, the ophthalmic nerve branch of CN V, coursed rostrally under the origin of the dorsal rectus muscle. In the emu, the nerve passed over the origin of the lateral rectus muscle before proceeding in a rostral direction under the dorsal rectus muscle's origin. In both species, the ophthalmic nerve passed under the trochlear nerve before proceeding over the origin of the medial rectus muscle (Figures 2.9, 2.10). The nerve ran along the dorsal margin of the medial rectus muscle before proceeding under the dorsal oblique muscle, distal to its origin. The ophthalmic nerve entered the maxilla via the *Foramen orbitonasale* (Figures 2.7, 2.8). In some specimens in both species, the distal part of the Harderian gland partly covered the latter foramen.

The *N. maxillaris* in the ostrich and emu entered the ventro-caudal orbit via the *Foramen n. maxillomandibularis* (Figure 2.7) together with the mandibular nerve. The maxillary nerve proceeded between *M. pseudotemporalis superficialis* posteriorly and *M. adductor mandibulae externus* anteriorly, before branching dorsally and ventrally. The dorsal branch of the maxillary nerve, the *N. supraorbitalis*, proceeded dorsally along the *Septum interorbitale* and terminated mid-orbit (Figure 2.7). In the emu, the supraorbital nerve proceeded somewhat ventral compared to the ostrich (Figure 2.7). The supraorbital nerve gave off a dorsal branch, presumably the *Ramus palpebralis caudodorsalis*, which entered the orbit ventral to the

supraorbital nerve (Figure 2.7) and proceeded dorsally along the anterior orbit within the periorbital connective tissue.

The ventral supraorbital *rami*, namely the *N. nasopalatinus* (dorsal) and *N. infraorbitalis* (ventral), innervated the caudal maxilla in both ostrich and emu (Figure 2.7). The *N. nasopalatinus* proceeded on the medial aspect of the *Arcus jugalis*, before entering the maxilla and innervating the mucosa covering the mid to proximal *Os palatinum*. In the emu, the nasopalatine nerve proceeded at a steeper angle before entering the maxilla compared to the ostrich where the nerve ran more horizontally from its origin (Figure 2.7). In both species, the *N. infraorbitalis* proceeded postero-ventrally over the *M. pseudotemporalis superficialis* before coursing along the anterior ventral orbit where it entered the maxilla posteriorly to the *N. nasopalatinus*.

2.3.2.5 *N. abducens*

Cranial nerve VI in both ostrich and emu entered the orbit via the *For. n. abducentis* (Figure 2.8), before coursing dorsal to the optic nerve where it innervated the lateral rectus on its anterior surface (Figures 2.9, 2.10). After innervating the lateral rectus muscle, the abducent nerve proceeded ventral to the *vagina tendinis* and entered the quadratus muscle anteriorly (Figures 2.9, 2.10). It was evident in the ostrich and emu that the distal branch of the abducent nerve proceeded ventral to the optic nerve before innervating the pyramidal muscle (Figures 2.9, 2.10). The continuation of the abducent nerve entered the pyramidal muscle at its dorso-rostral margin in both ostrich and emu (Figures 2.9, 2.10).

2.3.2.6 *N. facialis*

In both species, the *N. palatinus* of cranial nerve VII entered the orbit via the *Foramen n. facialis* located ventrally to the *Foramen n. maxillomandibularis* (Figure 2.8), before branching into a dorsal and ventral ramus (Figure 2.7). The ventral palatine ramus coursed along the ventral part of the orbit (Figure 2.7), whereas the dorsal ramus proceeded from caudally along the dorsal margin of the Harderian gland before communicating with the ethmoidal ganglion, ventral to the orbitonasal foramen (Figure 2.7). In the ostrich and emu, a *connexus* was evident between the ophthalmic nerve and the ethmoidal ganglion where the ophthalmic nerve exited the orbit (Figure 2.7). In neither species was it evident that the sphenopalatine ganglion communicated with the ventral palatine ramus or ethmoidal ganglion. In the emu, a *connexus*

was present between the infraorbital nerve and the ventral palatine ramus (Figure 2.7) at the insertion of *M. pseudotemporalis superficialis*.

2.4 Discussion

2.4.1 *M. bulbi oculi*

Cranial osteology as well as the morphology of the extrinsic ocular muscles in the ostrich (Webb, 1957, Martin & Katzir, 1995; Martin et al., 2001; Crole & Soley, 2016) and emu (Parker, 1866; Kesteven, 1942; Crole & Soley, 2016), has been described. Descriptions of the morphology of the *M. bulbi* in these species are however not extensive.

The ostrich and emu globe is large in comparison to cranial volume and thus the interorbital septum (*Septum interorbitale*) or posterior portion of the ossified orbit is particularly thin in these ratites (Parker, 1866; Kesteven, 1942; Webb, 1957, Martin & Katzir, 1995; Martin et al., 2001; present study). The latter is common to most avian species (King & McLelland, 1985; Baumel et al., 1993).

The avian *Musculi bulbi oculi* is comprised of four *Mm. recti* namely dorsal, ventral, medial and lateral; two *Mm. obliquus* namely dorsal and ventral, and two nictitating membrane muscles namely the *M. quadratus membranae nictitantis* and *M. pyramidal membranae nictitantis* (Chard & Gundlach, 1938; King & McLelland, 1985; Baumel et al., 1993; Ritchie et al., 1994). These eight extrinsic ocular muscles are evident in the ostrich embryo (Webb, 1957) as well as adult ostrich (Monfared & Bakhteyari, 2013; Crole & Soley, 2016; present study) and emu (Crole & Soley, 2016; present study). The attachments of the *M. bulbi* in the ostrich and emu, are comparable, with minor differences noted in the morphology.

The muscle and tendon fibres in each extrinsic ocular muscle in the ostrich and emu are orientated longitudinally from its origin to insertion (present study). Attachments of the recti muscles in the ostrich and emu are comparable in that these muscles originate from the border of the optic foramen (*Foramen n. optici*) (present study). It has previously been confirmed that the recti muscles originate from the border of the optic foramen in the ostrich (Mac Alister, 1864; Deeming, 1999). The latter has not been described in the emu, however the present study confirmed that that these muscles originate from the border of the optic foramen. Likewise, the origins of the oblique muscles are comparable between the ostrich and emu. It was evident in the present study, that the oblique muscles in the ostrich and emu originate from the *Os ectethmoidale*. The *M. quadratus membranae nictitantis* and *M. pyramidalis*

membranae nictitantis in both species appear robust (present study), which has previously been documented in the adult ostrich (Mac Alister, 1864). In the ostrich and emu, the nictitating membrane muscles, originate on the posterior sclera (present study).

No thorough descriptions of the origins of the extrinsic ocular muscle have previously been provided in either ostrich or emu. The present study however indicates that minor differences in the origins of the *M. bulbi* are evident between the two species, in that the ventral rectus muscle originates further rostrally in the emu compared to the ostrich. In the ostrich, the pyramidal muscle originates on the equator of the globe, compared to the emu, where the same muscle originates posteriorly relative to the equator (present study). The origin of ventral oblique muscle is covered by the neck and proximal secretory duct of the same gland (see Chapter 4). In comparison, the Harderian gland in the emu partly covers the origin of the ventral oblique muscle and lies further anteriorly because of the relatively small size of the gland (see Chapter 4). Previously, the Harderian gland in the ostrich has previously only been described as positioned between the medial and ventral recti muscles (Mac Alister, 1864; Deeming, 1999). The origins of the nictitating membrane muscles are however comparable in the ostrich and emu (present study). In the ostrich, the pyramidal muscle originates further anterior to the equator of the globe than is apparent in the emu (present study).

In the present study, it was noted that the morphology of the *M. bulbi* in the ostrich and emu are similar to other avian species, such as the sparrow (Slonaker, 1918), homing pigeon (Chard & Gundlach, 1938) and Tinamous (Elzanowski, 1987). The same extrinsic ocular muscles have been identified in the English sparrow (Slonaker, 1918), homing pigeon (Chard & Gundlach, 1938) and Tinamous (Elzanowski, 1987). The recti and oblique muscles in the ostrich and emu have a greater muscular component compared to tendon (present study), which is comparable to the English sparrow (Slonaker, 1918), homing pigeon (Chard & Gundlach, 1938) and Tinamous (Elzanowski, 1987). From the respective origin of each muscle in the ostrich and emu, the muscle fibres converge towards the insertion, as is evident in the Tinamous (Elzanowski, 1987).

The origins of the recti muscles have been thoroughly described in the Tinamous (Elzanowski, 1987) and are similar to that in the ostrich and emu (present study). In the ostrich and emu, the origins of the oblique muscles are similar to that described in the Tinamous (Elzanowski, 1987), in that the oblique muscles originate from the rostral interorbital septum. As is evident in the Tinamous (Elzanowski, 1987), the quadratus muscle in the ostrich and emu originates dorsally, deep to the dorsal oblique muscle, posterior to the equator (present study). The orientation of the pyramidal muscle in relation to the remainder of the extrinsic ocular muscles

in the ostrich and emu, is similar to the sparrow (Slonaker, 1918) and homing pigeon (Chard & Gundlach, 1938). The optic foramen is partly covered by firm connective tissue extending onto the optic nerve in the ostrich (Mac Alister, 1864; Deeming, 1999; present study) and emu, which is comparable to the English sparrow (Slonaker, 1918) and homing pigeon (Chard & Gundlach, 1938).

Minor differences in the morphology of extrinsic ocular muscles in the ostrich and emu are however evident, compared to other avian species, such as the sparrow (Slonaker, 1918), homing pigeon (Chard & Gundlach, 1938) and Tinamous (Elzanowski, 1987). Origins of the extrinsic ocular muscles in both species appear muscular in nature, compared to the Tinamous where most ocular muscles originated from a greater proportion of tendinous fibres (Elzanowski, 1987). The recti muscles in the ostrich and emu differ from the sparrow (Slonaker, 1918) and homing pigeon (Chard & Gundlach, 1938) in that these muscles attach to the osseous portion of the optic foramen and not the proximal part of the optic nerve or the sheath surrounding the latter nerve.

Further morphological variation is evident when comparing the ostrich and emu to other avian species. In the ostrich and emu, the pyramidal muscle originates further caudally on the posterior sclera, compared to the same muscle in the Tinamous (Elzanowski, 1987). In the Tinamous, the origins of the oblique muscles on the ectethmoid bone are covered by the Harderian gland (Elzanowski, 1987). The latter differs from the ostrich in that the origin of ventral oblique muscle on the ectethmoid bone, is covered by the neck and proximal secretory duct of the same gland (see Chapter 4). In comparison, the Harderian gland in the emu partly covers the origin of the ventral oblique muscle on the ectethmoid bone (see Chapter 4). The *Os ectethmoidale* forms part of the *Paries rostralis orbitae*, whereas the *Septum interorbitale* is likewise described as the *Paries medialis orbitae* (Baumel et al., 1993). Thus, the rostral part of the interorbital septum could be considered synonymous to the caudal part of the ectethmoid bone.

The insertions of the extrinsic ocular muscles differ to a greater extent compared to the respective origins, between the ostrich and emu (present study). In both species, the extrinsic ocular muscles insert posterior to the equator, with the exception of the ventral muscles as well as the lateral rectus muscle, which insert anterior to or unto the equator (present study). Variation in the location of the *vagina tendinis* was also apparent between the two species. In the emu, the *vagina tendinis* is positioned somewhat caudally on the posterior sclera, compared to the ostrich (present study). The greatest variations in the insertions of the *M.*

bulbi between the ostrich and emu, are evident in the ventral and lateral rectus muscles (present study).

The ventral rectus muscle rotates the globe ventrally and the lateral rectus muscle abducts the globe (Maggs et al., 2008). In the ostrich, the ventral rectus muscle inserted anteriorly to the equator, compared to the emu, where the same muscle unto the equator. Posterior insertions of extrinsic ocular muscles relative to the equator decreases the effective distance from origin to insertion in these muscles and thus the level arm by which these muscles act on the globe (Ansons & Davis, 2014). The efficiency of rotating the globe ventrally due to the anterior insertion of the ventral rectus in the ostrich, may differ from the emu. In the ostrich, the oblique insertion of the lateral rectus, may likewise influence efficiency of globe abduction, compared to the emu. Variation in the insertions of the ocular muscles between the ostrich and emu may be related to the difference in globe volume between the two species. However, further investigation is required as to determine the influence that the variation in extrinsic muscle insertion has on visual fields between the two species.

The insertions of the extrinsic ocular muscles in the ostrich and emu, are comparable to other avian species such as the Tinamous (Elzanowski, 1987), English sparrow (Slonaker, 1918) and homing pigeon (Chard & Gundlach, 1938). Each rectus and oblique muscle in the ostrich and emu inserts on the sclera via a thin, sheet-like tendon, which is likewise described in the English sparrow (Slonaker, 1918), homing pigeon (Chard & Gundlach, 1938) and Tinamous (Elzanowski, 1987).

The posterior insertion of the dorsal rectus muscle relative to the equator in ostrich and emu (present study) is comparable to the Tinamous (Elzanowski, 1987). In the ostrich and emu, the insertion of the medial rectus muscle is similar to the Tinamous (Elzanowski, 1987), in that the medial rectus muscle inserts posterior to the equator. The dorsal oblique's insertion in the ostrich and emu, is comparable the Tinamous (Elzanowski, 1987), in that the dorsal oblique muscle inserts dorsally on the equator, deep to the *M. rectus dorsalis* and covers the *M. quadratus membranae nictitantis*. The insertion of the ventral oblique muscle partly covers the insertion of the ventral rectus muscle in the ostrich and emu (present study). In the sparrow (Slonaker, 1918), pigeon (Chard & Gundlach, 1938) and Tinamous (Elzanowski, 1987) similar description have been given for the insertion of the ventral oblique muscle. The description of the ventral oblique muscle inserting obliquely as well as ventrally on the sclera, is likewise apparent in the Tinamous (Elzanowski, 1987).

The *M. quadratus membranae nictitantis* inserts on the proximal portion of the *tendo m. pyramidalis* via a *vagina tendinis* dorsal to the optic nerve in the ostrich and emu. A similar morphological description of the quadrate muscle is provided for the Tinamous (Elzanowski, 1987). The origin of the quadrate muscle in the emu is comparable to the observations made in the sparrow (Slonaker, 1918) and homing pigeon (Chard & Gundlach, 1938).

The quadrate muscle inserts on the *tendo m. pyramidalis* via a *vagina tendinis* in the adult ostrich and emu (present study), which has previously been described in the ostrich embryo (Webb, 1957). A similar description for the insertion of the quadrate muscle has been provided in other avian species (King & McLelland, 1985; Baumel et al., 1993), such as the English sparrow (Slonaker, 1918), homing pigeon (Chard & Gundlach, 1938) and Tinamous (Elzanowski, 1987). The morphological descriptions of the *tendo m. pyramidalis* in the ostrich and emu is comparable to that in the sparrow (Slonaker, 1918) and homing pigeon (Chard & Gundlach, 1938). In both ostrich and emu, the pyramidal tendon proceeds ventro-caudally over the posterior sclera, where it is partly covered by the lateral rectus muscle before inserting ventrally on the free margin of the nictitating membrane (present study). The insertion of the pyramidal tendon in the ostrich and emu is similar in the English sparrow (Slonaker, 1918), homing pigeon (Chard & Gundlach, 1938) and Tinamous (Elzanowski, 1987).

Morphological variation in the insertion of *M. bulbi* in the ostrich and emu (present study) is evident compared to that described in species such as the English sparrow (Slonaker, 1918), homing pigeon (Chard & Gundlach, 1938) and Tinamous (Elzanowski, 1987). In the ostrich and emu, the lateral rectus inserts on the equator (present study). The latter differs from the Tinamous where the insertion of this muscle is further ventral as well as posterior to the equator (Elzanowski, 1987). A prominent opening in the lateral rectus muscle allows for the passage of the ophthalmic nerve is present in duck (*Gallus sp.*) (Elzanowski, 1987). This opening is not evident however in the ostrich or emu (present study). The insertion of the lateral rectus muscle in the ostrich is unique in respect to the Tinamous (Elzanowski, 1987) and emu (present study), as this muscle inserts obliquely on the sclera.

Further variation in the morphology of the *M. bulbi* in the ostrich and emu is apparent, compared to that described in the Tinamous. The *vagina tendinis* in the ostrich and emu is collagenous, which differs from the ostrich embryo (Webb, 1957) and Tinamous (Elzanowski, 1987), where the same structure is described as being chondrified and muscular, respectively. Collagen is renowned for its tensile strength when subject to mechanical load (Benjamin et al., 2008). The action of moving the nictitating membrane, though no considerable mechanical load is involved, would involve the suspension of the pyramidal tendon and the pulley-like

action of the quadratus muscle on the pyramidal tendon when the membrane is moved (Coues, 1868). Thus, the attachment of the quadratus muscle around the pyramidal tendon by means of collagen, would allow for a durable suspensory mechanism.

Furthermore, the *M. bulbi* in the ostrich and emu differed in the following respect from other avian species. In the Tinamous, a parapyramidal muscle has been described (Elzanowski, 1987), which is not evident in the ostrich or emu. The significance of this difference remains to be determined.

2.4.2 Cranial nerves associated with the orbit

The avian cranial nerves have been thoroughly described (Baumel et al., 1993; Ritchie et al., 1994; Jones et al., 2007; Orosz & Bradshaw, 2007). In the ostrich and emu, the cranial nerves follow the general avian pattern (Parker, 1866; Kesteven, 1942; Webb, 1957; Crole & Soley, 2016, present study). The optic nerve is the largest of all the cranial nerves discussed in this study and exits the posterior sclera of the globe ventro-caudally in the ostrich and emu (present study). The latter description of the optic nerve, is comparable to previous studies on the optic nerve in avian species (Baumel et al., 1993) such as the sparrow (Slonaker, 1918; King & McLelland, 1985), Tinamous (Elzanowski, 1987) and *Falconiformes* (Jones, 2007).

In the homing pigeon, it has been described that the optic nerve exits the globe centrally (Chard & Gundlach, 1938). The description given in the homing pigeon differs from that in the ostrich, where the optic nerve is described exiting the globe ventro-rostrally (Deeming, 1999). A membranous sheath surrounds the optic nerve and attaches to the posterior sclera as the nerve exits the globe (present study). The membranous structure may partly consist of *Dura mater* extending unto the sclera as observed by in the ostrich (Deeming, 1999; Monfared & Bakhteyari, 2013). The *N. opticus* (CN II) exits the orbit via the *Foramen n. optici* (*Foramen opticum*) in the ostrich (Parker, 1866; Kesteven, 1942; Webb, 1957; Crole & Soley, 2016, present study) and emu (Parker, 1866; Kesteven, 1942; Crole, 2016, present study). The measurements taken indicate that the *N. opticus* and the associated chiasm in both species are in markedly close proximity in the ostrich (Parker, 1866; Deeming, 1999; Monfared & Bakhteyari, 2013; present study), emu (Parker, 1866; present study) as noted in other avian species (King & McLelland, 1985). The latter needs to be taken into consideration when ocular surgery, such as enucleation is performed in the ostrich and emu.

The *N. oculomotorius* (CN III) enters the orbit caudally to the optic foramen via the *For. n. oculomotorii* and innervates the dorsal, ventral and medial recti muscles as well as the ventral oblique muscle in both ostrich and emu (present study). Similar observations were made in

other avian species (Baumel et al., 1993; Jones, 2007), such as the domestic fowl (Baumel et al., 1993) and the English sparrow (Slonaker, 1918; King & McLelland, 1985). It was confirmed that the dorsal ramus of the *N. oculomotorius* innervates the dorsal rectus muscle in the adult ostrich (present study), as is evident in the ostrich embryo (Webb, 1957).

The oculomotor nerve likewise innervates the dorsal rectus muscle in the domestic fowl (Baumel et al., 1993) and the sparrow (Slonaker, 1918; King & McLelland, 1985). In the ostrich and emu, CN III enters the origin of the dorsal rectus muscle dorsal to the optic nerve (present study). In domestic fowl (Baumel et al., 1993), the ostrich embryo (Webb, 1957), adult ostrich and emu (present study), the ventral ramus of the *N. oculomotorius* communicates with the *Ganglion ciliare*. The latter differs from the sparrow where the dorsal ramus communicates with the ciliary ganglion (Slonaker, 1918). The ventral ramus of the oculomotor nerve innervates the ventral and medial recti and ventral oblique muscles in the ostrich and emu (present study) as is evident in the sparrow (Slonaker, 1918) and domestic fowl (Baumel et al., 1993). In the sparrow, the *N. oculomotorius* and *N. trigeminus* have a communicating ramus (Slonaker, 1918). The latter communicating ramus was not evident in the ostrich or emu (present study).

The *N. trochlearis* (CN IV) innervates the dorsal oblique muscle in the ostrich (Webb, 1957; Deeming 1999; present study) and emu (present study) as well as other avian species, such as the sparrow (Slonaker, 1918; King & McLelland, 1985), domestic fowl (Baumel et al., 1993), and birds of prey (Jones, 2007). In both ostrich and emu, the nerve enters the orbit via the *Foramen n. trochlearis* (present study). The trochlear foramen is positioned dorsally to the optic foramen in the ostrich (Crole & Soley, 2016; present study) and dorso-rostrally to the same foramen in the emu (Crole & Soley, 2016; present study). The trochlear nerve proceeds dorsally to the ophthalmic nerve before entering the dorsal oblique muscle in the ostrich and emu, which is comparable to the sparrow (Slonaker, 1918; King & McLelland, 1985), and domestic fowl (Baumel et al., 1993).

The *N. trigeminus* (CN V) in both ostrich and emu have two main orbital branches, the *N. ophthalmicus* and *N. maxillaris*, which enter the orbit via the *For. n. ophthalmici* and *For. n. maxillomandibularis* respectively (present study). The latter has previously been described in the adult ostrich and emu (Crole & Soley, 2016) and in the ostrich embryo (Webb, 1957). In the present study, it was noted that the ophthalmic foramen is positioned caudally to the optic foramen in both species (present study). Similar descriptions have been provided in the adult ostrich (Parker, 1866; Crole & Soley, 2016), as well as in other avian species such as the sparrow (Slonaker, 1918), Tinamous, Cassowary and Greater Rhea (Parker, 1866).

The *For. n. ophthalmici* in both ostrich and emu is located dorsally to the *For. n. oculomotorii* and is smaller in the emu compared to the ostrich (Crole & Soley, 2016; present study). Upon entering the orbit, the ophthalmic nerve runs dorsal to the optic nerve (Deeming, 1999; Crole & Soley, 2016, present study) before proceeding ventral to the dorsal rectus muscle (Crole & Soley, 2016; present study). In the emu, it is evident that the ophthalmic nerve passed under the origin of the lateral rectus muscle before proceeding under the origin of the dorsal rectus muscle, however deviations were evident between specimens (present study). The description of the initial path of the ophthalmic nerve is similar in the ostrich and emu to that in the sparrow (Slonaker, 1918).

The ophthalmic nerve communicates with the ciliary ganglion ventral to the *vagina fibrosa tendinis* (present study). The ciliary ganglion is located posteriorly and ventro-rostrally in the ostrich embryo (Webb, 1957). The present study confirmed that this ganglion is located on the posterior sclera in both ostrich and emu, dorso-caudally to the proximal part of the optic nerve. The ciliary ganglion is positioned further rostral to the quadratus muscle insertion, in the emu compared to the ostrich (present study). This ganglion is well described in avian species (Baumel et al., 1993) such as the sparrow (Slonaker, 1918) and fowl (Baumel et al., 1993) and the contributing nerves (CN III and CN V) in these species are comparable to the ostrich (Webb, 1957; present study) and emu (present study).

In both species, the ophthalmic nerve continues rostrally and passes under the trochlear nerve before exiting the orbit, as is suggested in the sparrow (Slonaker, 1918; King & McLelland, 1985) and domestic fowl (Baumel et al., 1993). The ophthalmic nerve enters the maxilla through the orbitonasal foramen (Crole & Soley, 2016; present study) and innervates the nasal gland as it exits the orbit (Webb, 1957; Deeming, 1999; present study). The innervation to the nasal gland has been described in several avian species such as domestic fowl (Baumel et al., 1993). Before exiting the orbit, the ophthalmic nerve proceeds ventral to the dorsal oblique muscle (Crole & Soley, 2016; present study).

In both species, the ophthalmic nerve communicates with the facial nerve via the ethmoidal ganglion, ventral to the orbitonasal foramen (present study), as suggested in domestic fowl (Baumel et al., 1993). The latter differs from observations made in the ostrich embryo, where the sphenopalatine ganglion communicates directly with the ophthalmic nerve (Webb, 1957). The maxillary nerve of CN V, enters the orbit at its ventro-caudal margin in both the ostrich and emu (Webb, 1957; Crole & Soley, 2016; present study) via the maxillomandibular foramen. The latter foramen is common to avian species (Baumel et al., 1993). In the ostrich

and emu, the maxillary branches which course through the orbit, follow the same general pattern as described in the domestic fowl (Baumel et al., 1993).

In both species, the posteriorly directed dorsal ramus of the ophthalmic nerve, namely the *N. supraorbitalis* (Baumel et al., 1993; present study), is likewise evident in the ostrich embryo (Webb, 1957). The caudo-dorsal palpebral ramus of the supraorbital nerve in the ostrich and emu is comparable to domestic fowl (Baumel et al., 1993) and runs within the periorbital tissue in the dorso-caudal region of the anterior orbit (present study). The ventral branches of the supraorbital nerve, namely the infraorbital and nasopalatine nerves, in the ostrich and emu (present study) are comparable to domestic fowl, in that these branches innervate the caudal maxilla (Baumel et al., 1993). The supraorbital nerve proceeds from the maxillomandibular foramen to the middle of the interorbital septum in both species and terminates further ventrally in the emu compared to the ostrich (present study). The external mandibular adductor muscle is positioned caudally to the maxillary nerve as it enters the orbit, in the ostrich embryo (Webb, 1957), adult ostrich and emu (present study).

The maxillary nerve enters the antero-caudal orbit and proceeds between *M. pseudotemporalis superficialis* located posteriorly and the *M. adductor mandibulae externus* located anteriorly, before dividing into dorsal and ventral branches. The *N. nasopalatinus*, which is referred to as the lateral branch of the maxillary ramus in the ostrich embryo (Webb, 1957), proceeds along the medial aspect of the *Arcus jugalis*, before entering the maxilla and innervating the mucosa covering the mid to proximal *Os palatinum* in both ostrich and emu. Webb (1957) describes the latter nerve innervating the epithelium of the palate in the vomer region in the ostrich, which is likewise evident in the present study. In the emu, the nasopalatine nerve proceeds at a steeper angle before entering the maxilla compared to the ostrich, where it is evident that the nerve runs more horizontally from its origin.

In both species, the ventral *N. infraorbitalis* proceeds postero-ventrally over the *M. pseudotemporalis superficialis* before coursing along the ventrum of the posterior orbit where it enters the maxilla posteriorly to the *N. nasopalatinus* (present study). Similar observations were made by Webb (1957) in the ostrich embryo, in that the medial branch of the maxillary ramus innervates the epithelium of the posterior palate ventral to the pterygoid muscles.

The *N. abducens* (CN VI) innervates the lateral rectus muscle and both muscles of the nictitating membrane in both ostrich and emu (Webb, 1957; present study). It is commonly described in avian species that the abducent nerve innervates the lateral rectus muscle and the muscles of the nictitating membrane (Slonaker, 1918; King & McLelland, 1985; Jones,

2007). The abducent nerve enters the quadrate muscle at its anterior surface, adjacent and dorsal to the optic nerve (present study). The initial branch of the abducent nerve in the ostrich and emu innervates the lateral rectus before proceeding to the quadrate muscle and lastly the pyramidal muscle (present study), as is suggested in the sparrow (Slonaker, 1918) and domestic fowl (Baumel et al., 1993).

In the ostrich embryo, the ventral ramus of the abducent nerve innervates the lateral rectus muscle and the dorsal ramus innervates the muscles of nictitating membrane (Webb, 1957). The branching of the abducent nerve into a dorsal and ventral ramus was not obvious in the present study. It is evident in the ostrich and emu that the branch innervating the pyramidal muscle proceeds ventral to the optic nerve before entering the muscle (present study), which is also apparent in the ostrich embryo (Webb, 1957). The route of the abducent nerve differs in the sparrow (Slonaker, 1918; King & McLelland, 1985) and domestic fowl (Baumel et al., 1993), in that the branch innervating the pyramidal muscle runs dorsal to the optic nerve before entering the same muscle.

The *N. facialis* (CN VII) in ostrich and emu enters the orbit via the *Foramen n. facialis* which is positioned ventral to the *Foramen n. maxillomandibularis*, as is evident in other avian species, such as domestic fowl (Baumel et al., 1993). In both ostrich and emu, the *N. palatinus* of cranial nerve VII enters the orbit ventral to the *Foramen n. maxillomandibularis* before branching into a dorsal and ventral ramus, which is consistent with the observations made in the domestic fowl (Baumel et al., 1993). In both ostrich and emu (present study), the dorsal palatine ramus of the facial nerve proceeds dorsally from the posterior ventral orbit, as suggested in domestic fowl (Baumel et al., 1993). The dorsal palatine ramus proceeds along the dorsal border of the Harderian gland in both ostrich and emu, before contributing to the ethmoidal ganglion positioned dorso-rostrally to the gland.

In both ostrich and emu, the ventral palatine ramus courses along the ventral orbit (present study) and is assumed to communicate with the *Ganglion sphenopalatinum* as is evident in domestic fowl (Baumel et al., 1993). The sphenopalatine ganglion could however not be accurately identified in the present study in the ostrich or emu. The sphenopalatine nerve communicates with the ophthalmic nerve via the sphenopalatine ganglion in the ostrich embryo (Webb, 1957). It is evident in the ostrich and emu that the dorsal palatine ramus is in close communication with the ganglion located ventral to the orbitonasal foramen. This is assumed to be the ethmoidal ganglion as is evident in other avian species such as domestic fowl (Baumel et al., 1993). The emu differs in that the palatine nerve enters the orbit somewhat

dorsal compared to the ostrich and a *connexus* is present between the infraorbital nerve and the ventral palatine ramus at the insertion of *M. pseudotemporalis superficialis*.

2.5 Conclusion

The morphology of the *M. bulbi* (excluding attachments) and its innervation in the ostrich and emu follow the general avian pattern and is comparable to avian species such as the house sparrow, homing pigeon and Tinamous and domestic fowl. It is assumed that the attachments in the ostrich and emu follow the general avian pattern, however such information in avian species is scant. The attachments of the extrinsic ocular muscles in the ostrich and emu were therefore compared to the Tinamous, due to detailed information being available in this species. The attachments of the lateral rectus and pyramidal muscles in the ostrich and emu differ most from that in the Tinamous. In the ostrich and emu, the extrinsic ocular muscles appear to have a greater muscular component than that of the Tinamous. The insertion of the quadrate muscle in both species differ from the Tinamous in that it is not muscular, but collagenous, which emphasise the importance of the *vagina tendinis* as a robust support and pulley.

Despite the attachments of the *M. bulbi* in the ostrich and emu being similar, some morphological variation exists between the two species. The variation in the insertions of these muscles between the two species are greater compared to the respective origins. Further investigation is required to determine whether and to what extent the variation in the insertions of the *M. bulbi* between the ostrich and emu influences the rotation of the globe. Due to the smaller sized Harderian gland in the emu, the location of the extrinsic ocular muscles relative to this gland, differs to that in the ostrich.

The course of the cranial nerves through the orbit and the innervation to the *M. bulbi* in the ostrich and emu, follow the general avian pattern. The route of CN VI in both species however differs from that in other avian species such as the sparrow and domestic fowl. The innervation to the *M. bulbi* and the course of the cranial nerves through the orbit, are similar in the ostrich and emu. However minor differences are evident between the two species, in that the route of the *N. ophthalmicus*, *N. supraorbitalis*, *N. nasopalatinus* and *N. palatinus*, differ somewhat between the ostrich and emu. In both species, the locations of the *foraminae* referred to in the present study are similar, with minor differences noted.

It can thus be concluded that the morphology of the *M. bulbi* and associated nerves are comparable between the ostrich and emu, with minor differences noted. This implies that

similar surgical techniques could be performed during enucleation or other ocular surgeries in these two ratites.

2.6 References

ANSONS, A. M. & DAVIS, H. (2014) *Diagnosis and Management of Ocular Motility Disorders*. 4th ed. UK: John Wiley & Sons Ltd.

BAUMEL, J. J., KING, A. S., BREAZILE, A. E., EVANS, H. E. & VAN DEN BERGE, J. C. (1993) *Handbook of Avian Anatomy: Nomina Anatomica Avium*. 2nd ed. Cambridge, Massachusetts: Nuttall Ornithological Club.

BENJAMIN, M., KEISER, E. & MILZ, S. (2008) Structure-function relationships in tendons: a review. *Journal of Anatomy*, 212, 211-228.

BOCK, W.J. (1963) The cranial evidence for ratite affinities. *Proceedings XIII International Ornithological Congress*. Washington DC: American Ornithologists' Union.

CALVINO-CANCELA, M., DUNN, R.R., VAN ETTEN, E.J.B. & LAMONT, L.L. (2006) Emus as non-standard seed dispersers and their potential for long-distance dispersal. *Ecography*, 29, 632-640.

CHARD, R. D. & GUNDLACH, R. H. (1938) The structure of the eye of the homing pigeon. *Journal of comparative psychology*, 25, 2, 249–272.

COOPER, R. G., HORBANCZUK, J. O., VILLEGAS-VIZCAINO, R., SEBEI, S. K., MOHAMMED, A. E. F. & MAHROSE, K. M. A. (2010) Wild ostrich (*Struthio camelus*) ecology and physiology. *Tropical Animal Health and Production*, 42, 363–373.

COUES, E. (1868) Bird's Eye Views. *The American Naturalist*, 2, 10, 505-513.

CROLE, M.R. & SOLEY, J.T. (2016) Comparative morphology, morphometry and distribution pattern of the trigeminal nerve branches supplying the bill tip in the ostrich (*Struthio camelus*) and emu (*Dromaius novaehollandiae*). *Acta Zoologica*, 97, 1, 49-59.

DEEMING, D.C. (ed.) (1999) *The ostrich: Biology, Production and health*. London: CAB International.

ELZANOWSKI, A. (1987) Cranial and eyelid muscles of the Tinamous (Aves: *Tinamiformes*). *Zoologische Jahrbucher. Abteilung fur Anatomie und Ontogenie der Tiere*, 116, 63-118.

JONES, M. P., PIERCE, K. E. & WARD, D. (2007) Avian Vision: A Review of Form and Function with Special Consideration to Birds of Prey. *Journal of Exotic Pet Medicine*, 16, 2, 69-8.

KESTEVEN, H.L. (1942) The ossification of the avian chondrocranium, with special reference to that of the emu. *Proceedings of the Linnean Society of New South Wales*, 67,213–237.

KING, A.S. & MCLELLAND, J. (eds.) (1985) *Form and Function in Birds*. Volume 3. London: Academic Press.

MAC ALISTER, A. (1864) On the Anatomy of the Ostrich (*Struthio camelus*). *Proceedings of the Royal Irish Academy*, 1-24.

MAGGS, D. J., MILLER, P. E. & OFRI, R. (2008) *Slatter's Fundamentals of Veterinary Ophthalmology*. 4th Ed. Missouri, USA: Saunders Elsevier. 330-332.

MARTIN, G.R., ASHASH, U. & KATZIR, G. (2001) Ostrich ocular optics. *Brain Behavior and Evolution*. 58, 2, 115-120.

MARTIN, G.R. & KATZIR, G. (1995) Visual fields in ostriches. *Nature*, 374, 2 March.

MAXWELL, E. E., (2009) Comparative ossification and development of the skull in palaeognathous birds (Aves: *Palaeognathae*). *Zoological Journal of the Linnean Society*. 156, 184–200.

MILLER, R. E. & FOWLER, M. E. (eds.) (2015) *Fowler's Zoo and Wild Animal Medicine*. Volume 8. Missouri, USA: Elsevier. 77

MONFARED, A. L & BAKHTEYARI, Z. (2013). Some Gross Anatomical Features on Ostriches' Eye and its Application for Clinical Treatment of Ocular Abnormalities. *Global Veterinaria*, 11, 1, 76-79.

OROSZ, S. E. & BRADSHAW, G. A. (2007) Avian Neuroanatomy Revisited: From Clinical Principles to Avian Cognition. *Veterinary Clinics of North America Exotic Animal Practice*, 10, 775-802.

PARKER, W.K. (1866) On the Structure and Development of the Skull in the Ostrich Tribe. *Philosophical Transactions of the Royal Society of London*, 156, 113-183.

PREDOI, G., BELU, C., DUMITRESCU, I., GEORGESCU, B. & ROSU, P. (2007) Comparative aspects regarding the skull bones in nandu (*Rhea Americana*) and ostrich (*Struthio camelus*). *LUCRĂRI ȘTIINȚIFICE MEDICINĂ VETERINARĂ*, 135, 7, 750-753.

RITCHIE, B.W., HARRISON, G.J. & HARRISON, L.R. (1994) *Avian Medicine: Principles and Application*. Florida, USA: Wingers Publishing Inc.

SALES, J. (2007) The emu (*Dromaius novaehollandiae*): a review of its biology and commercial products. *Avian and Poultry Biology Reviews*, 18, 1, 1–20.

SLONAKER, J. R. (1918) Physiological study of the anatomy of the eye and its accessory parts of the English sparrow (*Passer domesticus*). *Journal of morphology*, 31, 351-459.

WEBB. M. (1957) The Ontogeny of the cranial bones, cranial peripheral and cranial parasympathetic nerves together with a study of the visceral muscles of *Struthio*. *Acta Zoologica*, 81-201.

2.6 Figures

Table 2.1: A comparison of the attachments of the *M. bulbi oculi* of the ostrich and emu.

<i>Musculi bulbi oculi</i>	Species	Origin	Insertion
i) <i>M. rectus dorsalis</i>	Ostrich	Caudo-dorsal margin of the <i>For. n. optici</i>	Dorsally, posterior to the equator
	Emu		
ii) <i>M. rectus ventralis</i>	Ostrich	Ventral margin of the <i>For. n. optici</i>	Ventro-rostrally, anterior to the equator
	Emu	Ventro-rostrally	Ventro-rostrally, on
iii) <i>M. rectus lateralis</i>	Ostrich	Caudo-ventral margin of the <i>For. n. optici</i>	Obliquely caudally, on the equator
	Emu		Directly
iv) <i>M. rectus medialis</i>	Ostrich	<i>Septum interorbitale</i> , dorso-rostrally to the <i>For. n. optici</i>	Rostrally, posterior to the equator
	Emu		
v) <i>M. obliquus dorsalis</i>	Ostrich	<i>Os ectethmoidale</i> , caudoventral to the <i>For. orbitonasale</i>	Obliquely on the dorsal sclera, posterior to the equator, deep to the <i>M. rectus dorsalis</i> , and covered the <i>M. quadratus membranae nictitantis</i>
	Emu		
vi) <i>M. obliquus ventralis</i>	Ostrich	<i>Os ectethmoidale</i>	Obliquely on the ventral sclera, anterior to the equator and covered the pyramidal muscle and superficial to the <i>M. rectus ventralis</i>
	Emu		
vii) <i>M. quadratus membranae nictitantis</i>	Ostrich	Dorsally, posterior to the equator, on the posterior sclera	Proximal tendon of the pyramidal muscle, dorsal to CN II
	Emu		
viii) <i>M. pyramidalis membranae nictitantis</i>	Ostrich	Ventro-rostrally, on the equator	Ventral free margin of the nictitating membrane
	Emu	Ventro-rostrally, posterior to	

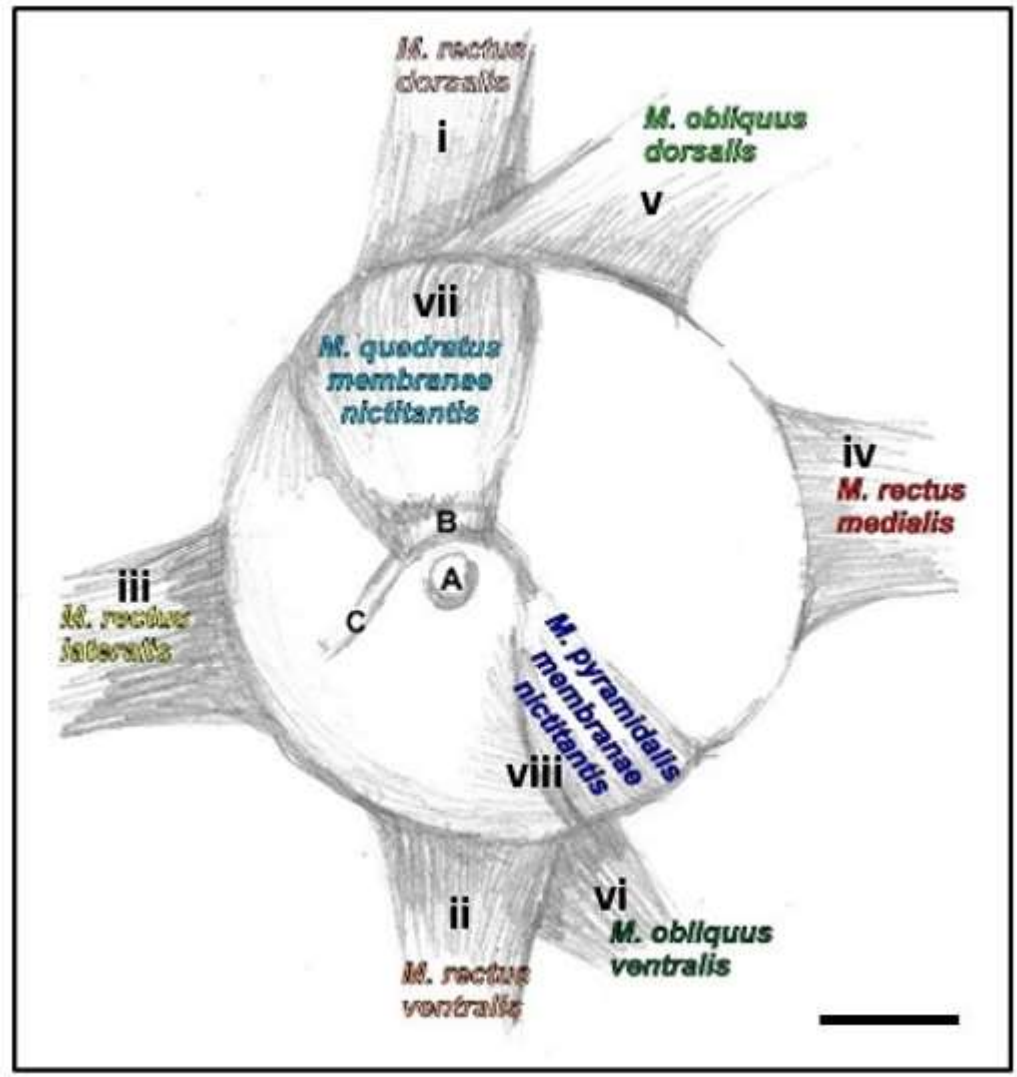


Figure 2.1: A schematic drawing of the left emu eye demonstrating the *M. bulbi oculi*. Posterior view. The extrinsic ocular muscles have been reflected. *N. optici* (cut) (A), *vagina fibrosa tendinis* (B) and *tendo m. pyramidalis* (C) (cut). Scale bar = 1 cm.

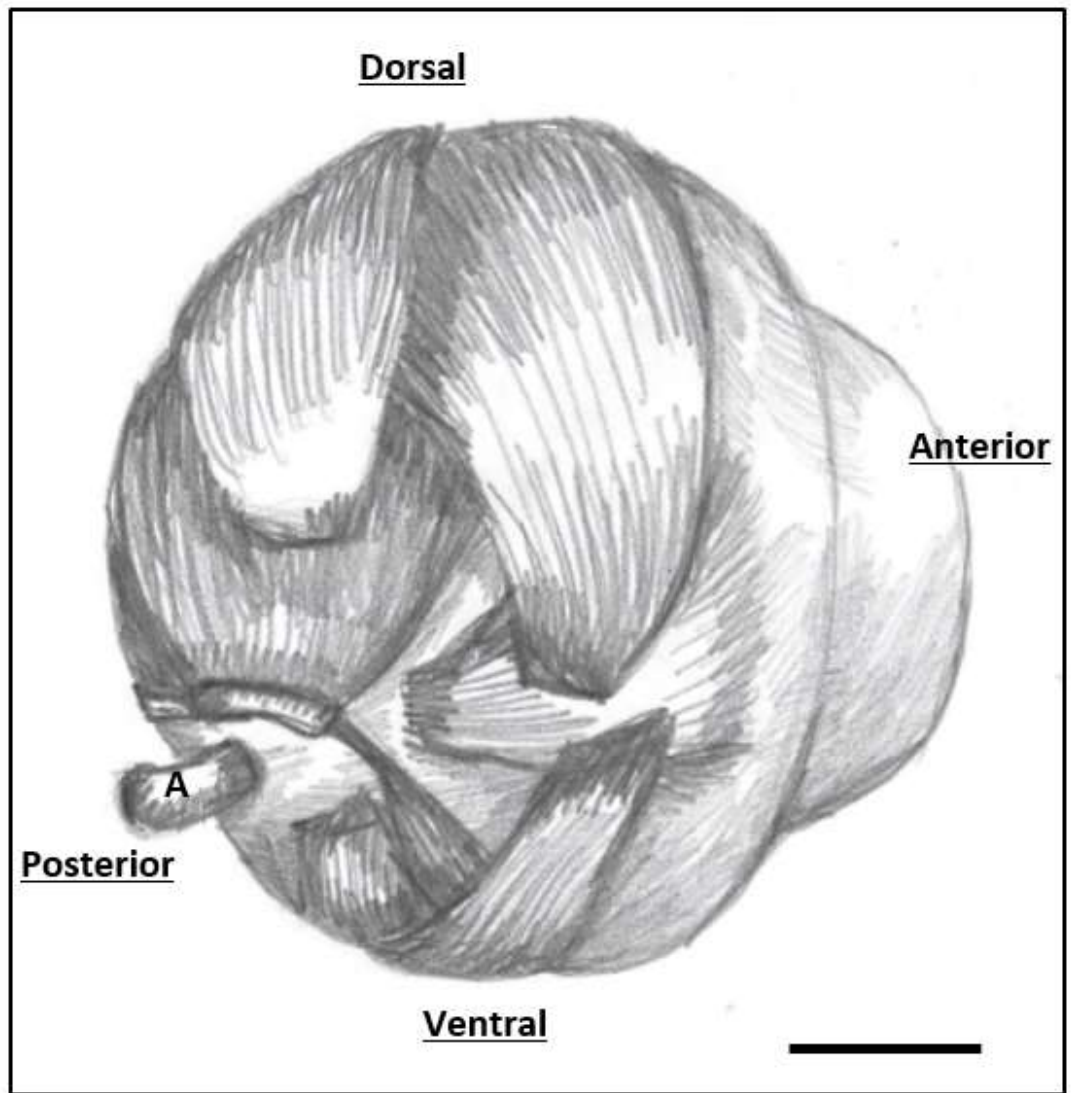


Figure 2.1.1: A schematic drawing of the left emu eye demonstrating the anatomical descriptions relevant to the globe. Note the cornea of the eye is positioned anteriorly in respect to the *N. optici* (cut) (A), which is located posteriorly. The extrinsic ocular muscles have been transected at origin. Scale bar = 1 cm.

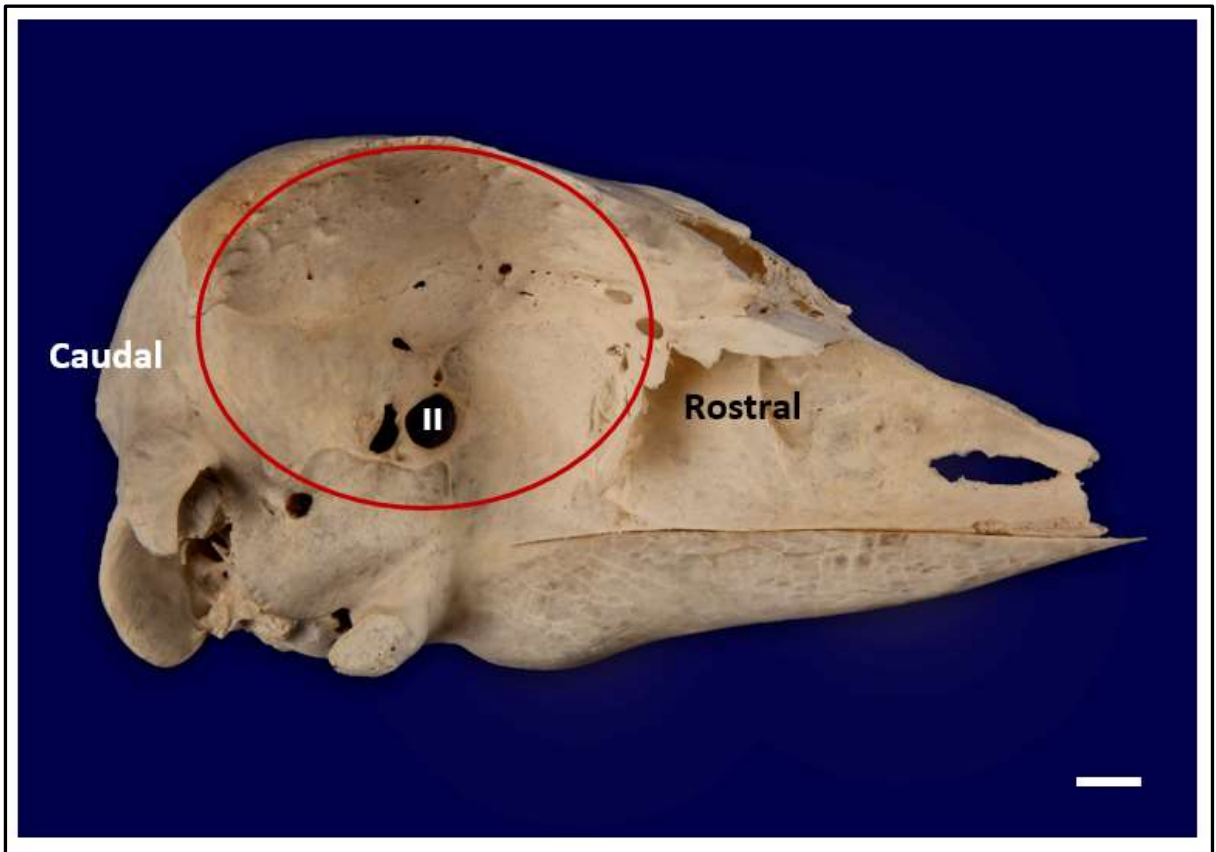


Figure 2.1.2: Right lateral view of the ostrich cranium, demonstrating the anatomical descriptions relevant to the orbit. The anterior orbital region is demarcated (red circle). Note the lateral orientation of the orbit within the cranium. The *Foramen n. optici* (II), located in the posterior orbit and the rostral and caudal extent of the orbit is noted. Scale bar = 1 cm.



Figure 2.2: Left eye of the ostrich (Left) and emu (Right), demonstrating the *M. bulbi oculi*. Posterior view. The extrinsic muscles have been reflected. *N. optici* (cut) (A), *vagina fibrosa tendinis* (B) and *tendo m. pyramidalis* (cut) (C). Coloured markers as well as numerals i to viii, correspond to Figure 2.1. Scale bar = 1 cm.

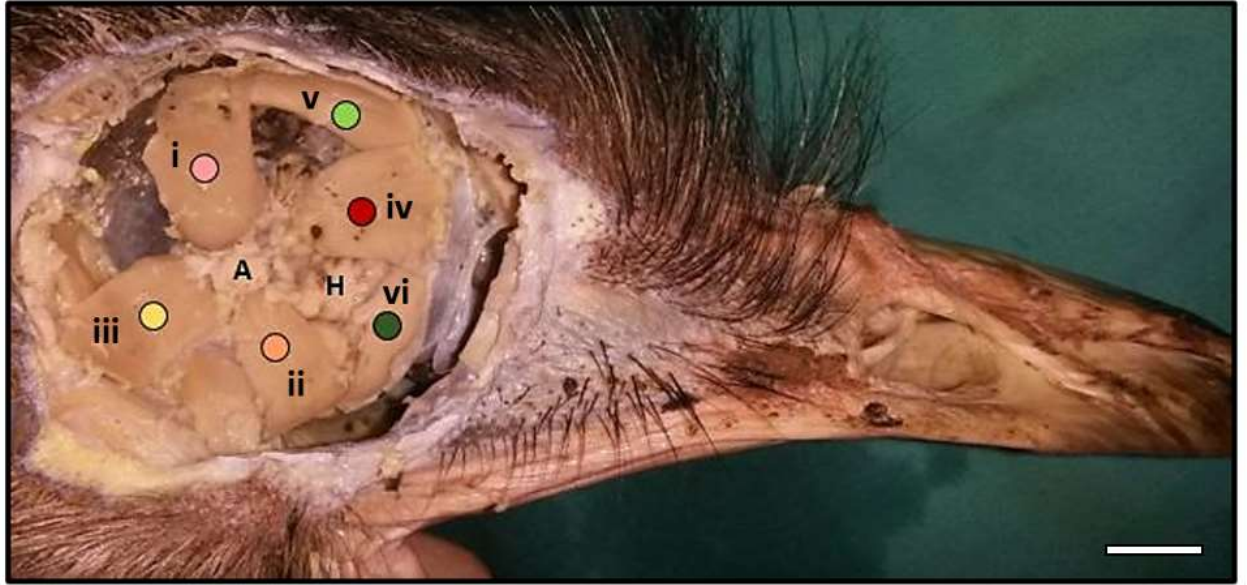


Figure 2.3: Right lateral view of the ostrich orbit. Extrinsic muscles of the eye have been transected near their insertions, the optic nerve cut and the globe removed. *N. optici* (A) and Harderian gland (H). Coloured markers as well as numerals i to viii, correspond to Figure 2.1. Scale bar = 1 cm.

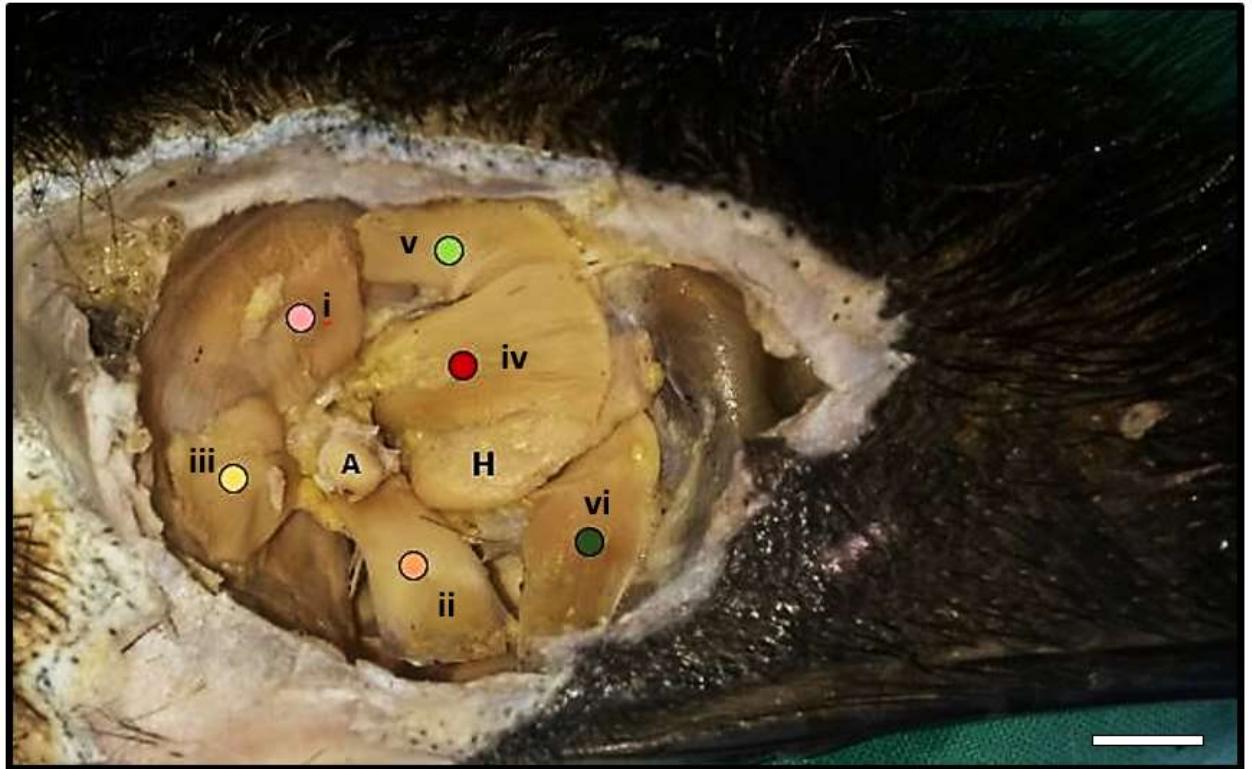


Figure 2.4: Right lateral view of the emu orbit. Extrinsic muscles of the eye have been transected near their insertions, the optic nerve cut and the globe removed. *N. optici* (A) and Harderian gland (H). Coloured markers as well as numerals i to viii, correspond to Figure 2.1. Scale bar = 1 cm.

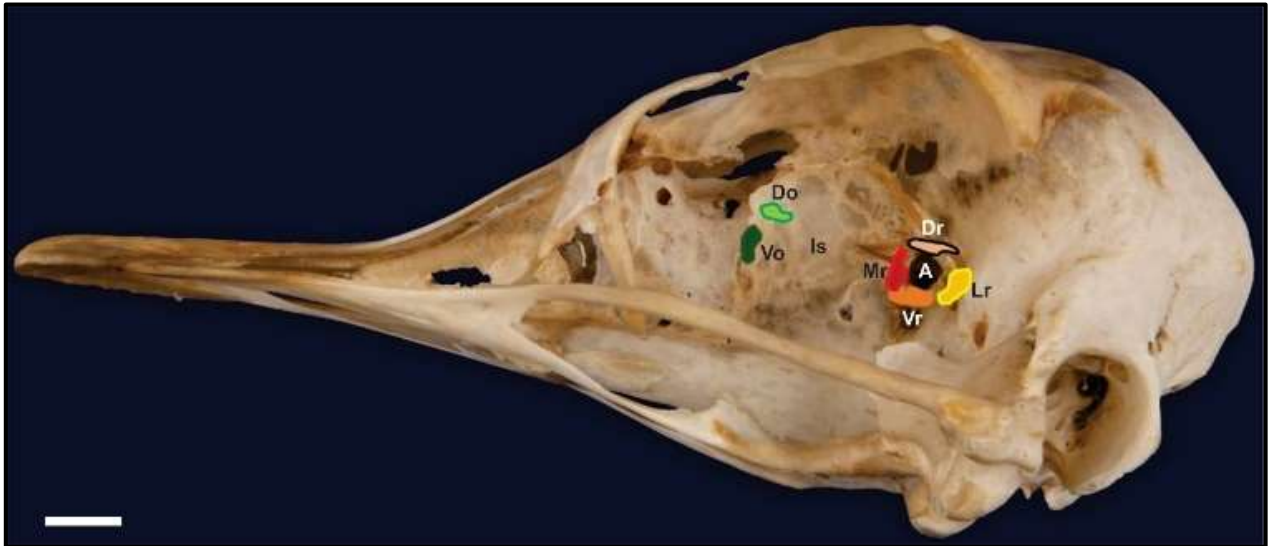


Figure 2.5: Ostrich cranium. Left lateral view. Origins of the extrinsic muscles of the eye. Dorsal oblique (Do), Ventral oblique (Vo), Dorsal rectus (Dr), Lateral rectus (Lr), Ventral rectus (Vr) and Medial rectus (Mr) muscles. Interorbital septum (Is), *For. n. optici* (A).
Scale bar = 1 cm.

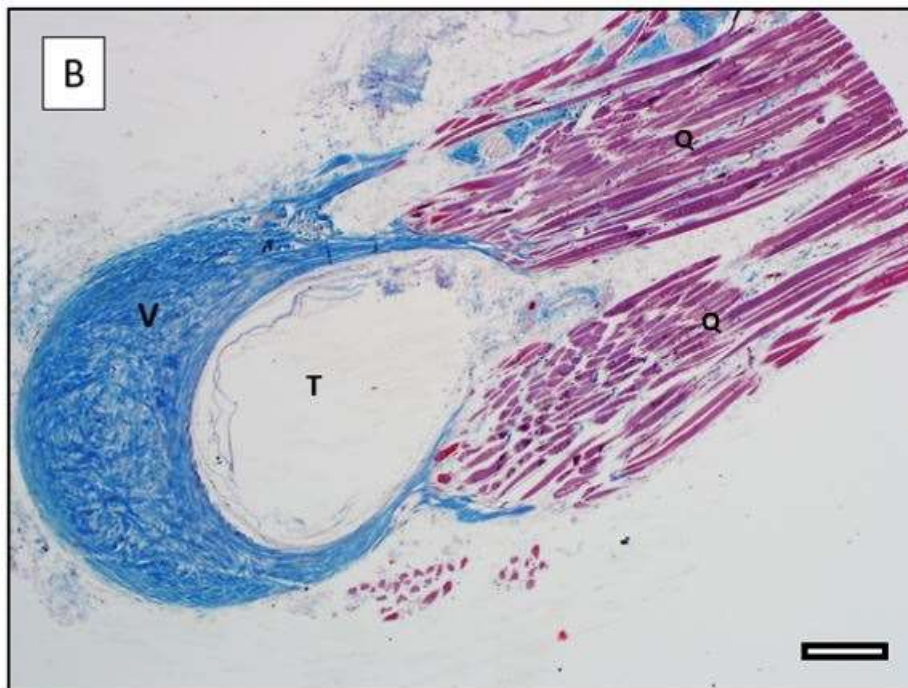
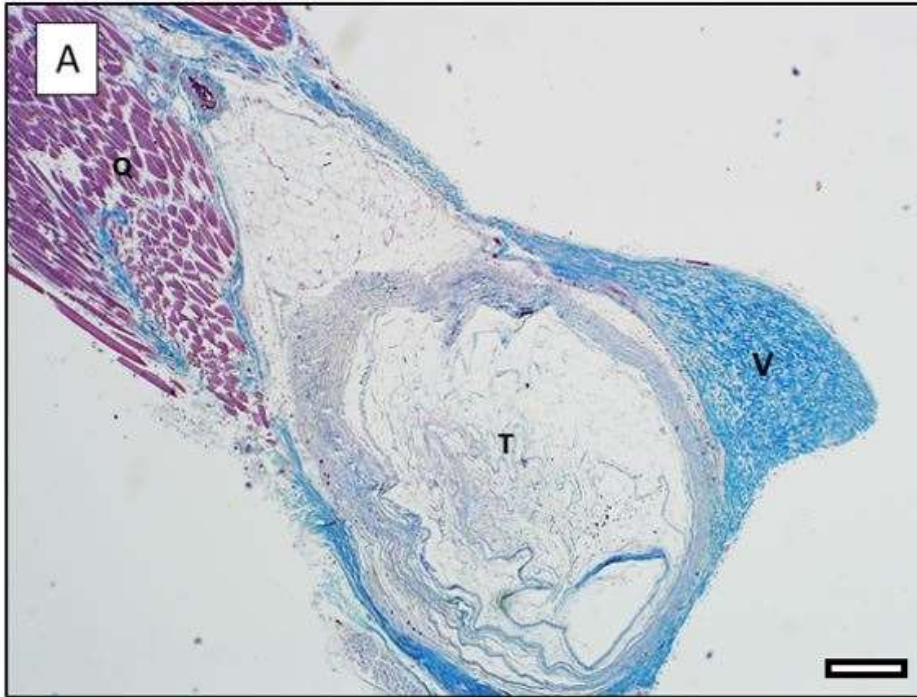


Figure 2.6: A transverse section of the *vagina tendinis* (V) of the quadrate muscle (Q) in the ostrich (A) and emu (B), stained with Masson Trichrome. Note the collagen and muscle fibres are stained blue and red respectively. The location of the *tendo m. pyramidalis* (T) relative to the quadrate muscle, is indicated. Scale bar = 200 μm .

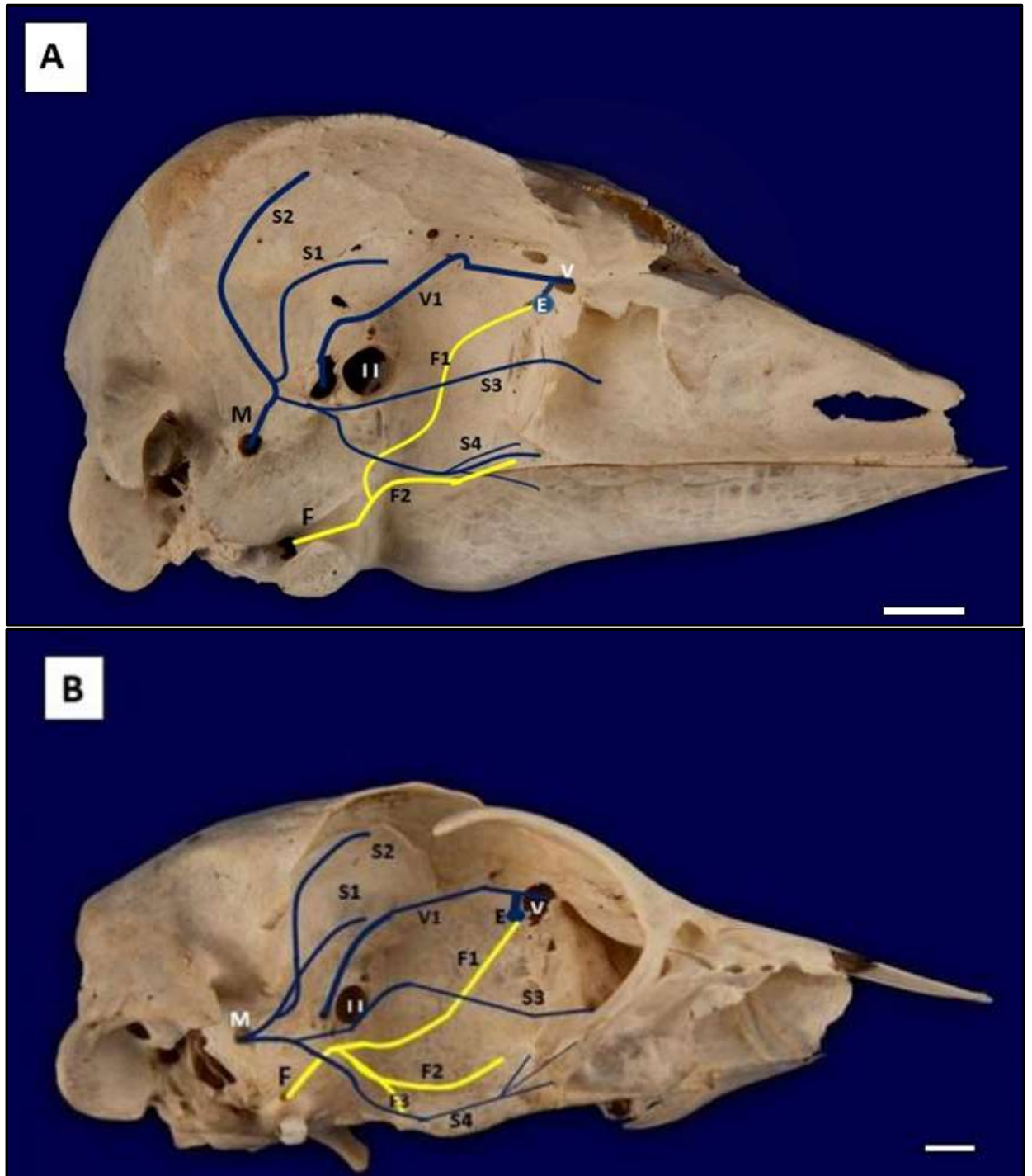


Figure 2.7: Right lateral view of an ostrich (A) and emu (B) cranium, and a schematic representation of the branches of CN V and VII within the orbit. *N. maxillaris* (M) after exiting the *For. maxillomandibularis*, branches into *N. supraorbitalis* (S1) which further branches into a *R. palpebralis* (S2), *N. nasopalatinus* (S3) and *N. infraorbitalis* (S4). The *N. palatinus* of the *N. facialis* after exiting the *For. n. facialis*, branches into a dorsal (F1) and ventral (F2) ramus. A *connexus* (F3) between F2 and S4, is present in the emu. *Foramen n. optici* (II); *Foramen orbitonasale* (V); *N. ophthalmicus* (V1); *Ganglion ethmoidale* (E). Scale bar = 0.5 cm.

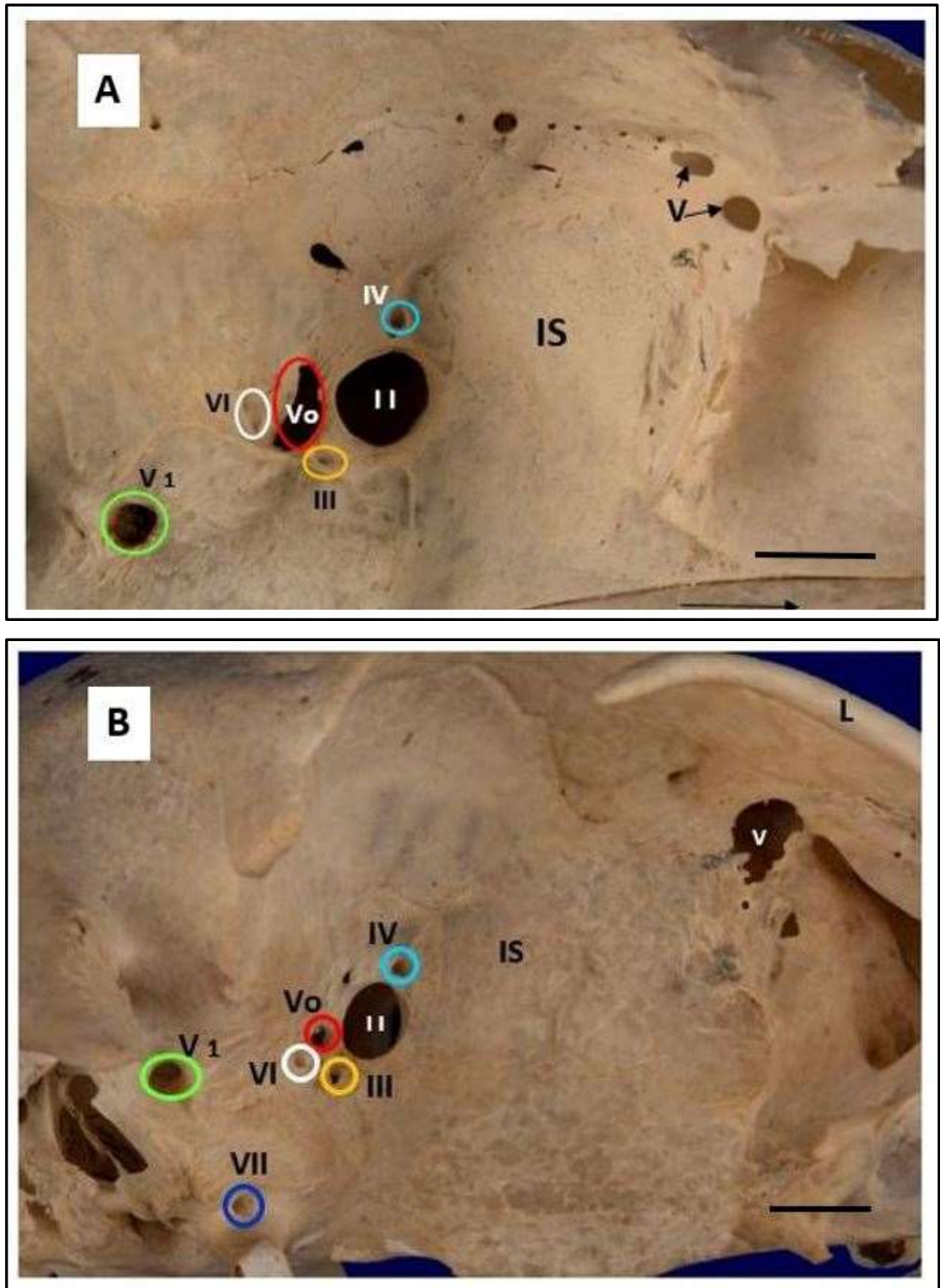


Figure 2.8: Right lateral view of an ostrich (A) and emu (B) showing the *foraminae* of CN II to CN VII within the orbit. *Os lacrimale* (L), *Septum interorbitale* (IS), *For. n. optici* (II), *For. n. oculomotorii* (III), *For. n. trochlearis* (IV), *For. n. ophthalmici* (Vo), *For. n. abducentis* (VI), *For. n. facialis* (VII), *For. N. maxillomandibularis* (V1), *For. orbitonasale* (V). Scale bar = 1 cm.

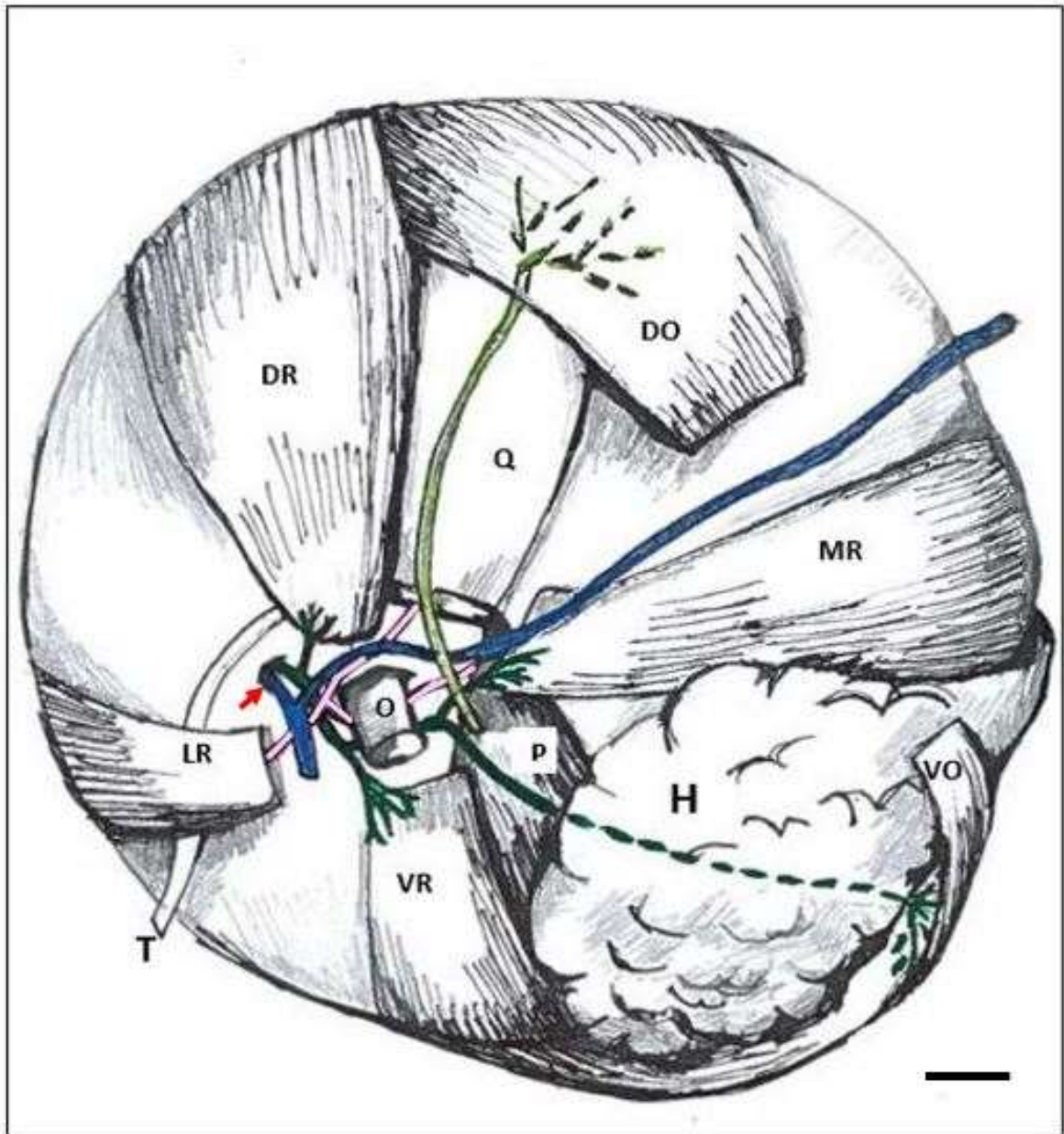


Figure 2.9: Posterior view of the left eye of the Ostrich after enucleation, showing the *M. bulbi oculi* (cut at origin) and its innervation. All cranial nerves were transected at the optic foramen and the tendon of the pyramidal, distally. *M. rectus dorsalis* (DR), *M. rectus ventralis* (VR), *M. obliquus dorsalis* (DO), *M. obliquus ventralis* (VO), *M. rectus lateralis* (LR), *M. rectus medialis* (MR), *M. quadratus membranae nictitantis* (Q), *M. pyramidalis membranae nictitantis* (P), Harderian gland (H), *Tendo. m. pyramidalis* (T), *Ganglion ciliare* (red arrow). Nerves: CN II (O), CN III (dark green), CN IV (light green), CN V (*N. ophthalmicus* cut at origin and distally - blue), CN VI (pink). Scale bar = 1 cm.

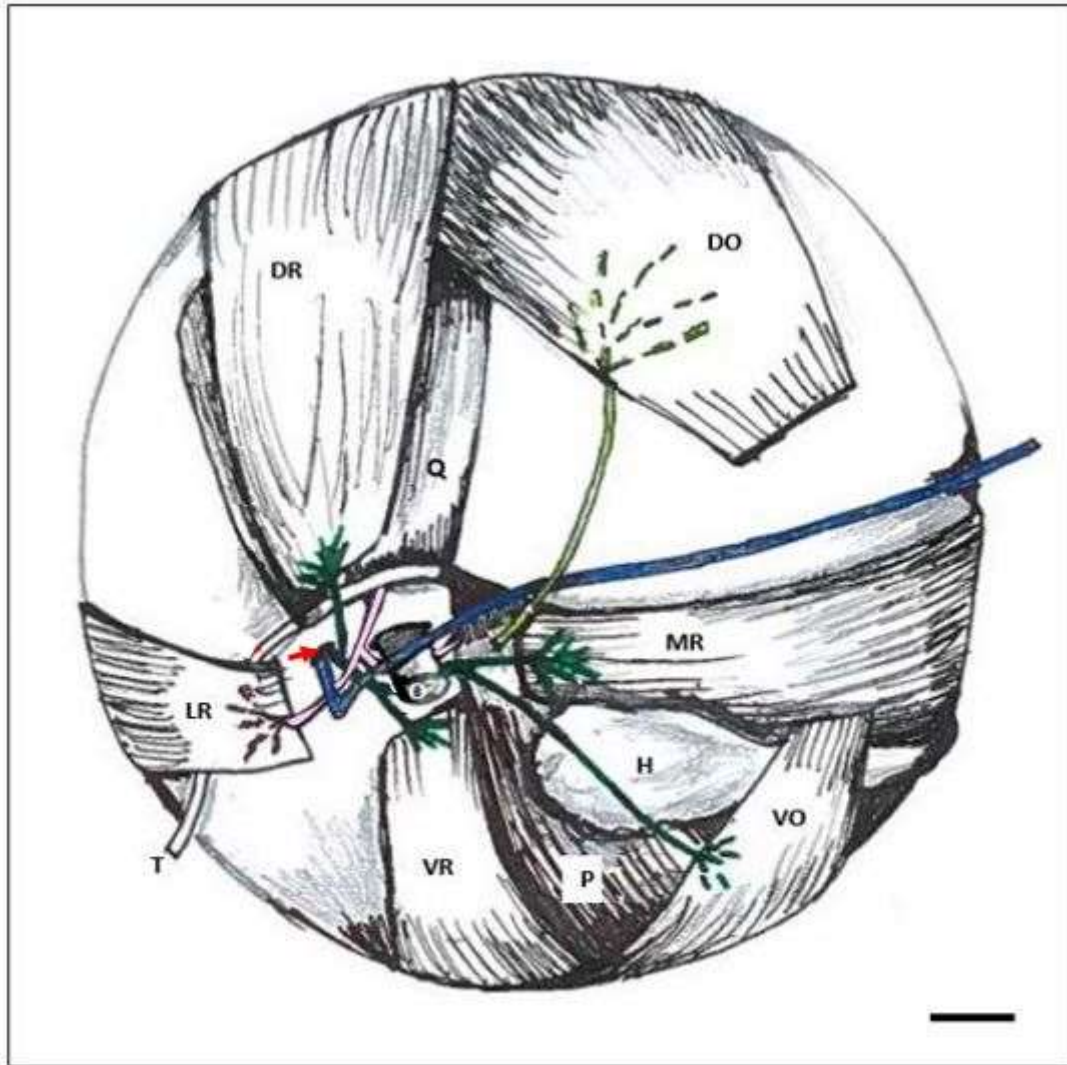


Figure 2.10: Posterior view of the left eye of the emu showing the *M. bulbi oculi* (cut at origin) and its innervation. All cranial nerves were transected at the optic foramen and the tendon of the pyramidal, distally. *M. rectus dorsalis* (DR), *M. rectus ventralis* (VR), *M. obliquus dorsalis* (DO), *M. obliquus ventralis* (VO), *M. rectus lateralis* (LR), *M. rectus medialis* (MR), *M. quadratus membranae nictitantis* (Q), *M. pyramidalis membranae nictitantis* (P), Harderian gland (H), *Tendo. m. pyramidalis* (T), *Ganglion ciliare* (red arrow). Nerves: CN II (O), CN III (dark green), CN IV (light green), CN V (*N. ophthalmicus* cut at origin and distally - blue), CN VI (pink). Scale bar = 1 cm.

CHAPTER 3

Morphometric characteristics of the *M. bulbi oculi* in the ostrich (*Struthio camelus*) and emu (*Dromaius novaehollandiae*).

3.1 Introduction

Morphometry is referred to as the dimensions of an object or the measurements of curvatures and the angles pertaining to an object (Pearsall, 2002). The data is used to calculate the functional properties of an object (Biewener, 2003; Payne et al., 2005; Hill et al., 2008). The volume, mass, length and density of a particular muscle can be used to calculate the isometric force it exerts (Biewener, 2003; Payne et al., 2005; Hill et al., 2008). The power generated by a muscle is related to the isometric force it exerts and its maximum contractile velocity (Biewener, 2003; Payne et al., 2005; Hill et al., 2008). Such data is useful in interpreting its functional properties.

Form and function in avian species has been extensively studied in neognathous species, such as *Passeriformes*, *Anseriformes*, *Galliformes* and *Psittaciformes* (King & McLelland, 1985; Baumel et al., 1993). The functionality of locomotory muscles has been explored in several neognathous species (Bennett, 1996; Tobalske, 2007; Meyers & McFarland, 2016). Examples include the contractile velocity, power as well as force generated by flight muscles in the cockatiel (*Nymphicus hollandicus*) (Biewener, 2003, 2011; Morris & Askew, 2010), golden eagle (*Aquila chrysaetos*) (Meyers & McFarland, 2016), bald eagle (*Haliaeetus leucocephalus*) (Meyers & McFarland, 2016), ring-neck dove (*Streptopelia risoria*) (Biewener, 2003), domestic pigeon (*Columba livia*) (Biewener, 2003), and mallard duck (*Anas platyrhynchos*) (Biewener, 2003). Morphometric studies on the locomotory muscles of avian species, are numerous in comparison to other functional muscle groups such as the extrinsic ocular muscles (*Musculi bulbi*) (Slonaker, 1918; Chard & Gundlach, 1937; Elzanowski, 1987; King & McLelland, 1985.).

Extraocular muscles allow for drifts, flicks, oscillations and tremors of the globe which ensure accurate focus of an image onto the retina when an object is viewed at close proximity, for example during foraging (King & McLelland, 1985). Avian species do not only rely on eye movements (effected by the *M. bulbi*) when observing their environment, grooming, foraging or flying, rather their light weight skull and flexible neck, allow for rapid, full range of movement

of the head (King & McLelland, 1985). Extrinsic ocular muscles are thin and allow limited movement of the large globe, as it is fitted tightly in the orbit of avian species (King & McLelland, 1985). The mean bulbar axial length of the ostrich is 38 mm (Martin et al., 2001) and is notably large, however it resembles the axial lengths recorded in albatross species (*Diomedea melanophris* and *Diomedea chrysostoma*) and the wedge-tailed eagle (*Aquila audax*) (Martin et al., 2001).

The ostrich eye is globose in shape (Martin et al., 2001), binocular vision is restricted and blind areas are present above and towards the back of the head (Martin & Katzir, 1995). This field of vision may be a protective mechanism against harsh sunlight that the ostrich is exposed to (Martin & Katzir, 1995). Studies have been conducted on the visual field of the ostrich (Martin & Katzir, 1995; Martin et al., 2001), as well as its ocular and cranial anatomy (Mac Alister, 1864; Parker, 1866; Webb 1957; Deeming, 1999). However scant in comparison, studies in the emu include; cranial osteology (Kestevens, 1942; Webb, 1957; Predoi et.al., 2007; Crole & Soley; 2016), retinal photoreceptors and *Pecten oculi* (Braekevelt, 1998; Hart et al., 2016).

A morphometric analysis to determine the power of the extrinsic eye muscles in the ostrich and emu will aid in understanding their functional significance. This will be of value in informing clinical procedures performed on the ostrich and emu eye. Both ratite species are of commercial importance and a functional eye is necessary to thrive. A thorough insight into the functional significance of the various muscles, could be of relevance in diagnosing and treating ophthalmological cases.

3.2 Materials and methods

Ten sub-adult (approximately 12 months old) ostrich (Klein Karoo Ostrich abattoir, Oudtshoorn, Western Cape, South Africa) and ten sub-adult (approximately 12 months old) emu (Oryx Abattoir, Krugersdorp, Gauteng, South Africa; Emu Ranch, Rustenburg, North-West Province, South Africa) heads from either sex were collected (protocol V066/ 11; V023/ 06), after slaughter of the birds for commercial use.

The heads were immersion fixed in 10% neutral-buffered formalin and stored in the University of Pretoria, Faculty of Veterinary Science's Anatomy department formalin tanks. The methods described below was that used for both species. To expose the globe, a circum-orbital incision was performed and the eyelids removed. To expose the globe, peri-orbital connective tissue was transected and removed, and the extrinsic ocular muscles transected at their respective origins.

The optic nerve was transected at the optic foramen, distal to this nerve's exit point from the globe. The entire globe was then removed from the orbit. In the present study the terms, quadrate muscle and *M. quadratus membranae nictitantis*, were used interchangeably. Pyramidal muscle was used in reference to the *M. pyramidalis membranae nictitantis*.

Excess connective tissue, nerves and blood vessels were removed from the globe, before the globe was placed in a measuring cylinder (Plasti 500 ml: 5 ml) and filled with 200 ml water. The volume of each globe (cm³) was calculated according to the amount of water displaced (mm). The volume of each globe was used to compare the means between species while adjusting for globe volume in order to compensate for the size variation in the two species.

The calculations and methodology recorded by Payne et al. (2005), were used as a model to determine the isometric force generation (Fmax), maximum contractile velocity (Vmax) and the power of each extrinsic eye muscle in both the ostrich and the emu. The following measurements were made in millimetres by using a digital calliper (Workzone GT-DC-02, Germany) and converted to centimeters before tabulating the values.

After transecting each muscle at its insertion, ten longitudinal incisions were made in the muscle belly, the length of each muscle fascicle measured and average of the ten measurements calculated. The pennation angle was calculated by measuring the angle between the muscle fascicles and the aponeurosis of its respective tendon (Payne et al., 2005). A protractor was used to determine the pennation angle. Tendon length was measured from its insertion point on the globe to the point where the muscle fascicles ended. Due to the variability in the tendo-muscular junction, three measurements were recorded for each tendon and the average used. The length of the tendon of the quadrate muscle was multiplied by two, as it looped around the tendon of the pyramidal muscle.

The maximum contractile velocity of each muscle was calculated by multiplying each average muscle fascicle length (meters) by a temperature constant (contractile velocity at 40 °C). The muscle fibre type was also taken into consideration. The fibres executing high velocity oscillatory motion and slow, low tension movement are type II and I fibres, respectively (Biewener, 2003; Briggs & Schachat, 2002), which are further sub-categorised (Biewener, 2003). The properties of avian locomotory muscle, as well as muscle fibre type related to function, maximum contractile velocity and posture, has been well documented (Meyers & McFarland, 2016) in comparison to the avian *M. bulbi*. The extrinsic ocular muscles in mammals and rodents are comprised of a mixture of these fibre types (Mayr, 1971, 1975; Briggs & Schachat, 2002; Rashed et al., 2010), which is also evident in the pigeon's medial

rectus muscle (Alvarado-Mallart, 1972). Thus, V_{max} was calculated according to the method used by Payne et al. (2005) and thus assuming that the extrinsic ocular muscles studied consist primarily of type IIA muscle fibres.

The maximum contraction velocity (V_{max}) of equine soleus muscle (muscle fascicle lengths per second) at 15 °C, is 1.33 (Payne et al., 2005). V_{max} is therefore calculated by multiplying muscle fascicle length by the temperature constant. The average body temperature of the ostrich is 39 to 40 °C (Deeming, 1999) which is approximately 2 °C higher than that in the horse (Gore et al., 2008). For every 10 °C rise in body temperature, the contraction velocity of muscle doubles (Payne et al., 2005). Thus, a new temperature constant was determined as follows: 15 °C = 1.33; 25 °C = 2.66; 35 °C = 5.32; 40 °C = 7.6). The V_{max} of each muscle was determined by multiplying the respective fascicle length (m) by 7.6.

A scalpel blade was used to separate the muscle from the tendon and thereafter each muscle weighed and the mass recorded in grams. A digital scale (New Classic MF, MS 4035 /01, Mettler Toledo) was used to determine the weight of all the muscles. Maximum isometric force generated by each muscle was calculated by multiplying the cross-sectional area of each muscle (muscle volume in cm^3 divided by fascicle length in cm) by the isometric stress constant of 0.3 MPa. The F_{max} , measured in Newtons (N), was multiplied by 100 to obtain centi-Newtons (cN). Payne et al. (2005) considered a pennation angle of more than twenty degrees to be significant. The cos of the pennation angle was multiplied by the cross-sectional area of the respective muscle in order to calculate the F_{max} (Payne et al., 2005).

In this study, $\cos(0^\circ)$ or $\cos(180^\circ)$ equals 1 and -1 respectively and thus the pennation angle was not included in calculating F_{max} as it had negligible effect on the result obtained. The volume of each muscle in cm^3 , was calculated by dividing its average mass in grams by the mammalian and avian muscle density constant of 1.12 g/cm^3 , as indicated by Bennett (1995, 1996) and Payne et al. (2005). The following formula used by Payne et al., (2005) was used in this study to calculate the power generated by each muscle (measured in Watts): $[(F_{max})(V_{max})] / 10$. The answer obtained was converted to micro-Watts (μW) by multiplying the value calculated in Watts, by one million. The power generated by the most powerful muscles were converted to μW per 0.5g by using the following formula: $(\mu\text{W} \cdot 0.5) / \text{muscle mass}$.

The muscle to tendon ratio was calculated by adding the average tendon length and fascicle length for each muscle. Thereafter it was determined what percentage of the muscle is comprised of tendon and of muscle fascicles respectively. The two percentages were then compared for each muscle. Mean, standard deviation, median and range of each parameter

were calculated in the ostrich and emu for each extrinsic ocular muscle. Normality was assessed using the Shapiro-Wilk test. The mean of each outcome was compared between species for each muscle using analysis of variance (ANOVA). Analysis of covariance (ANCOVA) was then used to compare the means between species while adjusting for the globe volume. The Bonferroni adjustment was used for comparing each parameter of each extrinsic ocular muscle in the two species. Statistical significance was assessed at $P < 0.05$. Statistical analyses were performed using Stata 14.2 (Stata Corp, College Station, TX, U.S.A.). In the present study, the term "significance" was used in reference to a statistically significant value.

3.3 Results

3.3.1 Globe volume

The average globe volume, calculated by the amount of water displaced, was 38 cm³ in the ostrich and 19 cm³ in the emu. Thus, the average volume of the eye globe in the ostrich was twice that of the emu (Table 3.1).

3.3.2 Muscle fascicle length

The mean fascicle length of the *M. bulbi* varied between 2.87 ± 0.21 and 2.35 ± 0.21 cm in the ostrich and 2.29 ± 0.28 and 1.84 ± 0.22 cm in the emu (Table 3.2). The longest and shortest muscles in the ostrich were the dorsal oblique and dorsal rectus muscles, respectively (Table 3.2). In the emu, the pyramidal was the longest and the ventral rectus the shortest muscle (Table 3.2). When unadjusted for globe volume there was a significant difference in the fascicle length of each muscle between the two species as the P-values obtained were below 0.05 (Table 3.3). However, when adjusted for globe volume, only the length of the dorsal oblique ($P < 0.05$) was significantly longer in the ostrich compared to that in the emu (Table 3.3).

3.3.3 Maximum velocity

The mean maximum contractile velocity of the extrinsic ocular muscles varied between 0.22 ± 0.02 and 0.18 ± 0.02 m/s in the ostrich and 0.17 ± 0.02 and 0.14 ± 0.02 m/s in the emu (Table 3.4). The muscles with the greatest contractile velocity were the dorsal oblique and pyramidal muscle, in the ostrich and emu respectively (Table 3.4). A maximum contractile velocity of 22 cm/s was obtained for the dorsal oblique muscle in the ostrich (fascicle length

of 3 cm) and 17 cm/s for the pyramidal muscle in the emu (fascicle length of 2 cm). The maximum contractile velocities of the dorsal oblique and pyramidal muscles were also expressed as 7 and 9 muscle fascicle lengths per second, respectively.

The dorsal rectus muscle in the ostrich and ventral rectus muscle in the emu displayed the lowest maximum contractile velocity (Table 3.4). When unadjusted for globe volume there was a significant difference in the maximum contractile velocity of each muscle between the two species, as the P-values obtained were below 0.05 (Table 3.5). However, when adjusted for globe volume, only the maximum contractile velocity of the dorsal oblique ($P < 0.05$) was significantly larger in the ostrich compared to that in the emu (Table 3.5).

3.3.4 Muscle mass

The mean muscle mass of the *M. bulbi* varied between 0.66 ± 0.04 and 0.29 ± 0.03 g in the ostrich and 0.30 ± 0.09 and 0.13 ± 0.04 g in the emu (Table 3.6). The heaviest muscles were the quadratus and medial rectus muscles, in the ostrich and emu respectively (Table 3.6). The pyramidal muscle of the nictitating membrane and the oblique ventral muscle were the lightest of the *M. bulbi* in the ostrich and emu respectively (Table 3.6). When unadjusted for globe volume, P-values of less than 0.05 were obtained for all of the muscles, thus indicating that muscle mass differed significantly between the two species (Table 3.7). However, when adjusted for globe volume all extrinsic ocular muscles, except for the ventral oblique and pyramidal muscles, had P values of less than 0.05, and were thus significantly heavier in the ostrich compared to those in the emu (Table 3.7).

3.3.5 Muscle cross-sectional area

The mean muscle cross sectional area varied between 0.24 ± 0.02 and 0.10 ± 0.02 cm² in the ostrich and 0.14 ± 0.04 and 0.05 ± 0.01 cm² in the emu (Table 3.8). The muscles with the greatest cross-sectional area were the quadratus and medial rectus muscles, in the ostrich and emu respectively (Table 3.8). The pyramidal muscle displayed the smallest cross-sectional area in both species (Table 3.8). P-values of less than 0.05 were obtained for all muscles, irrespective of being adjusted for globe volume or not (Table 3.9). Thus, the cross-sectional area of each muscle was significantly greater in the ostrich compared to that in the emu.

3.3.6 Maximum isometric force

The mean isometric force exerted by the extrinsic ocular muscles varied between 7.01 ± 0.55 and 3.04 ± 0.21 cN in the ostrich and 4.07 ± 1.24 and 1.54 ± 0.38 cN in the emu (Table 3.10). The *M. quadratus membranae nictitantis* and *M. rectus medialis* exerted the greatest force, in the ostrich and emu respectively (Table 3.10). The pyramidal muscle exerted the smallest force in both species (Table 3.10). P-values of less than 0.05 were obtained for all the muscles, irrespective of being adjusted for globe volume or not (Table 3.11). Thus the maximum isometric force generated by each muscle was significantly greater in the ostrich compared to that in the emu.

3.3.7 Muscle volume

The mean volume of the *M. bulbi* varied between 0.63 ± 0.04 and 0.27 ± 0.03 cm³ in the ostrich and 0.29 ± 0.09 and 0.12 ± 0.03 cm³ in the emu (Table 3.12). The muscles with the greatest volume were the quadratus muscle in the ostrich and medial rectus muscle in the emu (Table 3.12). The pyramidal muscle had the smallest volume in both species (Table 3.12). When unadjusted for globe volume, P-values of less than 0.05 were obtained for all muscles, thus indicating that muscle volume differed significantly between the two species (Table 3.13). However, when adjusted for globe volume all extrinsic ocular muscles, except for the ventral oblique and pyramidal muscles, had P-values of less than 0.05, and thus had a significantly greater volume in the ostrich compared to the emu (Table 3.13).

3.3.8 Muscle power

The power exerted by the extrinsic ocular muscles varied between 1405.83 ± 86.88 and 607.08 ± 64.67 μ W in the ostrich and 632.65 ± 199.08 and 263.84 ± 74.30 μ W in the emu (Table 3.14). The quadratus muscle was the most powerful in the ostrich, generating 1400 μ W and the medial rectus muscle the most powerful in the emu, generating 632 μ W (Table 3.14). Power generated by the quadratus and medial rectus muscles each amounted to 1000 μ W per 0.5 g. The pyramidal and the ventral oblique muscles were the least powerful in the ostrich and emu respectively (Table 3.14). When unadjusted for globe volume, P-values of less than 0.05 were obtained for all the muscles, thus indicating that the power generated by each extrinsic ocular muscle differed significantly between the two species (Table 3.15). However, when adjusted for globe volume all extrinsic ocular muscles, except for the ventral oblique and pyramidal muscles, showed P-values of less than 0.05, and were thus significantly more powerful in the ostrich compared to those in the emu (Table 3.15).

3.3.9 Muscle to tendon ratio

The *M. bulbi* in both species generally displayed shorter tendons which inserted onto comparatively long muscle fascicles (Table 3.16). The pyramidal muscle was an exception in both species, as the tendon was on average 1.6 times longer than the average muscle fascicle length. The quadratus muscles displayed the largest muscle to tendon ratio, in the ostrich and emu respectively (Table 3.16).

3.4 Discussion

The ostrich and emu are omnivorous avian species (Deeming, 1999; Calvino-Cancela et al., 2006; Sales, 2007). The ostrich mostly feed on shrubs and grasses and occasionally insects (Deeming, 1999; Martin et al., 2001) and foraging takes place primarily during daylight hours (Martin et al., 2001; Cooper et al., 2010). The emu feeds primarily on seeds, shrubs, fruits, grasses and insects (Calvino-Cancela et al., 2006; Sales, 2007; Miller & Fowler, 2015). Frontal binocular vision plays an important role in accurate pecking and foraging at close range (Martin & Katzir, 1995; Martin et al., 2001). Prey species have laterally positioned eyes which give a wide range of vision and enable accurate detection of predators (Martin, 1986; O'Regan & Levy-Schoen, 1987; Martin, 2005; Martin, 2011), which also applies to the ostrich (Martin & Katzir, 1995) and possibly the emu.

Avian extrinsic ocular muscles are remarkable in that a range of movements of the globe are made possible. These include saccadic or rapid motion, smooth motion as well as movement of the globes in the same (conjugate motion) or opposing directions (disconjugate motion) (Martin & Schovanec, 1998; Purves et al., 2001; Maggs et al., 2008). The various movements of the globe (King & McLelland, 1985), combined with head movement, accurately focusses an image onto the retina (O'Regan & Levy-Schoen, 1987; Martin & Katzir, 1995). The avian orbit accommodates a particularly large globe and therefore movement of the globe is restricted in comparison to mammals (King & McLelland, 1985; Martin & Katzir, 1995).

Palaeognathous species, such as the ostrich and emu possess a large globe size (Deeming, 1999; Martin et al., 2001; Krabichler et al., 2015; Hart et al., 2016), which was confirmed in the present study. The large globe size in the ostrich is not marked in comparison to albatross and eagle species (Martin et al., 2001). In avian species, enhanced convergent or divergent ocular movements and therefore a greater proficiency at eliminating blind areas of vision, have been associated with increased globe size (Fernandez-Juricic et al., 2008). The ostrich may

also have a comparably greater ability compared to the emu in eliminating blind areas of vision when head movement is not implicated.

It has been documented that the ostrich has a blind area of vision above the head, which is a protective mechanism against the harsh sunlight (Martin & Katzir, 1995). Movement of the head would however alter the blind area of vision (Martin, 2011). It must however be taken into consideration that extrinsic ocular muscles do not function independently (Maggs et al., 2008). Therefore, the motion initiated by a single extrinsic ocular muscle cannot be accurately accessed without taking into consideration the synergistic and antagonistic influences of the remaining ocular muscles (Maggs et al., 2008).

It was evident in the present study that the extrinsic ocular muscles displaying the longest fascicle lengths, also had greater contractile velocities (V_{max}). The dorsal oblique muscle in the ostrich is significantly longer and possesses a significantly greater contractile velocity compared to the remainder of the *M. bulbi* as well as the extrinsic ocular muscles in the emu (present study). It has been documented that the oblique insertion of an extrinsic ocular muscle causes greater velocity of motion of the globe (Bell, 1823). The oblique muscles function synergistically, thus the combined action of these muscles initiate rotation around the vertical axis of the globe (Bell, 1823). The greater the distance from origin to insertion of an extrinsic ocular muscle, the greater the level arm and torque acting on the globe (Haselwanter et al., 2004; Ansons & Davis, 2014).

Torque is the product of force and radius or lever arm length (Hill et al, 2008). Rotatory motion is increased as the force exerted on the globe increases (Ansons & Davis, 2014). The dorsal oblique muscle rotates the dorsum of the globe rostrally, also termed intortion (Maggs et al., 2008). The length of the dorsal oblique muscle in ostrich, may indicate an increased torque and thus increased intortion of the globe, compared to the emu (present study). The concomitant action of the ventral oblique muscle on the globe can however not be ignored.

Information is available on the contractile velocities of the extrinsic ocular muscles in mammals such as the rabbit (McLoon et al., 1985). The greatest maximum contractile velocity of the extrinsic ocular muscles in the rabbit is 20 fascicle lengths per second (McLoon et al., 1985), which is twice the values obtained in the ostrich and emu. Different methods were used to calculate velocity of extrinsic ocular muscle in the rabbit (McLoon et al., 1985), compared to the present study. It appears that no information is available on the contractile velocities of the *M. bulbi* in avian species, therefore the rabbit was used as comparison.

In avian species, information is available on the contractile velocities of locomotory muscles (Bennett, 1995; Bennett, 1996; Tobalske, 2007; Morris & Askew, 2010; Biewener, 2011). The contractile velocities of the dorsal oblique and pyramidal muscles in the ostrich and emu respectively, are half the value measured in the avian pectoral muscle (21.2 Lo per second, where Lo equals fascicle length at which maximum force is produced) (Morris & Askew, 2010). Extrinsic ocular eye muscles are capable of initiating saccadic, smooth and sustained motion without fatigue (Porter et al., 1995; Purves et al., 2001; Yu Wai Man et al., 2005; Maggs et al., 2008).

Comparatively, not all locomotory muscles are fatigue resistant (Porter et al., 1995). It is possible that the *M. bulbi* in the ostrich and emu are less efficient at contracting compared to the avian locomotory muscles. The latter is due to short, rapid and small ranges of motion being evident in eye movement (Purves et al., 2001; Maggs et al., 2008) Flight muscles in comparison, sustain high magnitude contractions (Morris & Askew, 2010; Biewener, 2011).

The medial rectus and quadratus muscles are significantly heavier and exert a greater isometric force in the ostrich compared to the emu (present study). Of the extrinsic ocular muscles in the ostrich, the medial rectus muscle exerts the greatest amount of isometric force second to the quadratus muscle. The medial rectus muscle adducts the globe (Maggs et al., 2008) and allows for frontal binocular vision (Martin, 2005). The ostrich has narrow frontal binocular vision, as the bill creates a blind spot in this area of vision (Martin & Katzir, 1995). However, narrowed frontal binocular vision is a convergent feature of avian species that rely primarily on vision for pecking (Martin and Katzir, 1995), making foraging more efficient (Fernandez-Juricic et al., 2008; Martin, 2011). The increased isometric force exerted by the medial rectus muscle in the ostrich (present study), supports the latter in that the ability to adduct the globe on a horizontal axis, may be increased. The latter is indicative of a narrow frontal binocular field of vision described previously in this species. In the present study, the medial rectus muscle in the emu exerted the greatest isometric force compared to the remaining extrinsic ocular muscles. Thereby indicating reliance on frontal vision for accurate pecking in this species.

The quadratus and the pyramidal muscles are innervated by CN VI (see Chapter 2) and therefore may contract simultaneously when initiating movement of the nictitating membrane across the cornea. The nictitating membrane muscles are positioned directly opposite to each other, but the resultant force acts in a single direction in order to initiate the movement of the nictitating membrane across the corneal surface (Coues, 1868). The action of the quadratus muscle is pulley-like in nature (Coues, 1868), due to this muscle keeping the *tendo m. pyramidalis* in position dorsal to the optic nerve (see Chapter 2). The quadratus muscle in both

species acts indirectly on the nictitating membrane via the pyramidal muscle tendon and therefore exerts a greater isometric force compared to the pyramidal muscle (present study). In the ostrich and emu, the remaining extrinsic ocular muscles do not act in a pulley-like manner (present study). The individual isometric forces exerted by these are greater than that of the pyramidal muscle as sufficient torque needs to be generated to move the globe (Ansons & Davis, 2014).

The power generated by an extrinsic ocular muscle is the product of maximum isometric force (F_{max}) and contractile velocity (V_{max}) of the muscle (present study). As the contractile velocity or isometric force exerted by an extrinsic ocular muscle in the ostrich and emu increases, the respective power generated by the same muscle intensifies. The *M. bulbi* in the ostrich is significantly more powerful compared to the emu (present study). However, the power generated by the quadratus muscle in the ostrich and medial rectus muscle per 0.5 g muscle mass, both equates to 1000 μ W.

The power output of the extrinsic ocular muscles in both species are negligible compared to the values obtained for the flight muscles in avian species such as the cockatiel (*Nymphicus hollandicus*). In the latter species, power output fluctuated and the least power generated per 0.5 g of pectoral muscle was 30 000 μ W (or 60 W per kg) (Tobalske, 2007). The low power output and force generated by the *M. bulbi* in both species is due to these muscles initiating rapid, non-sustained motion over a short-range. The latter has previously been described in human extrinsic ocular muscles (Porter et al., 1995; Purves et al., 2001; Yu Wai Man et al., 2005; Maggs et al., 2008).

3.6 References

ALVARADO-MALLART, R. (1972) Ultrastructure of the muscle fibres of an extraocular muscle of the pigeon. *Tissue and Cell*, 4, 2, 327–339.

BELL, C. (1823) On the Motions of the Eye, in *Illustration of the Uses of Muscles and Nerves of the Orbit*. *Philosophical Transactions of the Royal Society of London*, 113, 166-186.

BENNETT, M. B. (1995) Interrelationship of cranial muscles and tendons in a range of birds. *The Zoological Society of London*, 235, 33–42.

BENNETT, M. B. (1996) Allometry of the leg muscles of birds. *The Zoological Society of London*, 238, 435 – 443.

BIEWENER, A. A. (2003) *Animal Locomotion*. United Kingdom: Oxford University Press.

BIEWENER, A. A. (2011) Muscle function in avian flight: achieving power and control. *Philosophical transactions of the Royal Society B*, 366, 1496–1506.

BRIGGS, M. M. & SCHACHAT, F. (2002) The superfast extraocular myosin (MYH13) is localized to the innervation zone in both the global and orbital layers of rabbit extraocular muscle. *Journal of Experimental Biology*, 205, 3133–3142.

CALVINO-CANCELA, M., DUNN, R. R., VAN ETTEN, E. J. B. & LAMONT, L. L. (2006) Emus as non-standard seed dispersers and their potential for long-distance dispersal. *Ecography*, 29, 632-640.

CHARD, R. D. & GUNDLACH, R. H. (1938) The structure of the eye of the homing pigeon. *Journal of comparative psychology*, 25, 2, 249–272.

COOPER, R. G., HORBANCZUK, J. O., VILLEGAS-VIZCAINO, R., SEBEI, S. K., MOHAMMED, A. E. F. & MAHROSE, K. M. A. (2010) Wild ostrich (*Struthio camelus*) ecology and physiology. *Tropical Animal Health and Production*, 42, 363–373.

COUES, E. (1868) Bird's Eye Views. *The American Naturalist*, 2, 10, 505-513.

CROLE, M.R. & SOLEY, J.T. (2016) Comparative morphology, morphometry and distribution pattern of the trigeminal nerve branches supplying the bill tip in the ostrich (*Struthio camelus*) and emu (*Dromaius novaehollandiae*). *Acta Zoologica*, 97, 1, 49-59.

DEEMING, D. C. (ed.) (1999) *The ostrich: Biology, Production and health*. London: CAB International.

ELZANOWSKI, A. (1987) Cranial and eyelid muscles of the Tinamous (Aves: *Tinamiformes*). *Zoologische Jahrbucher. Abteilung fur Anatomie und Ontogenie der Tiere*, 116, 63-118.

FERNÁNDEZ-JURICIC, E., GALL, M. D., DOLAN, T., TISDALE, V. & MARTIN, G. R. (2008) The visual fields of two ground-foraging birds, House Finches and House Sparrows, allow for simultaneous foraging and anti-predator vigilance. *Ibis*, 150, 779-787.

GELATT, K. N. (ed.) (2014) *Essentials of Veterinary Ophthalmology*. 3rd Ed. UK: Wiley Blackwell. 516-517.

GELATT, K. N. & GELATT, J. P. (eds.) (2011) *Veterinary Ophthalmic Surgery*. UK: Saunders Elsevier. 52-57.

GELATT, K. N., GILGER, B. C. & KERN, T.J. (eds.) (2013) *Veterinary Ophthalmology Volume 1*. 5th Ed. UK: Wiley Blackwell. 44-45.

GORE, T., GORE, P. & GRIFFIN, J. M. (2008) *Horse Owner's Veterinary Handbook*. 3rd Ed. Howell Book House.

HART, N. S., MOUNTFORD, J. K., DAVIES, W. I. L., COLLIN, S. P. & HUNT, D. M. (2016) Visual pigments in a palaeognath bird, the emu *Dromaius novaehollandiae*: implications for spectral sensitivity and the origin of ultraviolet vision. *Proceedings of the Royal Society of London B*, 283, 20161063, 1-9.

HILL, A. W., WYSE, G. A. & ANDERSON, M. (2008) *Animal Physiology*. 2nd ed. Sunderland, Massachusetts: Sinauer Associates Inc.

KING, A. S. & MCLELLAND, J. (eds.) (1985) *Form and Function in Birds*. Volume 3. London: Academic Press.

MAGGS, D. J., MILLER, P. E. & OFRI, R. (2008) *Slatter's Fundamentals of Veterinary Ophthalmology*. 4th Ed. Missouri, USA: Saunders Elsevier. 330-332.

MARTIN, C. L. (2005) *Ophthalmic Disease in Veterinary Medicine*. London: Mason Publishing. 14-115.

MARTIN, G. R. (2011) Understanding bird collisions with man-made objects: a sensory ecology approach. *Ibis*. 153. 239-254.

- MARTIN, G. R. & KATZIR, G. (1995) Visual fields in ostriches. *Nature*, 374, 2 March.
- MARTIN, G. R., ASHASH, U. & KATZIR, G. (2001) Ostrich Ocular Optics. *Brain, Behavior and Evolution*, 58, 115 – 120.
- MARTIN, C. F. & SCHOVANEC, L. (1998) Muscle Mechanics and Dynamics of Ocular Motion. *Journal of Mathematical Systems, Estimation, and Control*. Birkhauser-Boston, 8, 2, 1998, 1-15.
- MAYR, R., GOTTSCHALL, J., GRUBER, H. & NEUHUBER, W. (1975) Internal structure of cat extraocular muscle. *Anatomy and Embryology*, 148, 1, 25-34.
- MAYR, R. (1971) Structure and distribution of fibre types in the external eye muscles of the rat. *Tissue and Cell*, 3, 3. 433–462.
- MCLOON, L. K., PARK, H. N., KIM, J. H., PREDOSA-DOMELLOF, F. & THOMPSON, L.V. (2011) A continuum of myofibers in adult rabbit extraocular muscle: force, shortening velocity, and patterns of myosin heavy chain colocalization. *Journal of Applied Physiology*, 111, 4, 1178-1189.
- MEYERS, R. A. & MCFARLAND, J. C. (2016) Anatomy and histochemistry of spread -wing posture in birds. Eagles soar with fast, not slow muscle fibres. *Acta Zoologica*, 97, July, 319–324.
- MILLER, R. E. & FOWLER, M. E. (eds.) (2015) *Fowler's Zoo and Wild Animal Medicine*. Volume 8. Missouri, USA: Elsevier. 77
- MORRIS, C. R. & ASKEW, G. N. (2010) The mechanical power output of the pectoralis muscle of cockatiel (*Nymphicus hollandicus*): the in vivo muscle length trajectory and activity patterns and their implications for power modulation. *Journal of Experimental Biology*, 213. 2770–2780.
- PAYNE, R. C., HUTCHINSON, J. R., ROBILLIARD, J. J., SMITH, N. C. & WILSON, A. M. (2005) Functional specialisation of the pelvic limb anatomy in horses (*Equus caballus*). *Journal of Anatomy*, 206, 557–574.

PEARSALL, J. (ed.) (2002) *Concise Oxford English Dictionary*. 10th Ed. revised. Oxford: Oxford University Press.

PURVES, D., AUGUSTINE, G. J. & FITZPATRICK, D. (eds.) (2001) *Neuroscience: Types of Eye Movements and Their Functions*. 2nd Ed. Sunderland: Sinauer Associates. [Online] available from: <https://www.ncbi.nlm.nih.gov/books/NBK10991/> [Accessed: 28 March 2017].

RASHED, R. M., EL-ALFY, S. H. & MOHAMED, I. K. (2010) Histochemical analysis of the muscle fibre types of rat superior rectus extraocular muscle. *Acta histochemical*, 112, 536–545.

SALES, J. (2007) The emu (*Dromaius novaehollandiae*): a review of its biology and commercial products. *Avian and Poultry Biology Reviews*, 18, 1, 1-20.

SLONAKER, J. R. (1918) Physiological study of the anatomy of the eye and its accessory parts of the English sparrow (*Passer domesticus*). *Journal of morphology*, 31, 351-459.

TOBALSKE, B. W. (2007). Biomechanics of bird flight. *Journal of Experimental Biology*, 210, 3135–3146.

3.7 Tables

Table 3.1: Globe volume from ten ostrich and ten emu as measured by the amount of water displaced (cm³) by the globe.

Bird Number	Globe volume	
	Ostrich	Emu
1	30	20
2	30	17.5
3	37.5	20
4	35	20
5	40	20
6	35	20
7	35	20
8	30	17.5
9	35	17.5
10	35	15
Average	37.75	18.75

Table 3.2: The range, mean and median muscle fascicle lengths (cm) of each extrinsic eye muscle in the ostrich and emu, arranged from longest to shortest. (SD: standard deviation)

<i>M. bulbi</i>	Ostrich (n = 10)			<i>M. bulbi</i>	Emu (n = 10)		
	Mean length \pm SD	Median length	Range		Mean length \pm SD	Median length	Range
1	2.87 \pm 0.21	2.97	2.46 - 3.08	4	2.29 \pm 0.28	2.31	1.85 - 2.83
2	2.86 \pm 0.29	2.78	2.49 - 3.36	3	2.07 \pm 0.16	2.06	1.74 - 2.27
3	2.76 \pm 0.41	2.78	1.98 - 3.25	2	2.05 \pm 0.19	2.10	1.67 - 2.29
4	2.69 \pm 0.30	2.51	2.44 - 3.18	5	1.95 \pm 0.11	1.93	1.80 - 2.18
5	2.68 \pm 0.20	2.68	2.38 - 2.94	7	1.93 \pm 0.30	2.02	1.38 - 2.29
6	2.55 \pm 0.21	2.50	2.28 - 2.94	1	1.89 \pm 0.30	1.89	1.41 - 2.38
7	2.37 \pm 0.38	2.41	1.70 - 2.84	8	1.86 \pm 0.25	1.87	1.27 - 2.12
8	2.35 \pm 0.21	2.37	2.01 - 2.65	6	1.84 \pm 0.22	1.85	1.36 - 2.20

Table 3.3: The difference or contrast in muscle fascicle lengths in the ostrich compared to the emu. In both species P-values ($P > |t|$) were obtained before and after adjustment for globe volume, where the *t*-value indicates the magnitude of the difference in measurements recorded compared to the sampled data's variability. P-values of less than 0.05 were considered significant and are highlighted. A standard error of 0.12 and 0.17 was obtained for the unadjusted and adjusted values respectively.

<i>M. bulbi</i>	Contrast (cm)		P - value	
	Unadjusted	Adjusted	Unadjusted	Adjusted
1	0.98	0.51	0.0	0.02
2	0.81	0.34	0.0	0.31
3	0.68	0.22	0.0	1.00
4	0.40	-0.06	0.01	1.00
5	0.74	0.28	0.0	0.78
6	0.71	0.25	0.0	1.00
7	0.44	-0.02	0.0	1.00
8	0.49	0.03	0.0	1.00

* 1. *M. obliquus dorsalis*, 2. *M. rectus lateralis*, 3. *M. rectus medialis*, 4. *M. pyramidalis membranae nictitantis*, 5. *M. quadratus membranae nictitantis*, 6. *M. rectus ventralis*, 7. *M. obliquus ventralis*, 8. *M. rectus dorsalis*.

Table 3.4: The range, mean and median (Vmax) maximum contractile velocity (m/s) generated by each extrinsic eye muscle in the ostrich and emu. Velocities are arranged from highest to lowest. (SD: standard deviation).

<i>M. bulbi</i>	Ostrich (n = 10)			<i>M. bulbi</i>	Emu (n = 10)		
	Mean velocity \pm SD	Median velocity	Range		Mean velocity \pm SD	Median velocity	Range
1	0.22 \pm 0.02	0.22	0.18 - 0.23	4	0.17 \pm 0.02	0.17	0.14 - 0.21
2	0.21 \pm 0.02	0.21	0.19 - 0.25	3	0.16 \pm 0.01	0.16	0.13 - 0.17
3	0.21 \pm 0.03	0.21	0.15 - 0.24	2	0.15 \pm 0.01	0.16	0.13 - 0.17
4	0.20 \pm 0.02	0.19	0.18 - 0.24	5	0.15 \pm 0.01	0.15	0.14 - 0.16
5	0.20 \pm 0.02	0.20	0.18 - 0.22	7	0.15 \pm 0.02	0.15	0.10 - 0.17
6	0.19 \pm 0.02	0.19	0.17 - 0.22	1	0.14 \pm 0.02	0.14	0.11 - 0.18
7	0.18 \pm 0.03	0.18	0.13 - 0.21	8	0.14 \pm 0.02	0.14	0.10 - 0.16
8	0.18 \pm 0.02	0.18	0.15 - 0.20	6	0.14 \pm 0.02	0.14	0.10 - 0.17

Table 3.5: The difference or contrast in maximum contractile velocity in the ostrich compared to the emu. P-values of less than 0.05 were considered significant and are highlighted. A standard error of 0.01 was obtained for the unadjusted and adjusted values.

<i>M. bulbi</i>	Contrast (m/s)		P - value	
	Unadjusted	Adjusted	Unadjusted	Adjusted
1	0.07	0.04	0.0	0.02
2	0.06	0.03	0.0	0.32
3	0.05	0.02	0.0	1.0
4	0.03	-0.01	0.01	1.0
5	0.06	0.02	0.0	0.84
6	0.05	0.02	0.0	1.0
7	0.03	0.0	0.0	1.0
8	0.04	0.0	0.0	1.0

* 1. *M. obliquus dorsalis*, 2. *M. rectus lateralis*, 3. *M. rectus medialis*, 4. *M. pyramidalis membranae nictitantis*, 5. *M. quadratus membranae nictitantis*, 6. *M. rectus ventralis*, 7. *M. obliquus ventralis*, 8. *M. rectus dorsalis*.

Table 3.6: The range, mean and median muscle mass (grams) of each extrinsic eye muscle in the ostrich and emu, arranged from heaviest to lightest. (SD: standard deviation)

<i>M. bulbi</i>	Ostrich (n = 10)			<i>M. bulbi</i>	Emu (n = 10)		
	Mean mass \pm SD	Median mass	Range		Mean mass \pm SD	Median mass	Range
1	0.66 \pm 0.04	0.68	0.57 - 0.71	2	0.30 \pm 0.09	0.26	0.23 - 0.52
2	0.58 \pm 0.17	0.58	0.20 - 0.75	1	0.23 \pm 0.04	0.22	0.17 - 0.31
3	0.54 \pm 0.06	0.56	0.46 - 0.59	4	0.20 \pm 0.05	0.21	0.11 - 0.26
4	0.42 \pm 0.04	0.42	0.35 - 0.50	5	0.19 \pm 0.03	0.18	0.16 - 0.26
5	0.42 \pm 0.04	0.58	0.36 - 0.50	3	0.16 \pm 0.04	0.15	0.11 - 0.26
6	0.35 \pm 0.10	0.32	0.25 - 0.55	8	0.14 \pm 0.03	0.14	0.10 - 0.19
7	0.31 \pm 0.09	0.34	0.16 - 0.47	6	0.13 \pm 0.04	0.11	0.09 - 0.20
8	0.29 \pm 0.03	0.56	0.46 - 0.59	7	0.13 \pm 0.04	0.11	0.08 - 0.22

Table 3.7: The difference or contrast in muscle mass in the ostrich compared to the emu. P-values of less than 0.05 were considered significant and are highlighted. A standard error of 0.03 and 0.04 was obtained for the unadjusted and adjusted values respectively.

<i>M. bulbi</i>	Contrast (g)		P - value	
	Unadjusted	Adjusted	Unadjusted	Adjusted
1	0.43	0.35	0.0	0.00
2	0.28	0.20	0.0	0.00
3	0.38	0.29	0.0	0.00
4	0.22	0.14	0.0	0.01
5	0.23	0.15	0.0	0.01
6	0.21	0.12	0.0	0.04
7	0.19	0.10	0.0	0.15
8	0.16	0.08	0.0	0.61

* 1. *M. quadratus membranae nictitantis*, 2. *M. rectus medialis*, 3. *M. obliquus dorsalis*, 4. *M. rectus lateralis*, 5. *M. rectus ventralis*, 6. *M. rectus dorsalis*, 7. *M. obliquus ventralis*, 8. *M. pyramidalis membranae nictitantis*.

Table 3.8: The range, mean and median muscle cross sectional area (cm²) of each extrinsic eye muscle in the ostrich and emu. Cross sectional areas are arranged from greatest to least. (SD: standard deviation).

<i>M. bulbi</i>	Ostrich (n = 10)			<i>M. bulbi</i>	Emu (n = 10)		
	Mean area ± SD	Median area	Range		Mean area ± SD	Median area	Range
1	0.24 ± 0.02	0.24	0.20 - 0.27	2	0.14 ± 0.04	0.12	0.11 - 0.24
2	0.19 ± 0.04	0.20	0.09 - 0.23	1	0.11 ± 0.02	0.11	0.08 - 0.15
3	0.18 ± 0.02	0.18	0.14 - 0.28	4	0.10 ± 0.01	0.12	0.11 - 0.24
4	0.16 ± 0.01	0.16	0.14 - 0.17	6	0.09 ± 0.02	0.09	0.06 - 0.11
5	0.14 ± 0.03	0.14	0.10 - 0.20	3	0.08 ± 0.02	0.08	0.06 - 0.11
6	0.14 ± 0.02	0.14	0.12 - 0.16	5	0.07 ± 0.02	0.07	0.05 - 0.12
7	0.12 ± 0.03	0.13	0.08 - 0.15	7	0.06 ± 0.01	0.06	0.05 - 0.09
8	0.10 ± 0.02	0.10	0.08 - 0.12	8	0.05 ± 0.01	0.05	0.04 - 0.07

Table 3.9: The difference or contrast in muscle cross sectional area in the ostrich compared to the emu. P-values of less than 0.05 were considered significant and are highlighted. A standard error of 0.01 was obtained for the unadjusted and adjusted values.

<i>M. bulbi</i>	Contrast (cm ³)		P - value	
	Unadjusted	Adjusted	Unadjusted	Adjusted
1	0.12	0.17	0.0	0.0
2	0.06	0.05	0.0	0.01
3	0.10	0.09	0.0	0.0
4	0.06	0.05	0.0	0.0
5	0.07	0.06	0.0	0.0
6	0.05	0.04	0.0	0.03
7	0.06	0.06	0.0	0.0
8	0.05	0.04	0.0	0.03

* 1. *M. quadratus membranae nictitantis*, 2. *M. rectus medialis*, 3. *M. obliquus dorsalis*, 4. *M. rectus ventralis*, 5. *M. rectus dorsalis*, 6. *M. rectus lateralis*, 7. *M. obliquus ventralis*, 8. *M. pyramidalis membranae nictitantis*.

Table 3.10: The range, mean and median (Fmax) maximum isometric force (cN) generated by each extrinsic eye muscle in the ostrich and emu. Isometric force is arranged from highest to lowest. (SD: standard deviation).

<i>M. bulbi</i>	Ostrich (n = 10)			<i>M. bulbi</i>	Emu (n = 10)		
	Mean force ± SD	Median force	Range		Mean force ± SD	Median force	Range
1	7.01 ± 0.55	7.08	6.0 - 7.10	2	4.07 ± 1.24	3.62	3.20 - 7.22
2	5.81 ± 1.17	6.02	2.78 - 6.76	1	3.32 ± 0.62	3.24	2.47 - 4.56
3	5.34 ± 0.66	5.48	4.30 - 6.23	4	2.94 ± 0.38	2.93	2.35 - 3.73
4	4.70 ± 0.25	4.68	4.28 - 5.16	5	2.74 ± 0.49	2.83	1.80 - 3.31
5	4.23 ± 0.45	4.26	3.51 - 4.86	3	2.46 ± 0.57	2.33	1.80 - 3.43
6	4.16 ± 0.93	4.08	3.06 - 5.90	6	2.21 ± 0.56	2.05	1.63 - 3.61
7	3.68 ± 0.78	3.89	2.35 - 4.63	7	1.81 ± 0.35	1.77	1.42 - 2.64
8	3.04 ± 0.44	3.07	2.25 - 3.68	8	1.54 ± 0.38	1.41	1.20 - 2.16

Table 3.11: The difference or contrast in maximum isometric force in the ostrich compared to the emu. P-values of less than 0.05 were considered significant and are highlighted. A standard error of 0.3 and 0.4 was obtained for the unadjusted and adjusted values, respectively.

<i>M. bulbi</i>	Contrast (cN)		P – value	
	Unadjusted	Adjusted	Unadjusted	Adjusted
1	3.69	3.50	0.0	0.0
2	1.74	1.55	0.0	0.01
3	2.89	2.70	0.0	0.0
4	1.76	1.58	0.0	0.0
5	1.49	1.30	0.0	0.03
6	1.95	1.77	0.0	0.0
7	1.89	1.68	0.0	0.0
8	1.49	1.31	0.0	0.03

* 1. *M. quadratus membranae nictitantis*, 2. *M. rectus medialis*, 3. *M. obliquus dorsalis*, 4. *M. rectus ventralis*, 5. *M. rectus lateralis*, 6. *M. rectus dorsalis*, 7. *M. obliquus ventralis*, 8. *M. pyramidalis membranae nictitantis*.

Table 3.12: The range, mean and median muscle volume (cm³) of each extrinsic eye muscle in the ostrich and emu. Volumes are arranged from greatest to least. (SD: standard deviation)

<i>M. bulbi</i>	Ostrich (n = 10)			<i>M. bulbi</i>	Emu (n = 10)		
	Mean volume ± SD	Median volume	Range		Mean volume ± SD	Median volume	Range
1	0.63 ± 0.04	0.64	0.53 - 0.66	2	0.29 ± 0.09	0.24	0.22 - 0.49
2	0.54 ± 0.16	0.55	0.18 - 0.71	1	0.22 ± 0.04	0.21	0.16 - 0.30
3	0.51 ± 0.05	0.53	0.43 - 0.56	4	0.19 ± 0.04	0.19	0.10 - 0.24
4	0.40 ± 0.04	0.40	0.33 - 0.47	5	0.18 ± 0.03	0.17	0.15 - 0.24
5	0.40 ± 0.04	0.40	0.34 - 0.47	3	0.15 ± 0.04	0.15	0.10 - 0.24
6	0.33 ± 0.10	0.30	0.24 - 0.52	6	0.13 ± 0.03	0.13	0.09 - 0.18
7	0.29 ± 0.08	0.32	0.15 - 0.39	7	0.12 ± 0.03	0.10	0.09 - 0.19
8	0.27 ± 0.03	0.28	0.20 - 0.30	8	0.12 ± 0.03	0.11	0.08 - 0.20

Table 3.13: The difference or contrast in muscle volume in the ostrich compared to the emu. P-values of less than 0.05 were considered significant and are highlighted. A standard error of 0.03 and 0.04 was obtained for the unadjusted and adjusted values respectively.

<i>M. bulbi</i>	Contrast (cm ³)		P – value	
	Unadjusted	Adjusted	Unadjusted	Adjusted
1	0.41	0.33	0.0	0.00
2	0.26	0.18	0.0	0.00
3	0.36	0.28	0.0	0.00
4	0.21	0.13	0.0	0.01
5	0.22	0.14	0.0	0.01
6	0.20	0.12	0.0	0.04
7	0.18	0.10	0.0	0.15
8	0.15	0.07	0.0	0.61

* 1. *M. quadratus membranae nictitantis*, 2. *M. rectus medialis*, 3. *M. obliquus dorsalis*, 4. *M. rectus lateralis*, 5. *M. rectus ventralis*, 6. *M. rectus dorsalis*, 7. *M. obliquus ventralis*, 8. *M. pyramidalis membranae nictitantis*.

Table 3.14: The range, mean and median power output (μW) generated by each extrinsic eye muscle in the ostrich and emu. Power output is arranged from greatest to least.

<i>M. bulbi</i>	Ostrich (n = 10)			<i>M. bulbi</i>	Emu (n = 10)		
	Mean power \pm SD	Median power	Range		Mean power \pm SD	Median power	Range
1	1405.83 \pm 86.88	1440.21	1201.42 - 1486.91	2	632.65 \pm 199.08	547.65	493.51 - 1108.02
2	1224.66 \pm 353.95	1226.89	413.92 - 1594.10	1	483.54 \pm 87.47	471.23	369.34 - 663.33
3	1144.74 \pm 118.45	1197.17	966.86 - 1259.79	4	424.10 \pm 95.45	437.27	225.0 - 543.40
4	900.53 \pm 85.18	896.82	747.17 - 1052.83	5	403.73 \pm 57.43	388.98	345.99 - 541.27
5	900.32 \pm 93.71	893.11	757.78 - 1050.71	3	344.93 \pm 85.35	326.89	221.82 - 548.0
6	741.44 \pm 219.88	674.47	535.97 - 1169.58	6	301.95 \pm 57.31	293.46	212.26 - 393.75
7	662.16 \pm 189.43	716.92	329.01 - 863.92	7	263.84 \pm 74.30	240.39	168.75 - 428.77
8	607.08 \pm 64.67	632.02	458.49 - 669.69	8	265.23 \pm 75.07	230.31	199.53 - 420.28

Table 3.15: The difference or contrast in power output in the ostrich compared to the emu. P-values of less than 0.05 were considered significant and are highlighted. A standard error of 64.49 and 93.11 was obtained for the unadjusted and adjusted values, respectively.

<i>M. bulbi</i>	Contrast (μW)		P – value	
	Unadjusted	Adjusted	Unadjusted	Adjusted
1	922.29	746.10	0.0	0.0
2	592.01	415.81	0.0	0.0
3	799.81	623.62	0.0	0.0
4	476.43	300.23	0.0	0.01
5	496.60	320.40	0.0	0.01
6	439.49	263.30	0.0	0.04
7	398.32	222.12	0.0	0.15
8	341.85	165.66	0.0	0.62

* 1. *M. quadratus membranae nictitantis*, 2. *M. rectus medialis*, 3. *M. obliquus dorsalis*, 4. *M. rectus lateralis*, 5. *M. rectus ventralis*, 6. *M. rectus dorsalis*, 7. *M. obliquus ventralis*, 8. *M. pyramidalis membranae nictitantis*.

Table 3.16: Muscle to tendon ratio (cm) of each extrinsic eye muscle in the ostrich and emu. Values are arranged from greatest muscle to tendon ratio to least.

<i>M. bulbi</i>	Muscle fascicle to tendon ratio		Average muscle fascicle length		Average tendon length		Combined fascicle and tendon length	
	Ostrich	Emu	Ostrich	Emu	Ostrich	Emu	Ostrich	Emu
1	6.27 : 1	6.73 : 1	2.68	2.02	0.40	0.30	3.08	2.32
2	5.45 : 1	6.36 : 1	2.78	2.10	0.51	0.33	3.28	2.43
3	4.72 : 1	3.94 : 1	2.50	1.89	0.53	0.48	3.03	2.37
4	4.20 : 1	5.72 : 1	2.78	2.06	0.35	0.36	3.13	2.42
5	3.54 : 1	3.12 : 1	2.41	1.87	0.68	0.60	3.09	2.47
6	2.78 : 1	2.93 : 1	2.97	2.31	1.08	0.79	4.04	3.10
7	1.39 : 1	2.28 : 1	2.37	1.85	1.70	0.81	4.07	2.66
8	1 : 1.71	1 : 1.85	2.51	1.93	4.30	3.56	6.81	5.49

* 1. *M. quadratus membranae nictitantis*, 2. *M. rectus medialis*, 3. *M. rectus ventralis*, 4. *M. rectus lateralis*, 5. *M. obliquus ventralis*, 6. *M. obliquus dorsalis*, 7. *M. rectus dorsalis*, 8. *M. pyramidalis membranae nictitantis*.

CHAPTER 4

Gross Morphology and Innervation of the *Apparatus lacrimalis* in the ostrich (*Struthio camelus*) and emu (*Dromaius novaehollandiae*).

4.1 Introduction

The gross morphology of the lacrimal apparatus in avian species has been extensively described (Slonaker, 1918; Chard & Gundlach, 1937; Mueller et al., 1971; Aitken & Survashe, 1977; King & McLelland, 1985; Burns, 1992; Baumel et al., 1993; Payne, 1994; Chieffi et al., 1996; Jones et al., 2007; Bayon et al., 2007; Orosz & Bradshaw, 2007). The avian lacrimal apparatus is comprised of two Harderian glands or *Gl. membranae nictitantis* (King & McLelland, 1985; Baumel et al., 1993; Jones et al., 2007; Bayon et al., 2007) and two lacrimal glands or *Gl. lacrimalis* (King & McLelland, 1985; Baumel et al., 1993).

Compared to neognathous species, the gross morphology of the lacrimal apparatus in palaeognathous species such as Tinamous (Elzanowski, 1987), emu (Aitken & Survashe, 1977) and ostrich (Mc Alister, 1864; Webb, 1957; Aitken & Survashe, 1977; Deeming, 1999; Altunay & Kozlu, 2004; Klećkowska-Nawrot et al., 2015a; Klećkowska-Nawrot et al., 2015b; Frahmand & Mohammadpour, 2015) is scantily described. In the ostrich, the Harderian gland is droplet shaped and light pink in colour (Altunay & Kozlu, 2004; Frahmand & Mohammadpour, 2015). This gland is positioned ventro-rostrally within the orbit in the ostrich and is in close proximity to the *Septum interorbitale* and the postero-ventral sclera (Mc Alister, 1864; Webb, 1957; Altunay & Kozlu, 2004; Frahmand & Mohammadpour, 2015; Klećkowska-Nawrot et al., 2015a).

4.1.2 *Gl. membranae nictitantis*

The ostrich Harderian gland is attached to the periorbital connective tissue that borders the extrinsic ocular muscles and lines the orbit (Altunay & Kozlu, 2004; Frahmand & Mohammadpour, 2015). This large gland is positioned between the medial and ventral recti muscles, external to the pyramidal muscle in the ostrich (Mac Alister, 1864; Deeming, 1999; Frahmand & Mohammadpour, 2015; Klećkowska-Nawrot et al., 2015a). Descriptions on the location and gross morphology of the emu Harderian gland is scantily described (Aitken & Survashe, 1977). The body of the gland is continuous with a secretory duct and secretions of this gland are carried to the inferior and inner border of the nictitating membrane by a single

duct in the ostrich (Mac Alister, 1864; Webb, 1957; Frahmand & Mohammadpour, 2015), namely the *ductus gl. membranae nictitantis* (King & McLelland, 1985). The avian Harderian gland plays an important role in local ocular immunity and forms part of the head associated lymphoid tissue in avian species (Aitken & Survashe, 1977; Altunay and Kozlu, 2004; Schat et al., 2014). The presence of lymphoid tissue is likewise evident in the ostrich (Frahmand & Mohammadpour, 2015; Klećkowska-Nawrot et al., 2015a) and emu (Aitken & Survashe, 1977).

In comparison to descriptions of the gross morphology of the avian Harderian gland, information on the innervation of this gland is scarce. The descriptions of the innervation to the Harderian gland in avian species varies markedly (Wight et al., 1971; Walcott et al., 1989; Baumel et al., 1993; Orosz & Bradshaw, 2007; Jones et al., 2007). Scant information is available on the innervation of the ostrich Harderian gland (Webb, 1957) and it appears that no descriptions of the latter are available in the emu. Comparatively, the gross morphology (Aitken & Survashe, 1977; Frahmand & Mohammadpour, 2015; Klećkowska-Nawrot et al., 2015a) and innervation (Webb, 1957) of the Harderian gland in the ostrich has been described in greater detail than the lacrimal gland (Deeming, 1999; Klećkowska-Nawrot et al., 2015b) and emu (Aitken & Survashe, 1977).

4.1.3 *Gl. lacrimalis*

Detailed gross morphological descriptions of the lacrimal gland in the ostrich (Deeming, 1999; Klećkowska-Nawrot et al., 2015b) and emu (Aitken & Survashe, 1977), are scant compared to neognathous species (King & McLelland, 1985; Baumel et al., 1993). In the ostrich, the red coloured, oval shaped (Aitken & Survashe, 1977; Klećkowska-Nawrot et al., 2015b) lacrimal gland is located ventral to the lateral canthus (Aitken & Survashe, 1977; Deeming, 1999), between the *M. recti lateralis / dorsalis* (Klećkowska-Nawrot et al., 2015b). Similar descriptions have been provided in the emu, in that the same gland is located at the lateral canthus and described as red in colour and oval to triangular in shape (Aitken & Survashe, 1977).

The secretions of lacrimal gland in the ostrich plays a particular important role in lubricating the cornea and limiting ocular inflammation (Klećkowska-Nawrot et al., 2015b). Depending on the species, this gland may have numerous or a single duct (*ductus gl. lacrimalis*), which carry secretions to the conjunctival space underneath the lower lid (King & McLelland, 1985; Baumel et al., 1993). In the ostrich and emu, varying descriptions exist on the secretory duct of the lacrimal gland. The gland is described as having numerous ducts (Klećkowska-Nawrot et al., 2015b) and in other instances as single (Aitken & Survashe, 1977).

The gross morphology of the lacrimal gland (Aitken & Survashe, 1977; Klećkowska-Nawrot et al., 2015b) in the ostrich and emu have been described, however it appears that the innervation to the lacrimal gland in these species has not been described. Information on the innervation of the lacrimal gland in neognathous species such as the domestic fowl (Orosz & Bradshaw, 2007) and birds of prey (Jones et al., 2007), is available. The avian lacrimal gland is innervated by both trigeminal and facial nerves (Jones et al., 2007), with the latter nerve providing para-sympathetic innervation to this gland (Orosz & Bradshaw, 2007).

The gross morphological details and innervation of the lacrimal apparatus have been described in several avian species (King & McLelland, 1985), such as the domestic fowl (Baumel et al., 1993; Orosz & Bradshaw, 2007), birds of prey (Jones et al., 2007), domestic duck (Burns & Maxwell, 1979; Oliveira et al., 2006) and turkey or *Meleagris gallopavo* (Maxwell et al., 1986). However scant information is available on the ratite lacrimal apparatus, with detailed descriptions on the gross morphology of lacrimal apparatus in the ostrich being available (Mac Alister, 1864; Webb, 1957; Aitken & Survashe, 1977; Deeming, 1999; Altunay & Kozlu, 2004; Klećkowska-Nawrot et al., 2015b; Frahmand & Mohammadpour, 2015). Similar descriptions in the emu are scant compared to the ostrich (Aitken & Survashe, 1977).

Comparative descriptions of both the lacrimal apparatus in the ostrich and emu would assist in related diagnostic and surgical procedures, in so doing promoting the welfare and productivity of these commercially important avian species.

4.2 Materials and Methods

The heads of 5 sub-adult ostriches (approximately 14 months old) and 5 sub-adult emus, of either sex, were collected from Klein Karoo Ostrich abattoir (Oudtshoorn, Western Cape, South Africa) and Oryx Abattoir (Krugersdorp, Gauteng, South Africa), respectively (protocol V066 / 11; V023 / 06), immediately after slaughter of the birds for commercial use.

These were thoroughly rinsed in running tap water to remove blood and other contaminants, immersion fixed in 10% buffered formalin and stored in fixative until further processing. In each species, a circum-orbital incision was made and the eyelids removed in order to expose the eye globe. The lacrimal gland was carefully exposed on the dorso-caudal sclera by removing the distal extremity of the *Os lacrimale*. A morphological description of the gland was provided. Thereafter, the lacrimal gland and its duct were loosened from the overlying bone and connective tissue. The entire globe was removed from the osseous orbit, after transecting the extrinsic ocular muscles at the origin and removing excess periorbital connective tissue. The

Harderian gland and its duct were loosened from the ventral orbit and surrounding connective tissue. The glandular tissue was immersion fixed in fresh 10% buffered formalin and stored in labelled bottles until further processing.

A digital scale (New Classic MF, MS4035 / 01, Mettler Toledo) was used to determine the mass of each gland and callipers (Workzone GT - DC - 02) were used to measure the length and width of the body of Harderian and lacrimal glands. The results were recorded and compared for each species. The lacrimal apparatus was preserved in 10% buffered formalin.

4.3 Results

4.3.1 *Gl. membranae nictitantis*

In the ostrich and emu, the gross morphology of the Harderian gland was comparable in the following respects:

The gland was composed of a body, neck and single secretory duct (Figures 4.3 to 4.5). The Harderian gland was positioned in the ventro-rostral orbit (see Chapter 2; Figure 4.1), in both species. The large, lobated, droplet shaped gland (Figures 4.3 to 4.5) covered a large portion of the posterior sclera where it was surrounded by a moderate amount of periorbital connective tissue. In both species, the anterior surface of the gland which was positioned against the sclera and was concave in nature, whereas its posterior surface was convex. The rostral margin of the body of the Harderian gland was convex, whereas its caudal margin was concave (Figures 4.3 to 4.5) and in close proximity to the optic nerve (Figure 4.1).

A thin connective tissue membrane covered the gland. In both species, the medial and ventral recti muscles were located anterior to the Harderian gland. The dorsal and ventral margins of the Harderian gland in the ostrich were bordered by the latter ocular muscles (Figure 4.1). In both species, this gland narrowed into a single duct within the antero-rostral region of the orbit, ventral to the *For. orbitonasale* (see Chapter 2). The duct ran over the anterior sclera before opening into a pouch in the ventral margin of the nictitating membrane.

The gross morphology of the Harderian gland differed between the ostrich and emu in the following respects:

The distinction between the body and neck was less prominent in the emu compared to the ostrich (Figure 4.3). This gland had negligible contact with ventral osseous orbit in the emu, compared to the ostrich. Pigmented and dense vascular regions were not obvious within the glandular tissue of the emu (Figures 4.3, 4.5). The Harderian gland in the emu was moderately

sized, poorly lobulated, droplet shaped gland (Figures 4.3, 4.5) and covered a lesser part of the posterior sclera and was covered by periorbital connective tissue. In the emu, the curvatures of the Harderian gland was less distinct compared to the ostrich (Figure 4.3).

In the emu, the medial and ventral recti muscles covered the dorsal and ventral margins of the same gland. The posterior margin and origin of the ventral oblique muscle in the ostrich was covered by the neck of the Harderian gland before it narrowed into a single duct (Figure 4.3), whereas the origin of the ventral oblique muscle was partly covered by the Harderian gland in the emu (Figure 4.1). The duct coursed rostrally, over to the origins of the oblique muscles in the ostrich and coursed anterior to the latter muscles in the emu, due to the comparatively small size of emu Harderian gland. The average length of the body of the ostrich Harderian gland was $29.59 \text{ mm} \pm 2.68$, whereas the width was $17.96 \text{ mm} \pm 0.89$ (Table 4.1). Average glandular mass was $3.2 \text{ g} \pm 0.6$ (Table 4.1). The average length of the body of the same gland in the emu was $18.76 \text{ mm} \pm 1.82$, and the width was $10.7 \text{ mm} \pm 0.78$, whereas the average mass of the gland was $0.65 \text{ g} \pm 0.056$ (Table 4.1).

In the ostrich and emu, the *N. ophthalmicus* joined the *Ganglion ethmoidale* ventral to the *For. orbitonasale* (see Chapter 2). Before coursing caudoventrally over the insertion of the medial rectus muscle as the *N. palatinus R. dorsalis*, a lesser branch, presumably the *R. gl. membranae nictitantis*, was evident innervating the Harderian gland as it entered the dorsoproximal margin of the gland.

4.3.2 *Gl. lacrimalis*

In the ostrich and emu, the gross morphology of the lacrimal gland was comparable in the following respects:

The gland consisted of a body, neck and a single secretory duct (Figures 4.4, 4.5). In both species, the lacrimal gland was positioned dorso-caudally on the anterior sclera (Figure 4.2). The body of the gland was elongated and oval in shape (Figures 4.4, 4.5). Periorbital connective tissue and fat covered the moderately lobated gland. The duct of the lacrimal gland extended from the narrowed ventral most region of the gland (Figures 4.4, 4.5) and continued in a rostroventral direction before emptying into the dorsal margin of the lower eyelid.

The gross morphology of the lacrimal gland differed between the ostrich and emu in the following respects:

The emu differed from the ostrich in that the extensive connective tissue made it difficult to determine the exact dimensions of the gland and the parts of the gland were poorly

distinguished from each other in the emu. Darker pigmentation was evident between the individual lobes of the gland in the ostrich, which was absent in the emu (Figures 4.4, 4.5). The average length and width of the body of the ostrich lacrimal gland was $9.7 \text{ mm} \pm 0.45$ and $7 \text{ mm} \pm 0.36$, respectively (Table 4.1). The average glandular mass was $0.65 \text{ g} \pm 0.06$ (Table 4.1). The average length of the body of this gland in the emu was $9.1 \text{ mm} \pm 0.67$ and the width $7.06 \text{ mm} \pm 0.69$, whereas the average mass of the gland was $0.087 \text{ g} \pm 0.015$ (Table 4.1).

It was determined that CN V had lesser branches extending from the ventro-caudal region of the anterior conjunctiva, dorsal to the *For. maxillomandibularis* (see Chapter 2), innervating the lacrimal gland in the ostrich and emu.

4.4 Discussion

4.4.1 *Gl. membranae nictitantis*

The ostrich and emu follow the general avian pattern in that the Harderian gland is the largest of the lacrimal apparatus (Slonaker, 1918; Baumel et al., 1993; Payne, 1994; Jones et al, 2007) and covers a large portion of the posterior sclera. Similar observations were made by Mac Allister (1864), Deeming (1999) and Klećkowska -Nawrot et al. (2015) in the adult ostrich and Webb (1957) in the ostrich embryo.

The ostrich Harderian gland is on average three times longer and two and a half times the wider compared to the lacrimal gland in the ostrich. The Harderian gland in the emu is twice the length and twice the width of the lacrimal gland in the same species (present study). The mass of the lacrimal apparatus in the ostrich was greater than that in the emu. However, it is evident that the difference in body mass between the ostrich and emu is not directly correlated to gland size, which differs from observations made in quail species (Dimitrov & Genchev, 2011). The importance of the Harderian gland in local ocular immunity and thus the large infiltration of lymphoid cells into the gland, provides a possible reason for the relatively large size of this gland compared to the lacrimal gland. Taking into consideration the difference in body mass between the two species, it is evident that the lacrimal gland of the emu is relatively large compared to the same gland in the ostrich. Whether the nature of the glandular secretion differ between the species or the secretory capacity of this gland in the emu is comparatively greater, warrants further investigation.

The location of the Harderian gland in the ostrich and emu is similar (present study) and follows the general avian pattern (Aitken & Survashe, 1977), as is evident in sparrow (*Passer*

domesticus) (Slonaker, 1918); the homing pigeon (Chard & Gundlach, 1937) and domestic duck (*Anas platyrhynchos*) (Oliveira et al., 2006). The present study confirmed that the Harderian gland in the ostrich is positioned ventro-rostrally within the orbit, which is similar to previous observations made (Mac Alister, 1864; Deeming, 1999; Altunay & Kozlu, 2004; Frahmand & Mohammadpour, 2015; Klećkowska-Nawrot et al., 2015). In the ostrich, a glandular impression is evident within the ventral osseous orbit, which is not apparent in the emu (present study). The Harderian gland in both species is positioned in close proximity to the *Septum interorbitale*, as noted in numerous avian species (Baumel et al., 1993) as well as the ostrich embryo (Klećkowska-Nawrot et al., 2015).

The attachment of the Harderian gland to the orbital structures in the ostrich and emu is comparable to various avian species (Shirama et al., 1996) such as the domestic duck (Burns & Maxwell, 1979; Oliveira et al., 2006), turkey (*Meleagris gallopavo*) and domestic fowl (*Gallus domesticus*) (Burns & Maxwell, 1979). In the present study, it was confirmed that this gland in both ostrich and emu is lightly attached to the periorbital connective tissue bordering the extrinsic ocular muscles, as observed by Altunay and Kozlu (2004) and Frahmand and Mohammadpour (2015) in the adult ostrich, as well as Klećkowska-Nawrot et al (2015).

The present study indicated that the location of the Harderian gland in the emu with respect to the ventral muscles differs from the ostrich, due to large size of this gland in the latter species (see Chapter 2). The ventral oblique muscle in the emu covers a greater portion of the gland compared to the ventral rectus muscle, and thus an impression is evident on the posterior surface of the gland. The present study confirmed the observations made by Frahmand and Mohammadpour (2015) and Klećkowska-Nawrot et al. (2015) in that the Harderian gland in the ostrich narrows as it courses rostrally. In the emu, similar descriptions were provided, in that the gland narrows into a single secretory duct as it courses rostrally (present study). The present study indicated that the posterior surface and rostral margin are convex in both species. In the ostrich, the caudal margin of the gland is in close proximity to the optic nerve (present study), as previously described in this species (Frahmand and Mohammadpour, 2015). Compared to the ostrich, the relative small size of the Harderian gland in the emu accounts for the greater distance between the caudal margin of this gland and the optic nerve (present study).

A connective tissue capsule covers the avian Harderian gland (Walcott et al., 1989; Shirama et al., 1996; Payne, 1994). The latter is evident in the adult ostrich (Frahmand & Mohammadpour, 2015; present study) and ostrich embryo (Klećkowska-Nawrot et al., 2015), as well as the emu (present study). In the ostrich, the capsule extends in between the prominent lobes (present study, Frahmand & Mohammadpour, 2015; Klećkowska-Nawrot et

al., 2015). The ostrich Harderian gland is lobated and droplet shaped (Altunay and Kozlu, 2004; Frahm and Mohammadpour, 2015; Klećkowska-Nawrot et al., 2015; present study). Comparatively, the emu Harderian gland is elongated and the lobes as well as capsular pigment less evident (present study).

The secretions of the Harderian gland in the ostrich and emu are carried via a single duct, which is similar to other avian species (Burns, 1979; Aitken & Survashe, 1977; Payne, 1994). Secretions are carried to the inferior and inner border of the nictitating membrane in the emu (present study), adult ostrich (Mac Alister, 1864; present study) and the ostrich embryo (Webb, 1957). In neither ostrich nor emu does it seem evident that the pyramidal muscle is involved in compressing the Harderian gland and in so doing allowing the secretions to be emptied unto the cornea, as suggested by Mac Alister in the ostrich (1864).

Previously, the innervation to the Harderian gland in the ostrich embryo has been described as arising from an antero-ventral branch from the sphenopalatine ganglion (Webb, 1957). The Harderian gland in both species receive parasympathetic innervation from the palatine branch of the facial nerve, namely *R. gl. membranae nictitantis* via the ethmoidal and sphenopalatine ganglia (Baumel et al., 1993; present study). Various descriptions of the innervation to this gland have been provided in neognathous species, including the inferior branch of the oculomotor nerve innervating the Harderian gland (Slonaker, 1918; Burns, 1992; Chieffi et al., 1996).

Innervation to the Harderian gland in the ostrich and emu is comparable to the domestic chicken (Baumel et al., 1993; Orosz & Bradshaw, 2007), and birds of prey (Jones et al., 2007). The Harderian gland in domestic fowl and birds of prey receive parasympathetic innervation from the branches of the facial nerve (Walcott et al., 1989; Baumel et al., 1993; Orosz & Bradshaw, 2007; Jones et al., 2007), principally the palatine branch with contribution from the ethmoidal and sphenopalatine ganglia (Baumel et al., 1993). The ventral branch has likewise been described as innervating this gland in domestic fowl (Wight et al., 1971).

4.4.2 *Gl. lacrimalis*

The present study indicated that there are notable morphological differences in the gross anatomy of lacrimal gland compared to the Harderian gland, in both species. In the ostrich and emu, the size of the lacrimal gland is smaller compared to the Harderian gland, which is consistent with the observations made in other avian species (Slonaker, 1918; Baumel et al., 1993; Mueller et al., 1971; Payne, 1994; Jones et al., 2007). The latter has been confirmed in

the immature ostrich and ostrich embryo (Klećkowska-Nawrot et al, 2015). In the ostrich, the location of the lacrimal gland in the dorsotemporal periorbital region, is comparable to the emu (present study), as well as previous descriptions provided on the ostrich (Deeming, 1999; Klećkowska-Nawrot et al., 2015) and other avian species such as the sparrow (Slonaker, 1918), homing pigeon (Chard & Gundlach, 1937) and birds of prey (Jones et al., 2007).

In both species, the lacrimal gland is positioned against the anterior sclera, dorso-caudally and is partly covered by the *Os lacrimale* (present study). The locality of the lacrimal gland in the domestic fowl is similar in that direct contact between the osseous orbit and the gland is evident (Mueller et al., 1971). In both species, the lacrimal gland is located anteriorly to the dorsal and lateral rectus muscles (present study), as is indicated by Klećkowska-Nawrot et al. (2015) in the ostrich embryo and immature ostrich. The present study indicated that the pyramidal tendon in the ostrich is positioned further ventral to the lacrimal gland than suggested by Klećkowska-Nawrot et al. (2015) in the immature ostrich and embryo. The present study suggested that the lacrimal gland in the ostrich is less closely associated with the periorbital connective tissue compared to the emu. It is evident that a thin connective tissue capsule surrounds the glandular parenchyma in the ostrich and emu (present study), as is described in the Japanese quail (*Coturnix Coturnix Japonica*) (Dimitrov & Genchev, 2011).

In the ostrich, the lacrimal gland differs morphologically in that distinct lobation is evident compared to the emu (present study). The present study indicated that the emu lacrimal gland is oval shaped and flatter compared to the ostrich which has a voluminous and tear drop shaped gland. In contrast, the sparrow and homing pigeon lacrimal gland is described as being triangular in shape (Slonaker, 1918; Chard & Gundlach, 1937).

In comparison to the variation existing in the gross morphology of the lacrimal gland between the ostrich and emu, interspecies variation in the innervation to this gland is not evident. The present study indicated that branches of the trigeminal nerve innervate the lacrimal gland in the ostrich and emu. It is not apparent in either species whether this gland receives para-sympathetic innervation from the facial nerve as is described in the domestic fowl (Orosz & Bradshaw, 2007) and birds of prey (Jones et al., 2007). Para-sympathetic innervation to the lacrimal gland is essential and thus it is likely that CN VII contributes to innervating the lacrimal gland in both ostrich and emu.

4. 5 Conclusion

The gross morphology and innervation to the lacrimal apparatus have been described in several avian species such as the domestic fowl, birds of prey, Japanese quail, duck and turkey. The only ratite which has been studied with regards to the lacrimal apparatus in greatest detail, is the ostrich. The aim of the present study was to use the ostrich as a model to which the morphology of the lacrimal apparatus in the emu could be compared, while taking into consideration the size difference between the species.

The Harderian gland is the larger of the lacrimal apparatus in both ostrich and emu and is morphologically distinct from the lacrimal gland. In both species, the gross morphology of the lacrimal apparatus differs markedly. Despite the innervation and location of these glands within the orbit being comparable, the size, shape and morphometry differ notably between the ostrich and emu. The lacrimal apparatus in the ostrich is more robust, distinctly lobated and pigmented compared the emu. When surgical and diagnostic procedures are performed on the lacrimal apparatus in these ratites, the morphometric and morphological variation between these species need to be taken into consideration.

4. 6 References

- AITKEN, I. D. & SURVASHE, B. D. (1977) Lymphoid cells in avian paraocular glands and paranasal tissues. *Comparative Biochemistry and Physiology Part A: Physiology*, 58, 3, 235-244.
- ALTUNAY, H. & KOZLU, T. (2004) The fine structure of the Harderian gland in the ostrich (*Struthio camelus*). *Anatomia, histologia, embryologia*, 33, 3, 141-145.
- BAUMEL, J. J., KING, A. S., BRAEZILE, A. E., EVANS, H. E. & VAN DEN BERGE, J. C. (1993) *Handbook of Avian Anatomy: Nomina Anatomica Avium*. 2nd Ed. Cambridge, Massachusetts: Nuttall Ornithological Club.
- BAYÓN, A., ALMELA, R. M. & TALAVERA, J. (2007) Avian ophthalmology. *European Journal of Companion Animal Practice*, 17, 3.
- BURNS, R. B. (1992) *Harderian Glands: Porphyrin Metabolism, Behavioral and Endocrine Effects*. The Harderian gland in birds, histology and immunology. Springer Berlin, Heidelberg, 155-163.

- BURNS, R. B. & MAXWELL, M. H. (1979) The structure of the Harderian and lacrimal gland ducts of the turkey, fowl and duck. A light microscope study. *Journal of anatomy*, 128, 2, 285.
- CHARD, R. D. & Gundlach, R. H. (1938) The structure of the eye of the homing pigeon. *Journal of comparative psychology*, 25, 2, 249–272.
- CHIEFFI, G., BACCARI, G. C., DI MATTEO, L., D'ISTRIA, M., MINUCCI, S. & VARRIALE, B. (1996) Cell biology of the Harderian gland. *International review of cytology*, 168, 1-80.
- DEEMING, D.C. (ed.) (1999) *The ostrich: Biology, Production and health*. London: CAB International.
- DIMITROV, D. S. & GENCHEV, A. G. (2011) Comparative morphometric investigations of the intraorbital glands of the Japanese Quails (*Coturnix coturnix japonica*). *Bulgarian Journal of Veterinary Medicine*, 14, 2, 124–127.
- FRAHMAND, S. & MOHAMMADPOUR, A. A. (2015) Harderian Gland in Canadian Ostrich (*Struthio camelus*): A Morphological and Histochemical Study. *Anatomia Histologia Embryologia*, 44, 178–185.
- JONES, M. P., PIERCE, K. E. & WARD, D. (2007) Avian Vision: A Review of Form and Function with Special Consideration to Birds of Prey. *Journal of Exotic Pet Medicine*, 16, 2, 69-68.
- KING, A. S. & MCLELLAND, J. (eds.) (1985) *Form and Function in Birds*. Volume 3. London: Academic Press.
- KLEĆKOWSKA-NAWROT, J., GOŹDZIEWSKA-HARLAJCZUK, K., BARSZCZ, K. & KOWALCZYK, A. (2015a) Morphological Studies on the Harderian Gland in the Ostrich (*Struthio camelus domesticus*) on the Embryonic and Post-natal Period. *Anatomia histologia embryologia*, 44, 2, 146-156.
- KLEĆKOWSKA-NAWROT, J., GOŹDZIEWSKA-HARLAJCZUK, K., NOWACZYK, R. & KRASUCKI, K. (2015b) Functional anatomy of the lacrimal gland in African black ostrich *Struthio camelus domesticus* in the embryonic and postnatal period. *Onderstepoort Journal of Veterinary Research*, 82, 1, 1-12.

MAC ALISTER, A. (1864) On the Anatomy of the Ostrich (*Struthio camelus*). *Proceedings of the Royal Irish Academy*, 1-24.

MAXWELL, M. H., ROTHWELL, B. & BURNS, R. B. (1986) A fine structural study of the turkey Harderian gland. *Journal of anatomy*, 148, 147-157.

MUELLER, A. P., SATO, K. & GLICK, B. (1971) The chicken lacrimal gland, gland of Harder, caecal tonsil, and accessory spleens as sources of antibody-producing cells. *Cellular immunology*, 2, 2, 140-152.

OLIVEIRA, C. A., TELLES, L. F., OLIVEIRA, A. G., KALAPOTHAKIS, E., GONCALVES-DORNELAS, H. & MAHECHA, G. A. (2006) Expression of different classes of immunoglobulin in intraepithelial plasma cells of the Harderian gland of domestic ducks *Anas platyrhynchos*. *Veterinary immunology and immunopathology*, 113, 3 - 4, 257-266.

OROSZ, S. E. & BRADSHAW, G. A. (2007) Avian Neuroanatomy Revisited: From Clinical Principles to Avian Cognition. *Veterinary Clinics of North America Exotic Animal Practice*, 10, 775-802.

PAYNE, A. P. (1994) The Harderian gland: a tercentennial review. *Journal of anatomy*. 185, 1-49.

RITCHIE, B. W., HARRISON, G. J. & HARRISON, L. R. (1994) *Avian Medicine: Principles and Application*. Florida, USA: Wingers Publishing, Inc.

SCHAT, K. A., KASPERS, B. & KAISER, P. (2014) *Avian Immunology*. 2nd ed. Academic Press.

SHIRAMA, K., SATOH, T., KITAMURA, T. & YAMADA, J. (1996) The Avian Harderian Gland: Morphology and Immunology. *Microscopy Research and Technique*, 34:16, 27.

SLONAKER, J. R. (1918) Physiological study of the anatomy of the eye and its accessory parts of the English sparrow (*Passer domesticus*). *Journal of morphology*, 31, 351-459.

WEBB, M. (1957) The Ontogeny of the cranial bones, cranial peripheral and cranial parasympathetic nerves together with a study of the visceral muscles of *Struthio*. *Acta Zoologica*, 81-201.

WALCOTT, B., SIBONY, P. A. & KEYSER, K. T. (1989) Neuropeptides and the Innervation of the Avian Lacrimal Gland. *Investigative Ophthalmology and Visual Science*. 30, July, 7.

WIGHT, P. A. L., BURNS, R. B., ROTHWELL, B. & MACKENZIE, G. M. (1971) Harderian Gland of Domestic Fowl .1. Histology, with Reference to Genesis of Plasma Cells and Russell Bodies. *Journal of Anatomy*, 110, Nov, 307.

4. 7 Figures

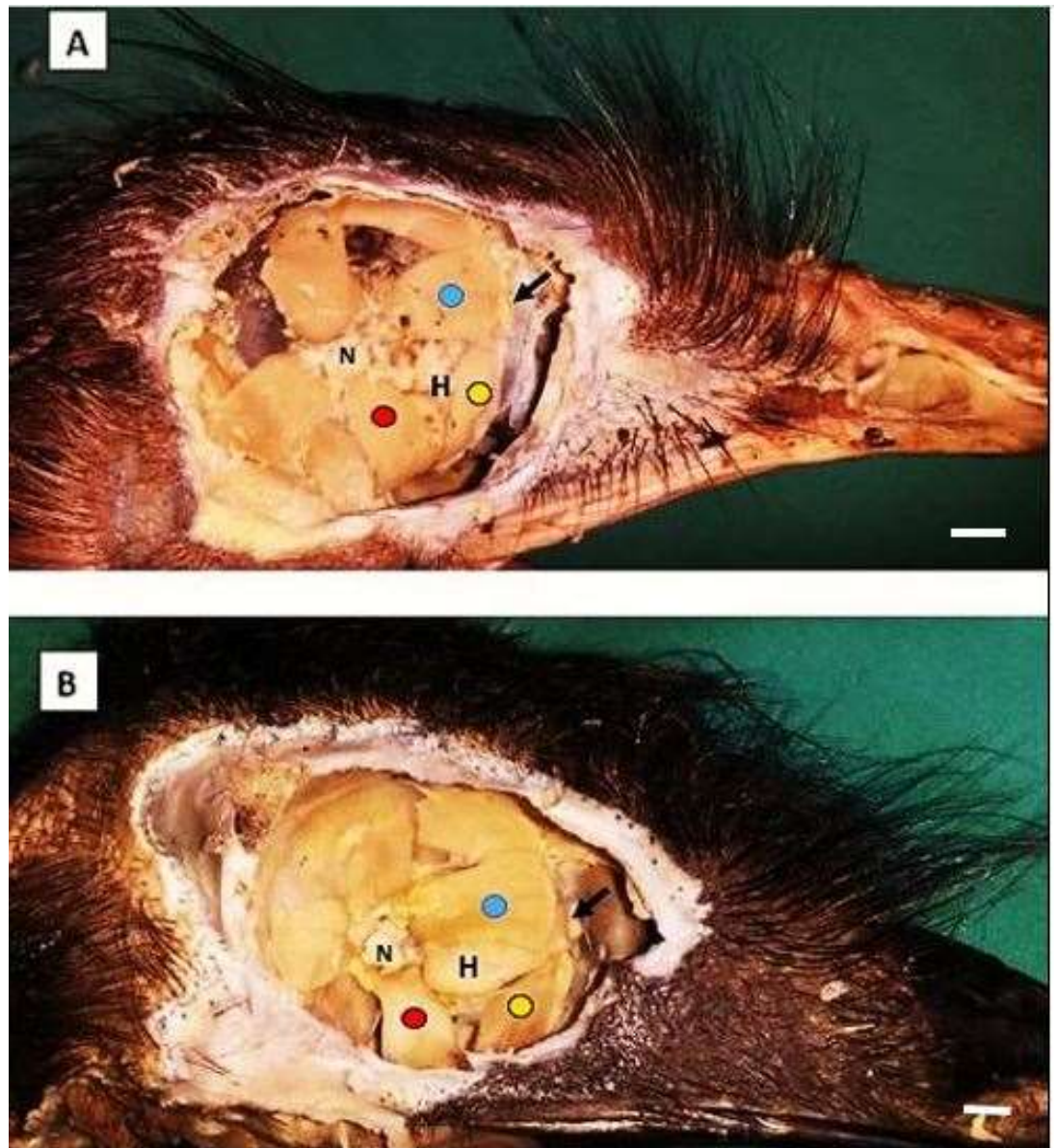


Figure 4.1: Right lateral view of the ostrich (A) and emu (B) orbit with the eye globe removed and extrinsic ocular muscles left intact (Medial rectus – Blue, Ventral oblique – Yellow, Ventral rectus – Red). The transected Optic nerve (N), as well as the exposed part of the Harderian gland (H) is indicated. The transected duct of the Harderian gland (arrow). Scale bar = 1 cm.

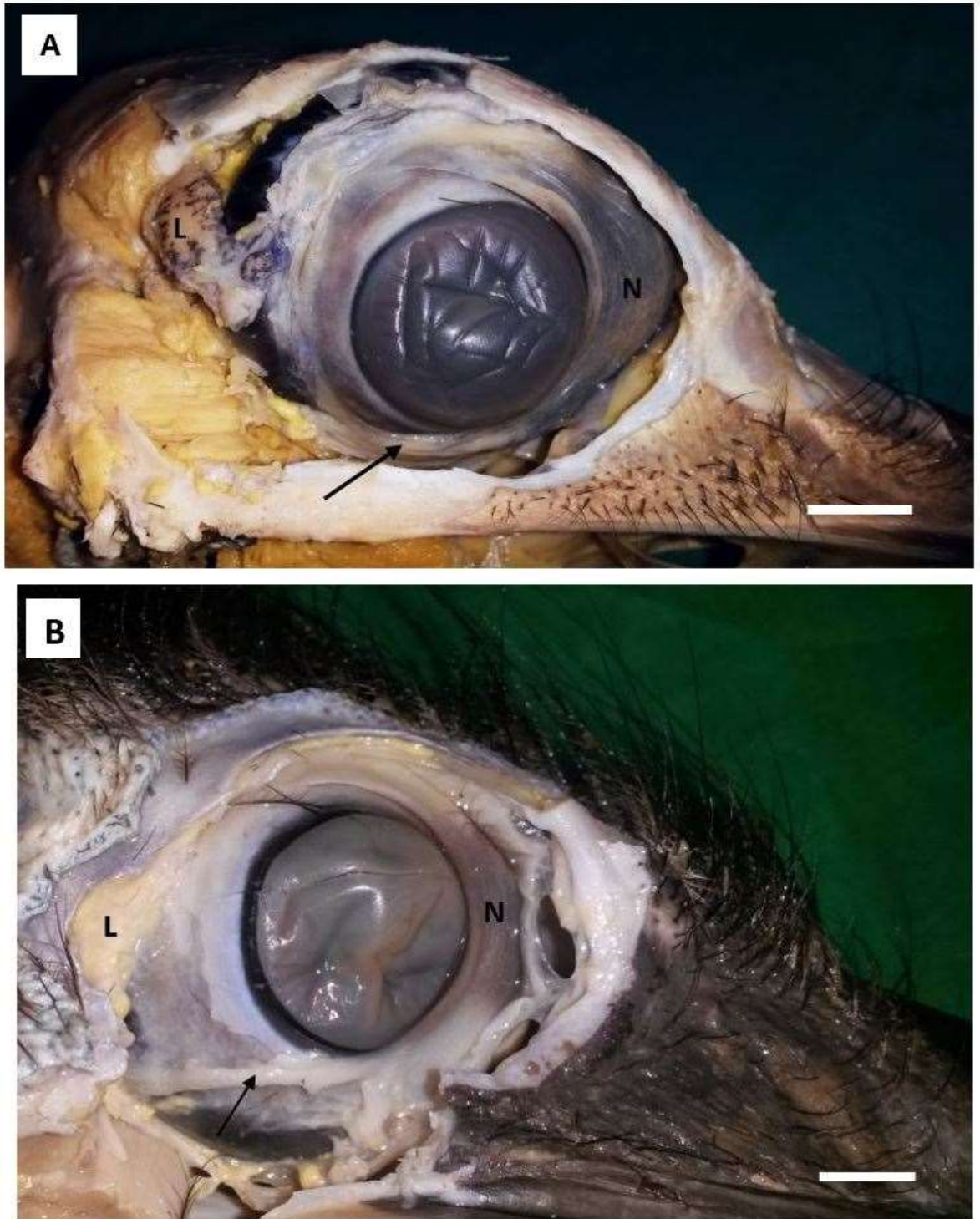


Figure 4.2: Right lateral view of the ostrich (A) and emu (B) with the osseous orbit and conjunctival tissue removed, in order to expose the lacrimal gland (L) at the lateral canthus. The eye globe was left intact. The pyramidal tendon (arrow) attaches to the nictitating membrane (N). Scale bar = 1 cm.

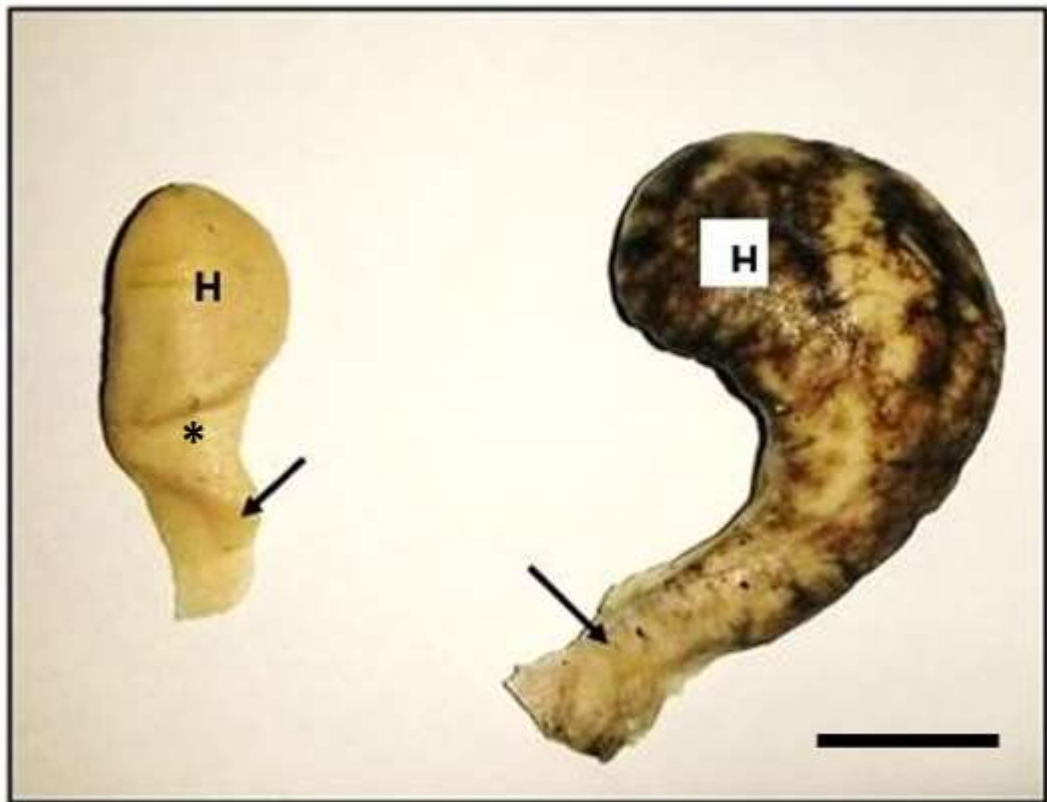


Figure 4.3: Harderian glands removed from orbit, ostrich (Right) and emu (Left). Transected duct of the Harderian gland (arrow). Harderian gland body (H). Note the distinct lobes and pigment evident in the ostrich Harderian gland and the impression made in the gland by the ventral oblique muscle in the emu (asterisk). Scale bar = 1 cm.



Figure 4.4: The Harderian (H) and lacrimal (L) glands removed from orbit of the ostrich. L and H indicate the body of these glands. Neck of the gland (short arrow). Secretory duct transected (long arrow). Note the distinct lobes and pigment evident in these glands. Scale bar = 1cm.

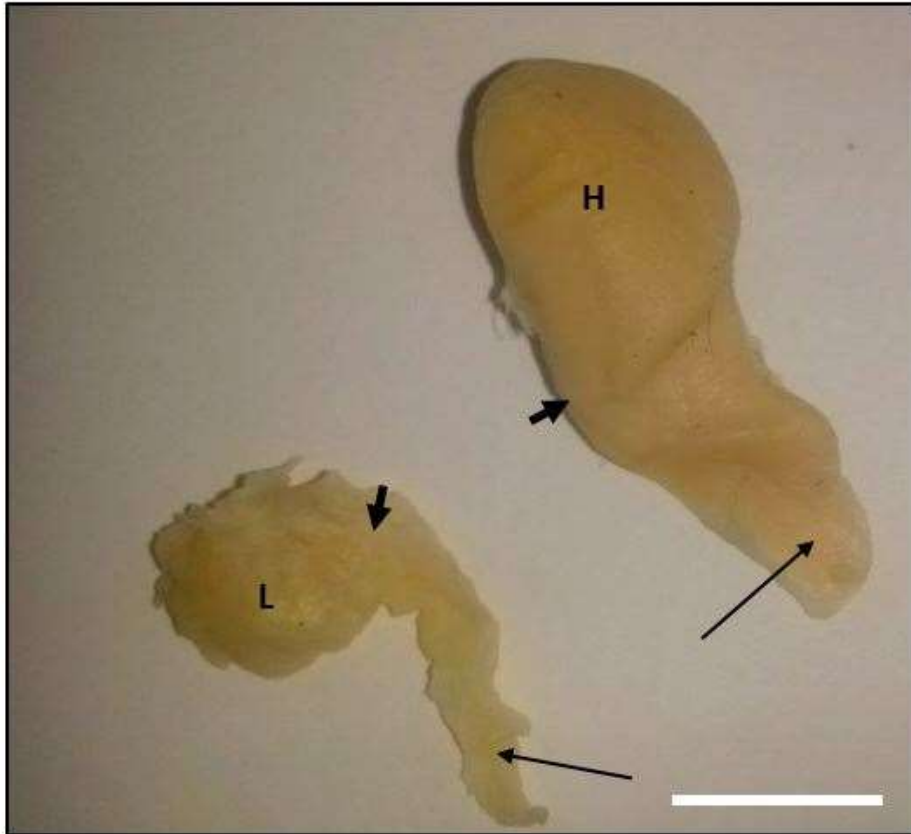


Figure 4.5: The Harderian (H) and lacrimal (L) glands removed from orbit of the emu. L and H indicate the body of these glands. Neck of the gland (short arrow). Secretory duct transected (long arrow). Scale bar = 1cm.

Table 4.1: Morphometric data from ten Harderian and ten lacrimal glands of both ostrich and emu.

		<u>Lacrimal gland</u>			<u>Harderian gland</u>		
Species	No.	Length (mm)	Width (mm)	Mass (g)	Length (mm)	Width (mm)	Mass (g)
Ostrich	1	9.6	7	0.4	28.4	17.3	2.8
	2	9.2	6.9	0.5	29.3	17	3.1
	3	10	7.3	0.49	27.6	17.3	2.7
	4	9.1	6.5	0.36	34	19.5	4.1
	5	10.2	7.5	0.33	28.8	17	3
	6	10	7.5	0.3	26.3	18	2.4
	7	9.6	6.7	0.48	30	19.2	3.1
	8	9.4	6.6	0.4	26.5	17.8	2.5
	9	9.8	7	0.42	31.6	18	3.8
	10	10.5	7.3	0.51	33.4	18.5	4
Average		9.74	7.03	0.42	29.59	17.96	3.15
Emu	1	9	7.6	0.088	22.2	12.3	0.74
	2	10	6.2	0.098	19.5	10	0.66
	3	9.6	7	0.08	19.3	10.5	0.65
	4	8.7	6.3	0.075	17.6	9.8	0.6
	5	10.2	7.5	0.1	18.3	10.7	0.63
	6	9	6.2	0.12	17.4	10.6	0.59
	7	8.5	7.2	0.07	16	10.6	0.56
	8	9.4	8	0.08	20.4	11.6	0.7
	9	8.2	6.7	0.076	19.7	11.2	0.7
	10	8.5	7.9	0.087	17.2	10	0.62
Average		9.1	7.1	0.087	18.76	10.7	0.65

CHAPTER 5

Histological Structure of the *Apparatus lacrimalis* in the in the Ostrich (*Struthio camelus*) and Emu (*Dromaius novaehollandiae*).

5.1 Introduction

The avian lacrimal apparatus consists of two exocrine, paraocular glands, the Harderian and lacrimal glands. Both glands are encapsulated and composed of secretory units or acini as well as attendant ducts. The various ducts empty into a larger single secretory duct and in most avian species mucin is the primary secretory product (Aitken & Survashe, 1977).

Lymphocytic infiltrates or the presence of plasma cells is a common histological feature of both these glands, however the extent and density of infiltrates vary between birds (Aitken & Survashe, 1977). Both glands are lobulated in most avian species, with the lobules varying in size (Aitken & Survashe, 1977). The nature of the lobules, whether compound tubulo-acinar, tubular or a mixture of both, differs between the two glands as well as between species of birds (Burns 1975; Aitken & Survashe, 1977; Burns, 1992). According to Aitken & Survashe (1977) the lacrimal apparatus in both the ostrich and emu conform to the general avian pattern.

The microscopic anatomy of the avian Harderian gland has been well documented, particularly with regards to the domestic fowl (Burns, 1977; Chieffi et al, 1996; Shirama et al, 1996; Schat et al, 2014), turkey (*Meleagris gallopavo*) (Burns & Maxwell 1979; Maxwell et al, 1986) and duck (Burns, 1976; Burns & Maxwell, 1979). Histological descriptions of the ostrich Harderian gland have been presented (Altunay and Kozlu 2004; Frahmand and Mohammadpour, 2015), and the histology of the lacrimal apparatus in the juvenile ostrich and ostrich embryo described (Klećkowska-Nawrot et al 2015).

The histological structure of the avian lacrimal gland has been thoroughly documented in various avian species such as the fowl, turkey and duck (Aitken & Survashe, 1977; Burns, 1976, 1979; Burns & Maxwell, 1979; Dimitrov, 2011; Dimitrov, 2015). The histological structure of the lacrimal gland in the juvenile ostrich and ostrich embryo has been described in detail by Klećkowska-Nawrot et al. (2015), however basic histological descriptions of this gland in the ostrich have also been given (Aitken & Survashe, 1977).

Despite the histological structure of the lacrimal apparatus has been described in several avian species, including the domestic fowl (Burns, 1977; Chieffi et al, 1996; Shirama et al, 1996; Schat et al, 2014), turkey (Burns & Maxwell 1979; Maxwell et al, 1986) and duck (Burns & Maxwell, 1979; Oliveira et al, 2006), only scant information is currently available on the microscopic anatomy of the ratite lacrimal apparatus. The ostrich is the most extensively studied ratite with regards to the histological structure of the lacrimal apparatus (Altunay and Kozlu, 2004; Klećkowska-Nawrot et al, 2015; Frahmand and Mohammadpour, 2015). The lacrimal apparatus in the emu has only been described briefly (Aitken & Survashe, 1977). A detailed, comparative description of the microscopic anatomy of the lacrimal apparatus in the ostrich and emu would assist in enhancing veterinary diagnostic and surgical procedures and in so doing promote the welfare and productivity of these commercially important birds.

5.2 Materials and Methods

The heads of 5 sub-adult ostriches (approximately 14 months old) and 5 sub - adult emus, of either sex, were collected immediately after slaughter from Klein Karoo Ostrich abattoir (Oudtshoorn, Western Cape, South Africa) and Oryx Abattoir (Krugersdorp, Gauteng, South Africa), respectively.

These were thoroughly rinsed in running tap water to remove blood and other contaminants, immersion fixed in 10% buffered formalin and stored in fixative until further processing. For each species, a circum-orbital incision was made and the eyelids removed in order to expose the eye globe. The lacrimal gland was carefully exposed at the lateral cantus of the eye by removing the distal extremity of the *Os lacrimale*. The lacrimal gland and its duct were loosened from the overlying bone and connective tissue. The eye globe was removed in entirety from the orbit, after transecting the extrinsic ocular muscles at origin and removing excess peri - orbital connective tissue.

The Harderian gland and its duct were loosened from the ventral orbit and surrounding connective tissue. The glandular tissue was immersion fixed in fresh 10% buffered formalin and stored in labelled bottles until further processing for light microscope. The samples were subsequently cut, dried by means of a graded ethanol series (70%, 80%, 96%, and 2x 100% ethanol) and further processed through 50:50 ethanol: xylol, 2x xylol and 2x paraffin wax (60 - 120 minutes per step) using a Shandon model 2LE Automatic Tissue Processor (Shandon, Pittsburgh, PA). After which the samples were manually imbedded into paraffin wax within plastic moulds. Sections were cut at 4 - 6 μm and stained with H & E. An Olympus BX 63 light microscope equipped with a DP 72 camera and Olympus cell Sens imaging software

(Olympus Corporation, Tokyo, Japan), were used to view the histological sections and record features of interest.

5. 3 Results

5.3.1 Harderian gland

The Harderian gland in both the ostrich and emu was clearly divided into a body and neck which was continuous with the main secretory duct (see Chapter 4). The general compound nature of the gland, indicated macroscopically by distinct lobation (Figure 5.1), was confirmed histologically (Figure 5.2). The body (Figure 5.2) and neck of the gland was divided into variably-sized lobes by well-developed trabeculae emanating from the connective tissue capsule (Figure 5.2). Several lobules, each of which represented a simple branched tubular gland, made up a lobe. The capsule and trabeculae were composed of densely arranged collagen fibres and interspersed fibroblasts. A rich vascular supply located in the capsule (Figure 5.3) entered the glandular parenchyma via the trabeculae. In some ostrich specimens, melanin pigment was evident within the capsule covering the body of the gland (Figure 5.1).

The parenchyma was arranged in the form of large, simple branched tubular glands (Figures 5.2, 5.3) separated by intervening layers of connective tissue (Figure 5.2). Flat, elongated myoepithelial cells and fibroblasts were evident in the inter-tubular connective tissue (Figure 5.6). The glands displayed a high degree of dichotomous branching, effectively forming prominent glandular units (Figure 5.2). The terminal secretory tubules were concentrated at the periphery of the glandular units, in some instances displaying a degree of coiling (Figure 5.2). Depending on the plane of section, these branches occasionally appeared as a collection of acini (Figures 5.2, 5.3). Each glandular unit, with its complement of branched secretory tubules, emptied into a secondary branch of the main secretory duct via a tertiary duct (Figure 5.2).

The epithelial lining of the secretory tubules was simple columnar in nature and rested on a well-defined basement membrane (Figure 5.3). The lining cells displayed a densely vacuolated cytoplasm and basally located round to oval shaped nuclei located basally (Figure 5.3). Apical blebbing was a consistent feature of these cells in both species with the blebs occasionally extending a considerable distance into the lumen of the tubules. Myoepithelial cells and fibroblasts were evident in the underlying connective tissue which carried variably sized blood vessels (Figure 5.4). The flattened myoepithelial cells were located adjacent to the basement membrane.

The epithelium lining the secretory tubules was continuous with that of the tertiary ducts into which they emptied (Figure 5.4 B). The epithelial lining of both the tertiary and secondary ducts was secretory in nature and composed of simple tall cuboidal to columnar cells. Cytological features of the cells were similar to those of the secretory tubules (Figures 5.3, 5.4). The distinction between secretory tubules and tertiary and secondary ducts could therefore only be made by the location and calibre of the various entities. Interstitial tissue surrounding the tertiary and secondary ducts, was composed of the same elements associated with the secretory tubules.

In both species, aggregates of lymphoid tissue, consisting of both lymphocytes and plasma cells, were evident in the interstitium between the secretory tubules and tertiary ducts (Figure 5.4), as well as being associated with the main secretory duct (Figures 5.7, 5.8) and its secondary branches (Figure 5.5). Tubular secretory units often appeared pushed apart by the high concentration of lymphoid tissue (Figure 5.6 B). The concentration of lymphocytes and plasma cells within the parenchyma differed between specimens within species as well as between the ostrich and emu. In general, it seemed evident that the ostrich Harderian gland had a greater concentration of lymphoid tissue than that of the emu.

The main secretory duct was flattened horizontally along its entire length (Figure 5.1) and opened at the inner border of the nictitating membrane (see Chapter 4). Proximally, the duct was continuous with the neck of the gland from where it proceeded into the body of the gland, branching just proximal to the mid-body into two to three secondary branches (Figure 5.1). These branches drained the tertiary ducts, emanating from the glandular units.

The main secretory duct was covered by a connective tissue capsule (Figures 5.1, 5.7) continuous with that of the body of the gland. Well-developed trabeculae projected into the glandular tissue adjacent to the lumen of the duct (Figure 5.7). The capsule was well vascularised (Figure 5.7) and in some ostrich specimens contained melanin pigment (Figure 5.7). Beneath the capsule was a layer of glandular tissue composed of simple branched tubular glands which opened directly into the main secretory duct (Figure 5.7). The branched nature of these glands was generally less complex than those forming the body or neck of the gland. A large portion of the main secretory duct, was lined by tubular units, thus giving a villus-like appearance to the interior of the main secretory duct (Figure 5.7). In places, the lumen of the tubular units was ill defined (Figure 5.6 A).

The simple columnar cells lining the main secretory duct were densely vacuolated and apical blebs extended into the lumen of the main secretory duct (Figure 5.8). Depending on the plane

of section the lining of the duct in both species, appeared pseudostratified in parts (Figure 5.8 B). The large lumen of the main secretory duct and its secondary branches, often contained homogenous, eosinophilic material, presumably indicative of the mucoid type secretion produced by the Harderian gland.

5.3.2 Lacrimal gland

As in the Harderian gland, the lacrimal gland in the ostrich and emu consisted of a body and neck which was continuous with a single secretory duct (see Chapter 4). The general compound nature of the gland, indicated macroscopically by distinct lobation (Figure 5.9), was confirmed histologically (Figure 5.10). The body (Figure 5.10) and neck of the gland were encapsulated by loose connective and adipose tissues in both species. The emu differed from the ostrich in that the amount of connective tissue made it difficult to determine the exact dimensions of the gland. In some ostrich specimens, melanin pigment was evident within the capsule covering the body of the gland (Figure 5.9).

Connective tissue trabeculae, carrying blood vessels, extended from the capsule into the glandular tissue (Figure 5.10). The connective tissue trabeculae divided the body of the gland into well-defined lobes (Figure 5.10). Several lobules, each composed of a large simple branched tubular gland, made up a lobe. Secretory tubules formed the bulk of each glandular unit and were concentrated at the periphery of the gland (Figure 5.10). The secretory tubules collectively drained into a tertiary duct which, in turn, drained into the secondary branches of the main secretory duct. The interstitium of the lacrimal gland in the ostrich and emu was relatively sparse due to the density of the secretory tubules (Figure 5.11). Flat, elongated myoepithelial cells (Figure 5.11), fibroblasts and blood vessels were evident in the interstitial tissue.

The epithelium lining the secretory tubules (Figure 5.11), tertiary ducts and secondary branches of the main secretory duct (Figure 5.12), varied from simple low columnar to simple columnar in nature. The epithelium of the secretory tubules (Figure 5.11) merged with that of the tertiary ducts. These cells were vacuolated and had round to oval-shaped, basally positioned nuclei (Figure 5.11). All epithelia rested on a basement membrane. The secondary branches of the main secretory duct were lined by a single layer of tall cuboidal to columnar cells (Figure 5.12), which merged into the epithelium of the tertiary ducts draining into them. The cells of the secondary branches showed similar structural features to those lining the secretory tubules (Figure 5.12) and tertiary ducts. In both species, cytoplasmic vacuoles were

often evident in the epithelial cells lining the tertiary ducts and secondary branches of the main secretory duct.

Due to the low concentration of lymphoid tissue present, adjacent tubular secretory units were not pushed apart (Figure 5.11), as was evident in the Harderian gland. In both species, the concentration of lymphoid cells was highest around the main secretory duct (Figure 5.13) and the secondary branches of this duct (Figure 5.12). Variations in the concentration of lymphoid tissue was evident within species as well as between the ostrich and emu.

A single voluminous, main secretory duct extended into the body of the gland in both species, before branching into secondary branches (Figure 5.9). The main secretory duct was not flattened horizontally as was observed in the Harderian gland, and emptied into the dorsal margin of the lower eyelid (see Chapter 4). Proximally, the duct was continuous with the neck of the gland. The main secretory duct entered the neck of the gland marginally off-centre and was distinct in the emu in that it appeared labyrinthine in nature (Figure 5.9). This appearance was due to extensive connective tissue trabeculae and branching of tubules being evident present in the mid and proximal parts of the main secretory duct. As the main secretory duct progressed into the body of the lacrimal gland in the ostrich and emu, it divided into secondary branches. In both species, the main secretory duct was covered by a connective tissue capsule (Figure 5.14) and adipose tissue. Connective tissue trabeculae, carrying blood vessels, extended from the capsule into the glandular tissue surrounding the main secretory duct (Figures 5.13, 5.14). In some ostrich specimens, melanin pigment was evident within the capsule covering the main secretory duct (Figure 5.14 A).

The columnar cells lining the main secretory duct were densely vacuolated and had round to oval shaped basally positioned nuclei (Figure 5.15). As in other parts of the gland, the epithelial lining lay on a basement membrane. Depending on the plane of section, the lining of the main secretory duct in both species, in parts, appeared pseudostratified or tall cuboidal in nature. A large portion of the main secretory duct was lined by tubular units, thus giving a villus-like appearance to the interior of the main secretory duct (Figures 5.13, 5.14). In other parts, the epithelial lining was thrown into folds (Figure 5.13), with no obvious tubular structures being evident. Dichotomous branching was less evident in the main secretory duct compared to the body of the lacrimal gland. The large lumen of the main secretory duct often contained homogenous, eosinophilic secretory material (Figures 5.13, 5.15).

5. 4 Discussion

5.4.1 Harderian gland

a. General features

In the ostrich and emu, the Harderian gland is composed of a body, neck and single secretory duct (See Chapter 4). In both species, the large, lobated, droplet shaped Harderian gland is positioned in the ventro-rostral orbit (see Chapter 4). The duct ran over the anterior sclera before opening into a pouch in the ventral margin of the nictitating membrane (see Chapter 4).

b. Lobation

The present study indicated that the body of the Harderian gland of both the ostrich and emu is clearly lobulated and encapsulated by dense connective tissue, as is also evident in the fowl (Schramm, 1980; Shirama et al., 1996; Schat et al., 2014) and turkey (Maxwell et al., 1986). As previously noted (Frahmand & Mohammadpour, 2015) and confirmed in this study, the lobes are unequal in size. The connective tissue capsule in both species divides the lobes into unequal sized lobules by trabeculae extending into the glandular parenchyma. The trabeculae carry a dense network of blood vessels and display cells which resemble fibroblasts (present study), features that had previously been confirmed in the adult ostrich (Altunay & Kozlu, 2004; Frahmand & Mohammadpour 2015).

Previous studies indicated that a dense blood supply in the avian Harderian gland assists in the active transfer of substances such as lipids which have thermo-insulatory and bactericidal properties, between the epithelial cells and blood vessels (Payne, 1994). The prominent blood supply evident in the ostrich and emu Harderian glands, may thus point to the active transport of such substances taking place within the Harderian gland of these ratites.

Melanin pigment is evident in the capsule of the ostrich Harderian gland, but not in the emu or in previous studies referring to the ostrich Harderian gland. Further investigation as to the possible function of melanin pigment within the capsule of the ostrich Harderian gland is required.

c. Structure of the i. secretory tubules, ii. Basement membrane and iii. Tertiary and secondary tubules

i. Lobules are primarily composed of secretory acini, which is a common feature of the avian Harderian gland (Aitken & Survashe, 1977; Schramm, 1980; Maxwell et al., 1986; Burns, 1992; Shirama et al., 1996; Schat et al., 2014). In the ostrich (Aitken & Survashe, 1977; Frahmand & Mohammadpour, 2015), emu (Aitken & Survashe, 1977), domestic fowl (Schat et al., 2014) and turkey (Maxwell et al., 1986), the Harderian gland has been described as displaying peripherally located acini in each lobule. However, the present study indicated that lobules in the ostrich and emu are composed of branched tubular units which terminate at the periphery of the lobule in either a straight or coiled manner. In both species, these tubular units are lined by a single layer of columnar cells that are highly vacuolated (present study). In comparison, previous studies described the adult ostrich (Frahmand & Mohammadpour, 2015) and ostrich embryo or juvenile ostrich (Klećkowska-Nawrot et al., 2015a) as having a sparsely vacuolated cytoplasm. The simple columnar nature of the lining cells of the tertiary ducts and secretory tubules, has also been confirmed in the domestic fowl (Wight et al., 1971), turkey (Maxwell et al., 1986) and ostrich (Frahmand & Mohammadpour, 2015).

In the ostrich and emu, blebs are evident at the apical margin of the cells lining the ducts and secretory tubules, possibly representing secretory vesicles. These vesicles may be indicative that the mode of secretion is merocrine in nature, as is common in the avian Harderian gland (Burns, 1992; Maxwell & Burns, 1979). Similar observations have previously been made in the adult ostrich (Frahmand & Mohammadpour, 2015). The Harderian secretions in ostrich and emu are presumed to be a mixture of mucins and lipids, as suggested in the juvenile ostrich and ostrich embryo (Klećkowska-Nawrot et al., 2015a) as well as domestic fowl (Chieffi et al., 1996; Burns 1992) and turkey (Maxwell et al., 1986).

ii. A basement membrane is present at the basal margin of the tubular units in both ostrich and emu. A similar to observation has previously been made in the adult ostrich (Frahmand & Mohammadpour, 2015), as well as in the domestic fowl (Schat et al., 2014), where the acini are bordered by a basement membrane. Flat, elongated cells resembling myoepithelial cells are present near the basal margin of tubular units in both species. Myoepithelial cells are evident in the Harderian gland of various avian species (Shirama et al., 1996), such as the turkey (Maxwell et al., 1986), as well as in the adult ostrich (Altunay & Kozlu, 2004; Frahmand & Mohammadpour, 2015), juvenile ostrich and ostrich embryo (Klećkowska-Nawrot et al., 2015a).

iii. The avian Harderian gland is comprised of a single main secretory duct which branches into secondary and tertiary ducts. Tertiary ducts are common to most avian species (Burns, 1992; Aitken & Survashe, 1977) such as the turkey (Maxwell et al., 1986), rockhopper penguin (Burns, 1992) and domestic fowl (Wight et al., 1971). In the present study, it was evident that several secretory tubules secrete into secondary branches of the main secretory duct, via tertiary ducts. Thus, each lobule is drained by a secondary duct which branches from the main secretory duct. The avian Harderian duct system is described as being lined by a single layer of columnar to cuboidal cells (Burns & Maxwell; 1979; Maxwell & Burns, 1979; Shirama et al., 1996).

Tertiary and secondary ducts in both ostrich and emu, are lined by a single epithelial layer of columnar to high cuboidal cells (present study). From previous studies, a morphological distinction could not be made between tertiary and secondary ducts (Wight et al., 1971; Frahmand & Mohammadpour, 2015). The transition of epithelium in the domestic fowl from acini to smaller tertiary and secondary ducts is not obvious (Wight et al., 1971), which was also evident in the present study. Previously it has been indicated that high cuboidal cells line the main secretory duct and its secondary branches, in the ostrich (Frahmand & Mohammadpour, 2015).

All tubules as well as ducts are lined by secretory epithelium in the ostrich and emu Harderian glands. This may be suggestive that more voluminous secretions are required in these ratites, considering the environmental and antigenic insult the ocular tissues have to endure. It has previously been documented that the fatty and mucoid secretions of these tubules and smaller ducts, contribute to lubricating and nourishing the avascular cornea (Burns, 1992). However, further investigation is required as to determine whether the structure of the Harderian gland tubules and ducts are so adapted in response to particular harsh climatic conditions and other environmental insults the ostrich and emu are exposed to.

d. Interstitial tissue

The avian Harderian gland commonly has a cell rich interstitium (Schramm, 1980; Maxwell et al., 1986; Burns, 1992; Shirama et al., 1996; Schat et al., 2014), which has also previously been confirmed in the adult ostrich and ostrich embryo (Altunay & Kozlu, 2004; Klećkowska-Nawrot et al., 2015a; Frahmand & Mohammadpour, 2015). Various cells have been identified in the glandular interstitium of the fowl and turkey, of which B-lymphocytes and plasma cells predominate (Burns, 1977; Burns, 1975; Davelaar & Kouwenhoven, 1980; Schramm, 1980; Maxwell et al., 1986; Savage et al., 1992; Olah et al., 1996; Shirama et al., 1996). However,

macrophages and lymphoblasts are also evident in the glandular interstitium of the domestic fowl (Schramm, 1980; Olah et al., 1996), which were not obvious in the present study or documented in previous studies conducted on the ostrich (Altunay & Kozlu, 2004; Klećkowska-Nawrot et al., 2015a; Frahmand & Mohammadpour, 2015). Macrophages are directly involved in the immune response initiated by the avian Harderian gland (Schramm, 1980; Schat et al., 2014). Thus, in conjunction with a high concentration of plasma cells in the ostrich and emu, would point to the important immunological role the Harderian gland has in response to antigen stimulation.

In the present study, dense aggregates of lymphocytes and plasma cells were identified in the interstitium and sub-epithelial tissue of the Harderian gland in several specimens. Similar observations were made previously in the turkey (Maxwell et al., 1986); domestic fowl (Burns, 1977; Shirama et al., 1996; Savage et al., 1992; Davelaar & Kouwenhoven, 1980; Schramm, 1980), rook (*Corvus frugilegus* L.) (Burns, 1975), adult ostrich (Altunay & Kozlu, 2004; Frahmand & Mohammadpour, 2015) and ostrich embryo (Klećkowska-Nawrot et al., 2015). It has been documented that the avian Harderian gland mounts an immune response when stimulated by antigens in the ocular region or upper respiratory tract (Shirama et al., 1996; Savage et al., 1992; Davelaar & Kouwenhoven, 1980; Schramm, 1980). Thus, the large concentration of lymphoid cells observed in both the ostrich and emu Harderian glands, is indicative of the important role this gland plays in local immunity in the eyes and upper-airways (present study).

High concentrations of plasma cells have been identified around main secretory duct of the Harderian gland in several avian species (Aitken & Survashe, 1977; Shirama et al., 1996), including the domestic fowl (Walcott et al., 1989). In previous studies on the ostrich Harderian gland, a moderate infiltration of plasma cells in aggregates of ten to fifty cells was noted, whereas extensive sheets of plasma cells were evident towards the main secretory duct in the emu (Aitken & Survashe, 1977). Such marked distinction in the pattern of lymphoid infiltration, was not evident between the two species in the present study, however.

It is evident from the present study, that large aggregations of lymphoid cells infiltrated the tissue surrounding the main secretory duct and its secondary branches, as well as being evident throughout the parenchyma of the Harderian gland in both species. It has previously been indicated that the epithelium of the secretory duct of the avian Harderian gland (Burns & Maxwell, 1979; Schramm, 1980), plays an important role in antigen uptake. The structure of the main secretory duct epithelium in the ostrich and emu Harderian gland, may thus allow for an increased rate of antigen uptake by creating a greater surface area for antigen contact.

In a previous study, the glandular tissue in the ostrich Harderian gland was not impinged by lymphoid aggregates, whereas the same tissue was notably distorted in the emu (Aitken & Survashe, 1977). It is evident from the present study however, that the arrangement of the glandular tissue in both ostrich and emu was in most specimens, distorted by impinging lymphoid aggregates. In the duck, turkey and domestic fowl (Olah et al., 1996; Schat et al., 2014), dense lymphoid cell aggregates as well as germinal centres were noted surrounding the main secretory duct (Burns & Maxwell, 1979). Germinal centres were not evident in the ostrich or emu in the present study.

e. Main secretory duct

The main secretory duct in the ostrich and emu is surrounded by a connective tissue capsule which carries blood vessels (present study), as is apparent in the Harderian gland of the domestic fowl, duck and turkey (Burns & Maxwell, 1979). In both species, the Harderian gland has a single duct (present study), which is also noted in domestic fowl (Burns, 1977; Burns & Maxwell 1979; Burns, 1992; Shirama et al., 1996), duck and turkey (Burns & Maxwell 1979). The latter has previously been described in the adult ostrich (Aitken & Survashe, 1977; Frahmand & Mohammadpour, 2015) and emu (Aitken & Survashe, 1977). The main duct is positioned off-centre as it enters the body of the gland in both species.

The epithelium of the main secretory duct in the domestic fowl, turkey and duck, is described as villus-like in nature (Burns and Maxwell, 1979). The main secretory duct in the ostrich and emu is lined by tubular secretory units that empty into the main duct lumen, giving it a villus-like appearance. In both species, the epithelial lining of the secretory units merge with that of the main secretory duct.

The main duct epithelium varies between avian species, such as the duck, turkey and domestic fowl, where the epithelial cells range from stratified to pseudo-stratified and cuboidal to columnar in shape (Burns & Maxwell, 1979; Maxwell & Burns, 1979). Previous studies indicated that the epithelium of the main duct in the adult ostrich is stratified cuboidal in nature (Frahmand & Mohammadpour, 2015). However, the present study showed that the main secretory duct in the ostrich and emu is lined primarily by a simple columnar epithelium. A apparent stratified appearance of the epithelium in some parts of the duct is mainly due to the oblique plane of section.

The epithelial cells lining the main duct in the ostrich and emu have a vacuolated, light coloured to clear cytoplasm. Similar observations were previously made in domestic fowl, duck and

turkeys, in that the vacuolated appearance of these epithelial cells indicate the presence of secretory content (Burns & Maxwell, 1979) which is lipid as well as mucoid in nature (Payne, 1994). The vacuolated appearance of the main duct epithelium in the ostrich and emu is thus suggestive of active secretion of cellular content into the duct lumen. It has previously been described that goblet cells also contribute to Harderian gland secretions in avian species (Burns & Maxwell, 1979; Maxwell & Burns, 1979).

Goblet cells are sparsely dispersed between the main duct epithelial cells in the ostrich and are scant in the emu (present study). In comparison, these cells contain mucopolysaccharides and are numerous in the Harderian gland of fowl, duck and turkey (Burns & Maxwell, 1979; Maxwell & Burns, 1979). Further investigation is required as to determine the extent to which goblet cells contribute to the secretory content of the Harderian gland in the ostrich and emu compared to epithelial cells.

In previous studies, it was noted that mucus is a primary secretory product of the main secretory duct in avian species such as the duck and turkey (Payne, 1994; Burns & Maxwell, 1979). Furthermore, the presence of lipid droplets in the epithelial cells of the main secretory duct, has previously been described (Payne, 1994). The villus-like structure of the main duct epithelium in the ostrich and emu could increase the surface area from which secretions are released, contributing to the volume of secretory content.

f. Gland classification

The avian Harderian gland is described as varying from compound tubular to compound tubulo-acinar and the excretory product being primarily mucoid (Aitken & Survashe, 1977; Maxwell et al., 1986; Chieffi et al., 1996). This gland is classified into three main types according to lobule structure and the epithelium lining the ducts of the gland (Burns, 1975; Aitken & Survashe, 1977; Burns, 1992). The terms tubulo-acinar and tubulo-alveolar are used interchangeably (Burns, 1975; Aitken & Survashe, 1977; Maxwell et al., 1986; Burns, 1992; Chieffi et al., 1996).

Type I Harderian glands are compound in nature, characterised by tubulo-alveolar type lobules emptying into a main secretory duct (Aitken & Survashe, 1977; Burns, 1992). Type I glands have a characteristically high concentration of plasma cells evident in the interstitial tissue (Burns, 1975; Aitken & Survashe, 1977; Burns, 1992). The Type I Harderian gland is characterised by having lobules composed of a single epithelial cell type (Aitken & Survashe,

1977; Burns, 1992). In comparison, Type II glands differ with regards to the structure of the lobules (Aitken & Survashe, 1977; Burns, 1992).

The lobules in the Type II Harderian glands are characterised by being compound tubular in nature (Aitken & Survashe, 1977; Burns, 1992). Plasma cells are not as numerous in a Type II gland compared to a Type I Harderian gland (Aitken & Survashe, 1977; Burns, 1992). Type III glands display characteristics of both Type I and II glands and are thus composed of a mixture of compound tubular and compound tubulo-alveolar lobules (Aitken & Survashe, 1977; Burns, 1992). In Type III Harderian glands, plasma cells are associated with the lobules which are tubulo-alveolar in nature (Aitken & Survashe, 1977; Burns, 1992).

Previous studies indicated that the Harderian gland in ostrich (Aitken & Survashe, 1977; Altunay & Kozlu, 2004; Frahm and Mohammadpour, 2015; Klećkowska-Nawrot et al., 2015a) and emu (Aitken & Survashe, 1977), are compound tubulo-acinar in nature and thus a Type I gland. Other avian species such as the domestic fowl, turkey, greater rhea and kiwi, have also been described as having the latter Harderian gland type (Aitken & Survashe, 1977). In both ostrich and emu, tertiary tubules may terminate at the gland periphery by coiling (present study), giving the appearance of acini, which are evident in tubulo-acinar type glands.

The main secretory duct opens into two to three secondary branches before diverging into smaller tertiary branches in both species (present study). It is thus evident from the present study that the ostrich and emu Harderian gland is compound in nature by virtue of lobules emptying into a main secretory duct. The lobules in both species are tubular in nature, which is typically characteristic of a Type II Harderian gland which is common to aquatic avian species such as duck and geese (*Anser anser*), but not to ratites (Aitken & Survashe, 1977; Burns, 1992). Lobules are however composed of a single epithelial cell type, with lymphoid aggregates being evident in the interstitial tissue as well as surrounding the main secretory duct, which is commonly noted in Type I glands (present study).

In reference to aforementioned classification of the avian Harderian gland, the ostrich and emu Harderian glands display more Type I characteristics, compared to that evident in Type II glands. The ostrich and emu display characteristic of a Type I gland, with the exception of the lobules being tubular in nature. It is evident from the present study that lobules in the ostrich and emu are composed of branched tubular units which often terminate at the periphery of the lobule in coiled manner. It is possible that this terminal branching pattern could have been misinterpreted as being alveoli, in previous studies. There are differing opinions as to whether

the gland type is related to habitat (Burns, 1992) and further investigation is required as to determine the reason for these ratites having Harderian glands not typical of a particular type.

5.4.2 Lacrimal gland

a. General features

In both species, the Lacrimal gland consists of a body, neck and a single secretory duct and is positioned dorso-caudally on the anterior sclera (see Chapter 4). The body of the gland is lobated and oval in shape (see Chapter 4). The duct of this gland extends from the ventral margin of the gland and continues in a rostroventral direction before emptying into the dorsal margin of the lower eyelid (see Chapter 4).

b. Lobation

The present study indicated that the body of the lacrimal gland in both ostrich and emu, is divided into variably sized lobes by connective tissue trabeculae into the glandular parenchyma. Similar descriptions have been given for the adult ostrich and emu (Aitken & Survashe, 1977) and juvenile ostrich (Klećkowska-Nawrot et al., 2015b), as well as the duck and domestic fowl (Burns, 1976). In both species, the lacrimal gland has prominent connective tissue trabeculae compared to the Harderian gland, dividing the gland into well-defined lobes, as noted above. This is related to cell rich interstium present in the ostrich and emu Harderian gland and the important immunological function it has in these species, compared to the lacrimal gland.

The trabeculae in both species are composed of dense connective tissue with dense network of interspersed blood vessels, and cells which resemble fibroblasts. Similar observations were made in the juvenile ostrich (Klećkowska-Nawrot et al., 2015b), however capsular adipocytes were not evident in the present study, although extra-capsular adipocytes were. The body and duct of the lacrimal gland in the ostrich was voluminous and well defined from the extra-capsular parts, compared to the emu. Thus, the extra-capsular cells appear more numerous in the emu compared to the ostrich (present study). The rich blood supply to the lacrimal gland in both ostrich and emu, is suggestive of the active secretory role this gland has in both species. The melanin pigment evident in the capsule surrounding the gland in the ostrich lacrimal gland, is not evident in the emu. This pigment has not been described previously in either species.

c. Structure of the i. secretory tubules and ii. Tertiary and secondary tubules

i. In both ostrich and emu, the lacrimal gland lobules are composed of large tubular secretory units which are concentrated towards the gland's periphery and terminate in a non-coiled or coiled manner (present study). In contrast, the lacrimal gland in the adult ostrich and emu (Aitken & Survashe, 1977), and in the juvenile ostrich (Klećkowska-Nawrot et al., 2015b) is described as having secretory acini concentrated towards the gland periphery. The coiling of terminal tubules may give the impression of having an acinar-like structure when viewed in cross section however.

The secretory units in the ostrich and emu are lined by a single layer of columnar cells which are vacuolated (present study). These cells have a round to oval nucleus situated basally. Similar observations were made with regards to the epithelial lining of the acini in the adult ostrich and emu (Aitken & Survashe, 1977) and the juvenile ostrich (Klećkowska-Nawrot et al., 2015b). The presence of a basement membrane closely associated with elongated elements resembling myoepithelial cells, has previously been made regarding the lacrimal gland acini in the duck, domestic fowl (Burns, 1976) and juvenile ostrich (Klećkowska-Nawrot et al., 2015b). In both species, the epithelial cells lining the tubular secretory units are arranged with the apical margins directed towards a lumen into which the secretions empty. Similar descriptions have been provided for the acini in the duck, domestic fowl (Burns, 1976), the adult ostrich (Aitken & Survashe, 1977) and juvenile ostrich (Klećkowska-Nawrot et al., 2015b).

ii. In the present study, it was evident that the glandular units, each representing a lobule, secrete into secondary branches of the main duct, via tertiary ducts. Thus, each lobe is drained by a secondary duct into the main secretory duct. A similar branching pattern has been documented in the turkey (Burns & Maxwell, 1979), domestic fowl and duck (Burns, 1976; Burns & Maxwell, 1979), as well as the juvenile and ostrich embryo (Klećkowska-Nawrot et al., 2015b). Secondary branches of the main secretory duct emu display a labyrinthine type branching pattern compared to ostrich, where the branching is simple (present study). Tertiary tubules may terminate at the gland periphery by coiling, giving the appearance of acini, which are evident in tubulo-acinar type glands. The lacrimal gland in the ostrich and emu is therefore compound in nature, composed of branched tubular secretory units.

As is evident in the Harderian gland, all tubules and ducts are lined by secretory epithelium in the ostrich and emu lacrimal glands. This may suggest that even more voluminous secretions are required in these ratites, considering the environmental insults the ocular tissues have to

endure. It has previously been documented that the secretions from these tubules and smaller ducts, contribute to the tear fluid, lubricating and nourishing the avascular cornea in the ostrich (Klećkowska-Nawrot et al., 2015b). However, further investigation is required as to determine whether the structure of the lacrimal gland tubules and ducts are so adapted in response to particular harsh climatic conditions and other environmental insults the ostrich and emu are exposed to.

d. Interstitial tissue

The interstitium in the ostrich and emu lacrimal gland is sparsely populated compared to the Harderian gland in both species. Few cells resembling plasma cells and lymphocytes are evident infiltrating the interstitial tissue of the lacrimal gland in either species (Aitken & Survashe, 1977; present study). The tubular units are however in close association with adjacent units as lymphoid cells are not numerous and do not push the tubular units apart. This differs from the observations made in the Harderian gland, where tubular units were often pushed apart by aggregations of lymphoid tissue. This would indicate the relative importance the Harderian gland has in local ocular immunity in the ostrich and emu, compared to the lacrimal gland.

Previous studies indicated that lymphocytes are more numerous in the juvenile ostrich and ostrich embryo compared to plasma cells (Klećkowska-Nawrot et al., 2015b). However, in the present study this was not apparent in either species. It is evident however, that aggregations of lymphoid tissue concentrate around the main secretory duct and the various duct branches of the lacrimal gland in both species, with the concentration of lymphoid tissue varying within as well as between species.

Diffuse infiltrates or clusters of lymphoid cells are evident in the lacrimal gland duct of the turkey, domestic fowl and duck (Burns & Maxwell, 1979). The ostrich and emu differ from the turkey, domestic fowl and duck, in that germinal centres with a distinct cortex and medulla were not evident in this study. Aggregations of lymphoid tissue are concentrated around the ducts in both Harderian and lacrimal glands, however these aggregations of cells are dispersed in between secretory units and are more concentrated in the Harderian gland compared to the lacrimal gland, in both ostrich and emu. Both glands play a part in local ocular immunity and responding to antigens presented in the secretory duct with the Harderian gland contributing most to local immunity (Aitken & Survashe, 1977; Burns & Maxwell, 1979; Schat et al., 2014; Klećkowska-Nawrot et al., 2015b). The present study also indicated that a relatively smaller concentration of lymphoid cells surrounding the main secretory duct of the

lacrimal gland, is indicative of the fact that this gland has a negligible immunological role in the ostrich and emu, compared to the Harderian gland.

e. Main secretory duct

The main secretory duct in the ostrich and emu is surrounded by a connective tissue capsule which carries numerous blood vessels, suggesting that this gland is active in its secretory role. A single main secretory duct in both species extends from the ventral margin of the lacrimal gland and empties at the dorsal margin of the lower eyelid. This differs from previous descriptions given, where the lacrimal gland in the ostrich is described as having numerous ducts opening into the lower eyelid (Klećkowska-Nawrot et al., 2015b).

The main secretory duct in the ostrich and emu is surrounded by tubular units that empty into the main duct lumen, giving a villus-like appearance to the lumen of the main duct (present study). Thus, the main duct in the turkey, domestic fowl and duck has been previously described as having villi protruding into the duct lumen (Burns & Maxwell, 1979). The present study indicated that the main secretory duct in the ostrich and emu consists of a single layer of tall cuboidal to columnar cells that were vacuolated. Similar observations were previously made in the turkey, domestic fowl and duck (Burns & Maxwell, 1979). The structure of the secretory duct epithelium in the ostrich and emu is comparable to that in the Harderian gland, in that it may allow for a greater surface area from which lacrimal secretions can be released.

The secretion of the lacrimal gland is described as being mucoid in the turkey, domestic fowl and duck (Burns & Maxwell, 1979) as well as the adult ostrich and emu (Aitken & Survashe, 1977). Previous studies indicated that the secretion in the juvenile ostrich is mucoserous in nature and thus the epithelial cells has a high mucopolysaccharide content (Klećkowska-Nawrot et al., 2015b). However further studies would need to be conducted to determine the composition of lacrimal secretions in the ostrich compared to the emu, as no information is available in this regard.

f. Gland classification

It is evident from previous studies that the lacrimal gland in the ostrich and emu (Aitken & Survashe, 1977) and Mulard duck (*Anas sterilis*) (Dimitrov & Nikiforov, 2005), as well as in the ostrich embryo (Klećkowska-Nawrot et al., 2015b), is compound tubulo-alveolar in nature. The present study however revealed that the lacrimal gland in the ostrich and emu has one lobule type, which is namely compound tubular in structure.

5. 5 Conclusion

The general histological structure of the ostrich and emu lacrimal apparatus is similar to other avian species, however there are notable differences.

In both species, the glands are compound tubular in nature, whereas in most other birds, the lacrimal apparatus is described as being compound tubulo-alveolar in nature. It is evident that the Harderian gland in ostrich and emu is categorised as a type II gland, due to its compound tubular structure. However, this gland type is not common to terrestrial avian species and high concentrations of lymphoid aggregates are not associated with Type II glands. To what extent habitat has influenced the appearance of the structural peculiarities may require additional studies on other ratite species such as rhea, cassowary and kiwi. Compared to other avian species, germinal centres are not evident within the lymphoid aggregations in the ostrich and emu. Further investigation is required into whether the latter observation is related to the concentration of B and T lymphocytes evident in the Harderian gland. Prominent melanin pigment was observed in the lacrimal apparatus of the ostrich, which is not evident in that of the emu. The significance of this difference remains to be determined.

Minor differences are evident when comparing the Harderian and lacrimal glands of the ostrich and emu. However, the lacrimal apparatus of both species reflects structural similarities which they share with other avian species such as the turkey, domestic fowl and duck, with respect to the following features:

Lobes are divided into smaller lobules by connective tissue trabeculae, which extend from the capsule which surrounds the body, neck and duct of the lacrimal apparatus. A single duct is evident in the ostrich and emu, which is common to avian species compared to numerous secretory ducts. The ducts are lined by a single layer of columnar to cuboidal epithelial cells, which may vary in different sections of a duct. The interstitium of the Harderian and lacrimal glands in the ostrich and emu contain fibroblasts, myoepithelial cells, connective tissue, numerous blood vessels, lymphocytes or plasma cells.

Lymphoid aggregations are evident in high concentrations around the main secretory ducts of the lacrimal apparatus. These cells are however not confined to the main duct in the Harderian glands of both species. There is evidence from the present study that the histological structure of the lacrimal apparatus in the ostrich and emu allows for a greater secretory capacity, as well as optimal response to antigen stimulation in the case of the Harderian gland. These

features may reflect a response to the harsh, dry climatic conditions these ratites are adapted to.

Some differences are, however, apparent between the two components of the lacrimal apparatus and between the two ratites studied. Compared to the lacrimal gland, the Harderian gland displays a high concentration of lymphoid cells interstitially, indicative of the primary role that this gland plays in local immunity. This was indicated by the fact that the tubular secretory units were pushed apart by infiltrating lymphoid tissue in the Harderian glands of both species, which was not apparent in the lacrimal glands. Due to the tubular architecture being obscured by impinging lymphoid cells in the Harderian glands of both species, lobules are comparably better defined in the lacrimal glands. It appears that the ostrich Harderian gland has a greater concentration of lymphoid tissue than that of the emu, whereas the concentration of lymphoid tissue in the lacrimal gland is similar between the two species. The degree of antigenic insult, immune status, as well as age of the ratite needs to be taken into consideration before making conclusions on the lymphoid cell response in the ostrich Harderian gland compared to that of the emu.

It can be concluded that the lacrimal apparatus in the ostrich and emu plays an important immunological role. However, the Harderian gland in both species plays a primary immunological role in comparison to that of the lacrimal gland. Further investigation would be required to accurately describe the diversity of lymphoid cells present in these glands, their origin as well as their unique contribution to local immune function. Future studies need to take into consideration to what extent the age of the ratites, environmental insult as well as pathogenic stress influence the structural peculiarities apparent in the lacrimal apparatus.

5.6 Figures

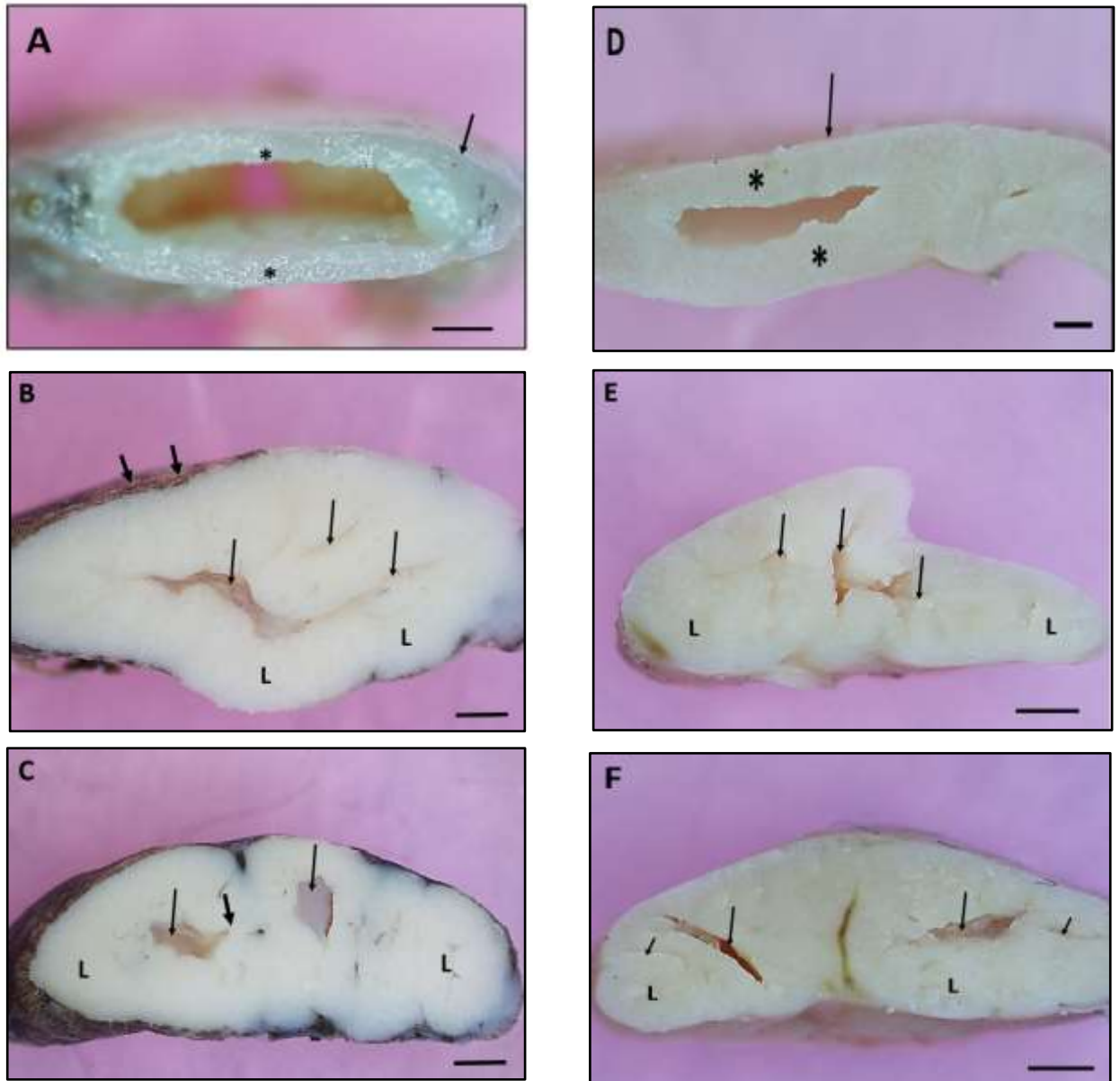


Figure 5.1: A series of transverse sections through the Harderian gland of the ostrich (A to C) and emu (D to F) illustrating the progression of the main secretory duct through the body of the gland. (A and D). The main secretory duct displaying a substantial layer of glandular tissue (asterisks) covered by a capsule (arrow). (B and E). Secondary branching of the main secretory duct (arrows) in the proximal body of the gland. Note the lobes (L), distinct capsule (short arrows) and the pigmentation in the ostrich. (C and F). Distal body of the gland showing termination of the secondary branches (arrows) into which tertiary ducts open (short arrows). Lobes (L). Scale bar = 500 μ m (Fig. A and D); 1mm (Fig. B, E and F); 2mm (Fig. C)

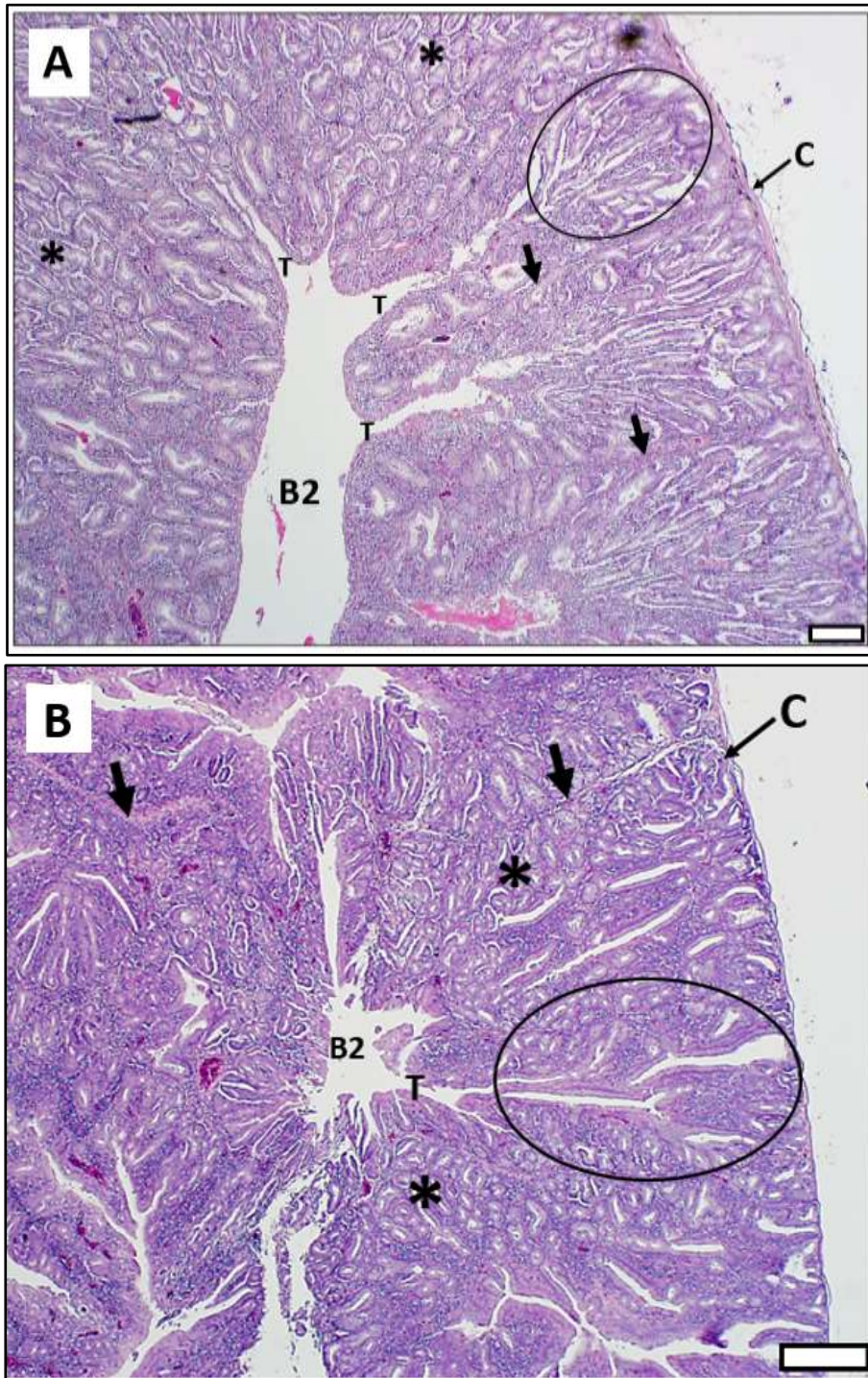


Figure 5.2: The body of the Harderian gland of the ostrich (A) and emu (B) showing the compound tubular nature of the gland. The gland is divided into lobes by trabeculae (short arrows) extending from the connective tissue capsule (C). Each lobe is divided into lobules (encircled) each of which represent a large, simple branched tubular gland. Note the degree of coiling displayed by the terminal secretory tubules (asterisks). Each tubular secretory unit is drained via a tertiary duct (T) into secretory branches of the main secretory duct (B2). Scale bar = 200 μ m.

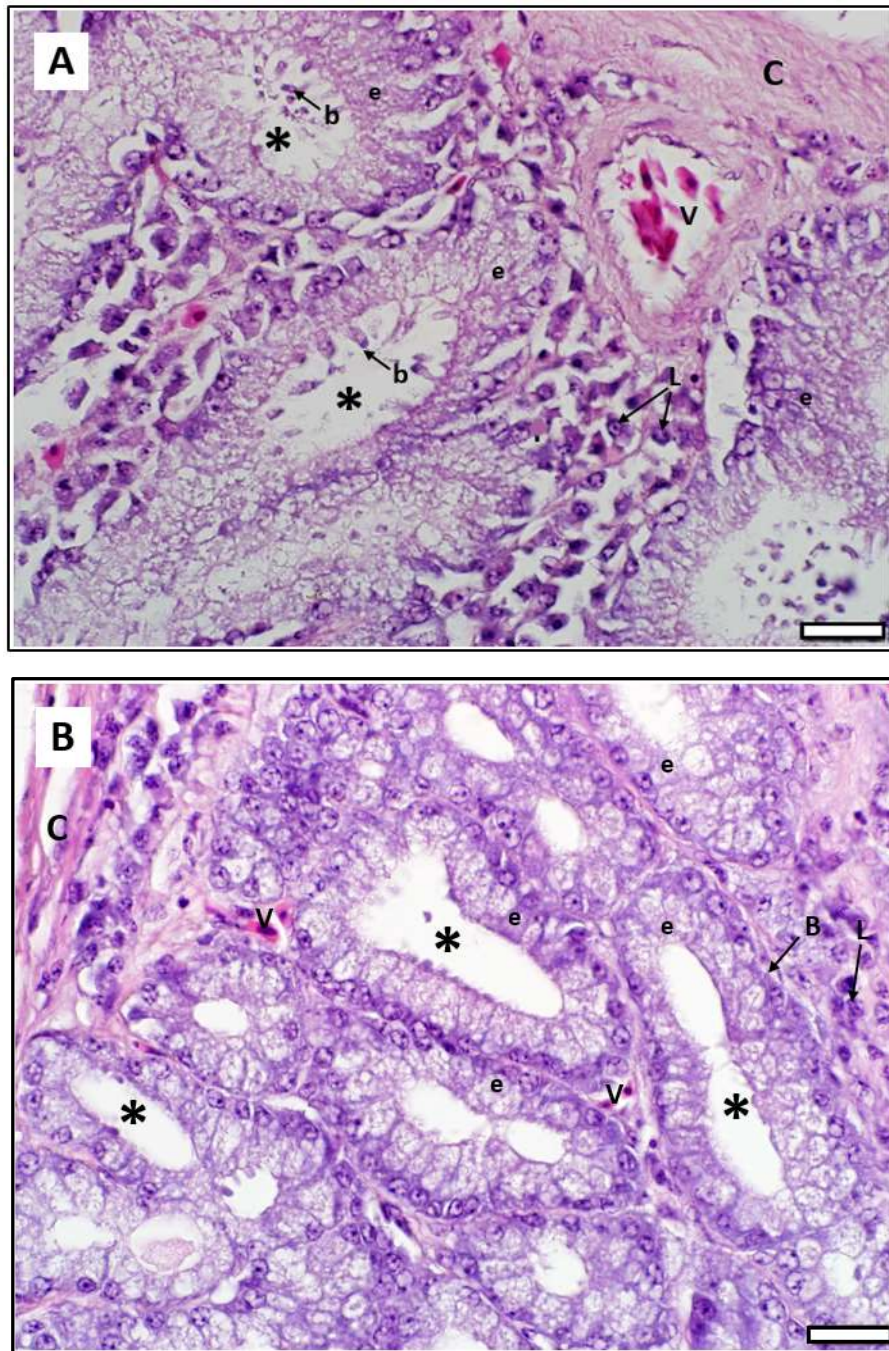


Figure 5.3: The body of the Harderian gland of the ostrich (A) and emu (B) showing terminal tubular units adjacent to the gland capsule (C). The tubules are composed of a simple columnar epithelium (e), resting on a basement membrane (B). Individual cells display densely vacuolated cytoplasm and basally positioned nuclei. Apical blebs (b) extend into the tubule lumen (asterisks) in figure A. Bloodvessels (V) and individual lymphoid cells (L) are evident in the underlying connective tissue. Scale bar = 20 μ m.

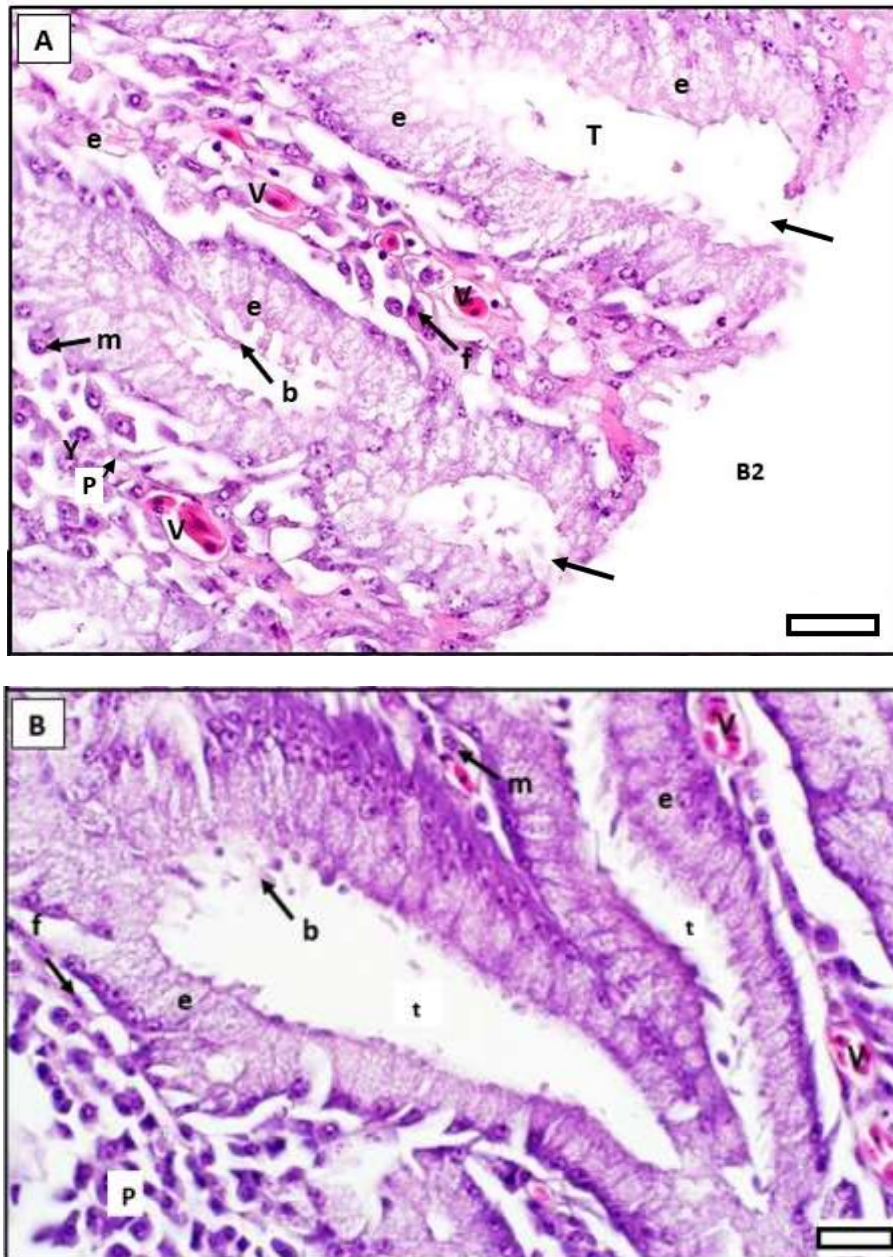


Figure 5.4: Body of the Harderian gland of the ostrich (A) and the emu (B). (A). In (A) tertiary ducts are observed opening (arrows) into a secondary branch (B2) of the main secretory duct, while in (B) two secretory tubules (t) unite to form a tertiary duct (T). Note the vacuolated lining epithelium (e), apical blebs (b), blood vessels (V), cells resembling fibroblasts (f), plasma cells (p) and myoepithelial cells (m). Scale bar = 20 μ m.

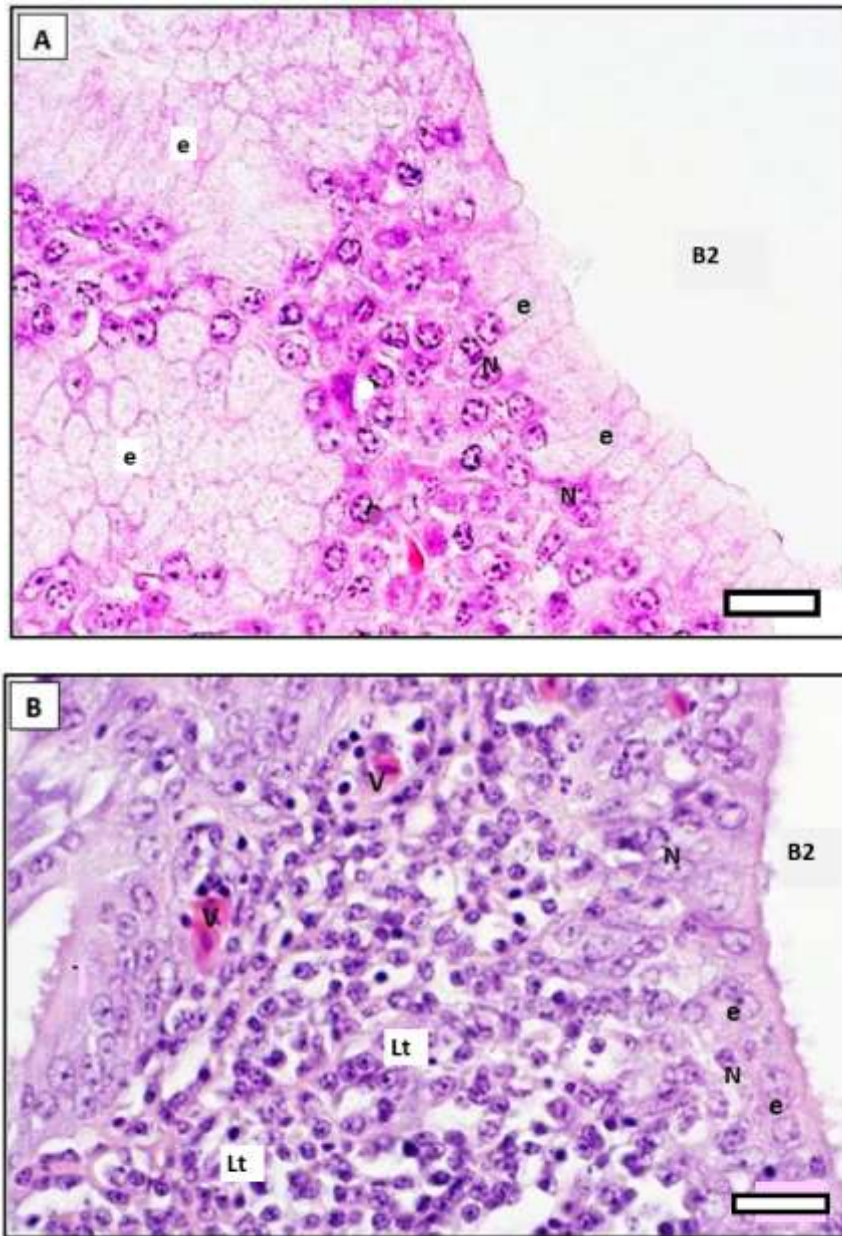


Figure 5.5: Secondary branches (B2) of the main duct in the mid-body of the ostrich (A) and emu (B) Harderian gland. In (A) the vacuolated epithelial cells (e) appear simple columnar with basally positioned nuclei (N). The adjacent tissue represents superficially sectioned epithelial elements. In (B) the epithelium (e) appears simple tall cuboidal in nature. Note the aggregates of lymphoid tissue (Lt) composed mainly of plasma cells, positioned close to the duct lumen. Blood vessels (V), nuclei (N). Scale bar = 20 μ m.

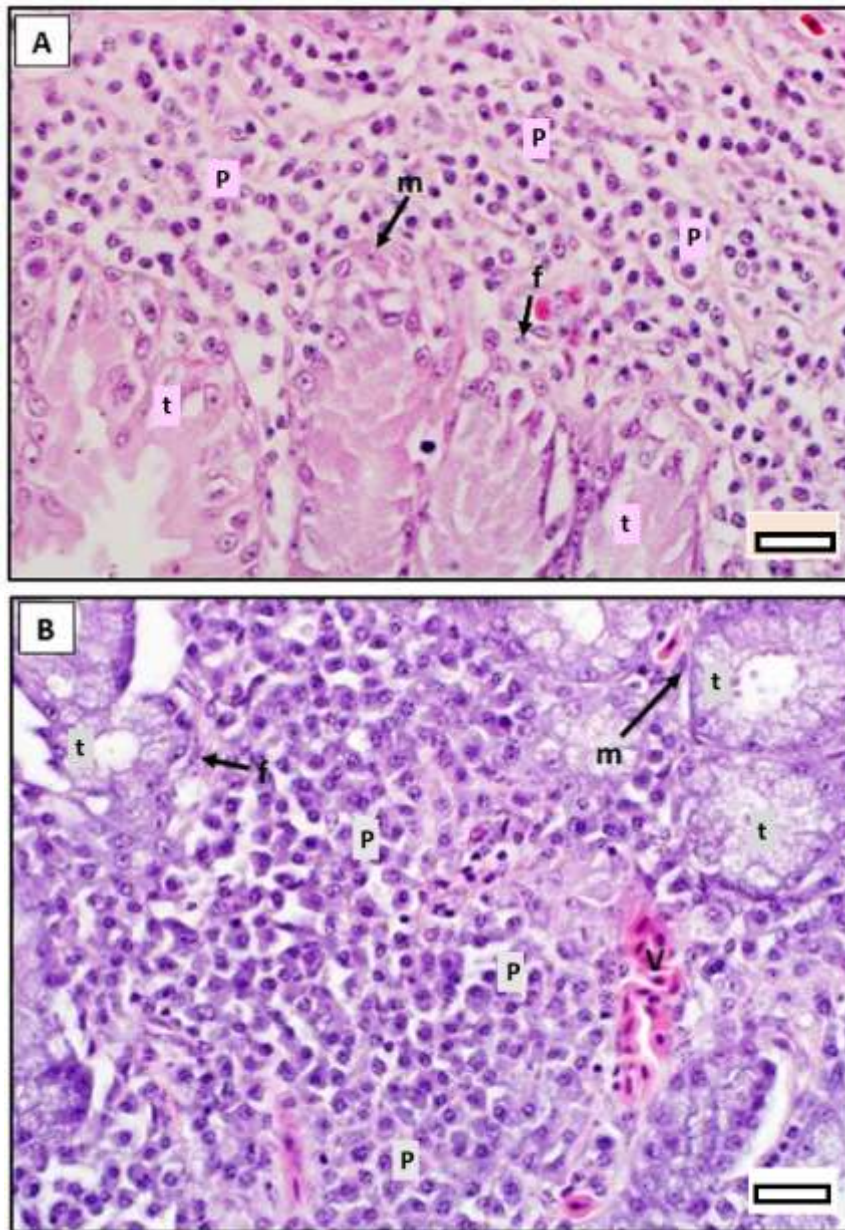


Figure 5.6: The body of the Harderian gland in the ostrich (A) and emu (B), showing secretory tubules (t). In (B) it is evident that these tubules appear pushed apart by adjacent lymphoid tissue composed primarily of plasma cells (P). Fibroblasts (f), myoepithelial cells (m) and blood vessels (V) lie interspersed in the surrounding connective tissue. Scale bar = 20 μm .

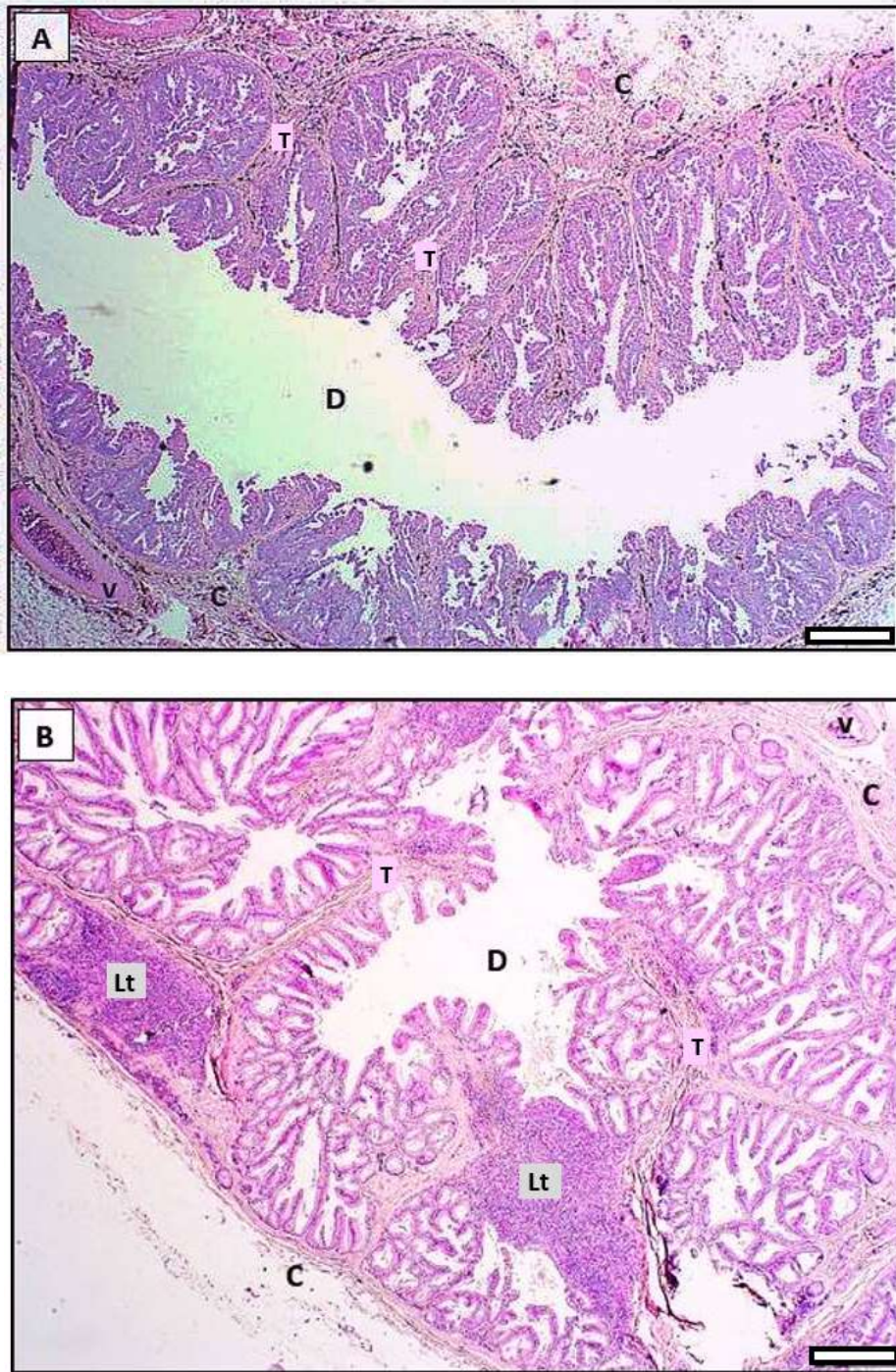


Figure 5.7: The main secretory duct (D) of the Harderian gland in the ostrich (A) and emu (B). The duct is covered by a connective tissue capsule (C) which extends as trabeculae (T) into the underlying layer of glandular tissue. Dark melanin pigment is evident in the capsule of the ostrich which is well vascularized (V) in both species. The underlying connective tissue has aggregates of interspersed lymphoid tissue (Lt) in the emu. Scale bar = 200 μ m.

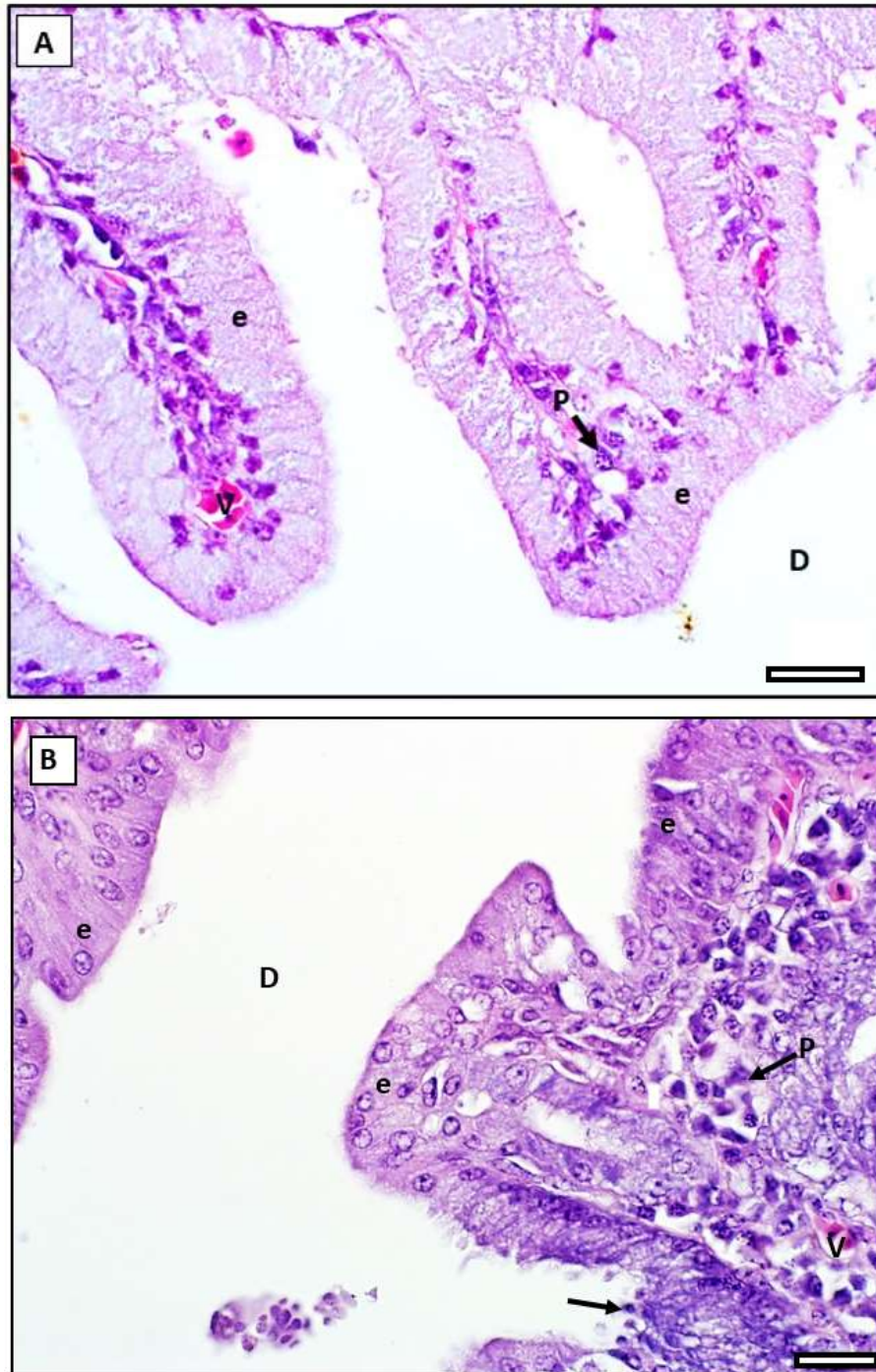


Figure 5.8: The main secretory duct of the Harderian gland in the ostrich (A) and emu (B). The epithelium of the duct (D) consists of a single layer of columnar cells (e) with densely vacuolated cytoplasm and a basally positioned nucleus. Blood vessels (v) and plasma cells (P) are interspersed in the underlying connective tissue. In places, apical blebs (arrow) extend into the duct lumen. Note in (B) that the epithelial lining appears pseudostratified. Scale bar = 20 μm .

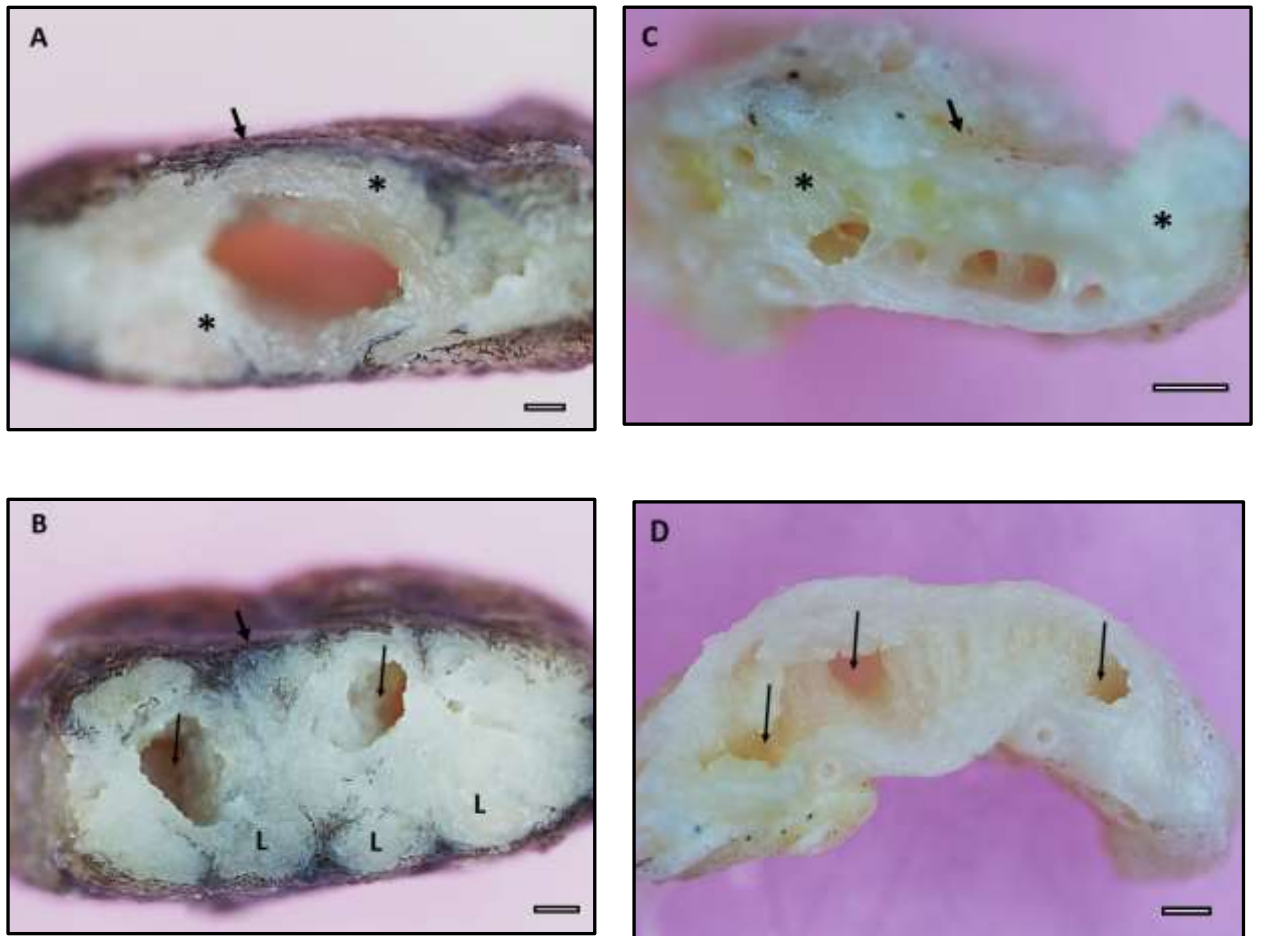


Figure 5.9: A series of transverse macroscopic sections through the lacrimal gland of the ostrich (A and B) and emu (C and D), illustrating the progression of the proximal main secretory duct through the body of the gland. (A and C) The proximal main secretory duct displaying a substantial layer of surrounding glandular tissue (asterisks) covered by a connective tissue capsule (arrow). Note the large calibre of the duct in the ostrich and the labyrinthine appearance of the duct in the emu due to the specific arrangement of the glandular tissue. (B and D) Secondary branching (long arrows) of the main secretory duct in the proximal to mid-body of the gland. Note the capsular pigmentation in the ostrich (short arrow) as well as the prominent lobation (L). Scale bar = 500 μm (Figs. B to D); 200 μm (Fig. A).

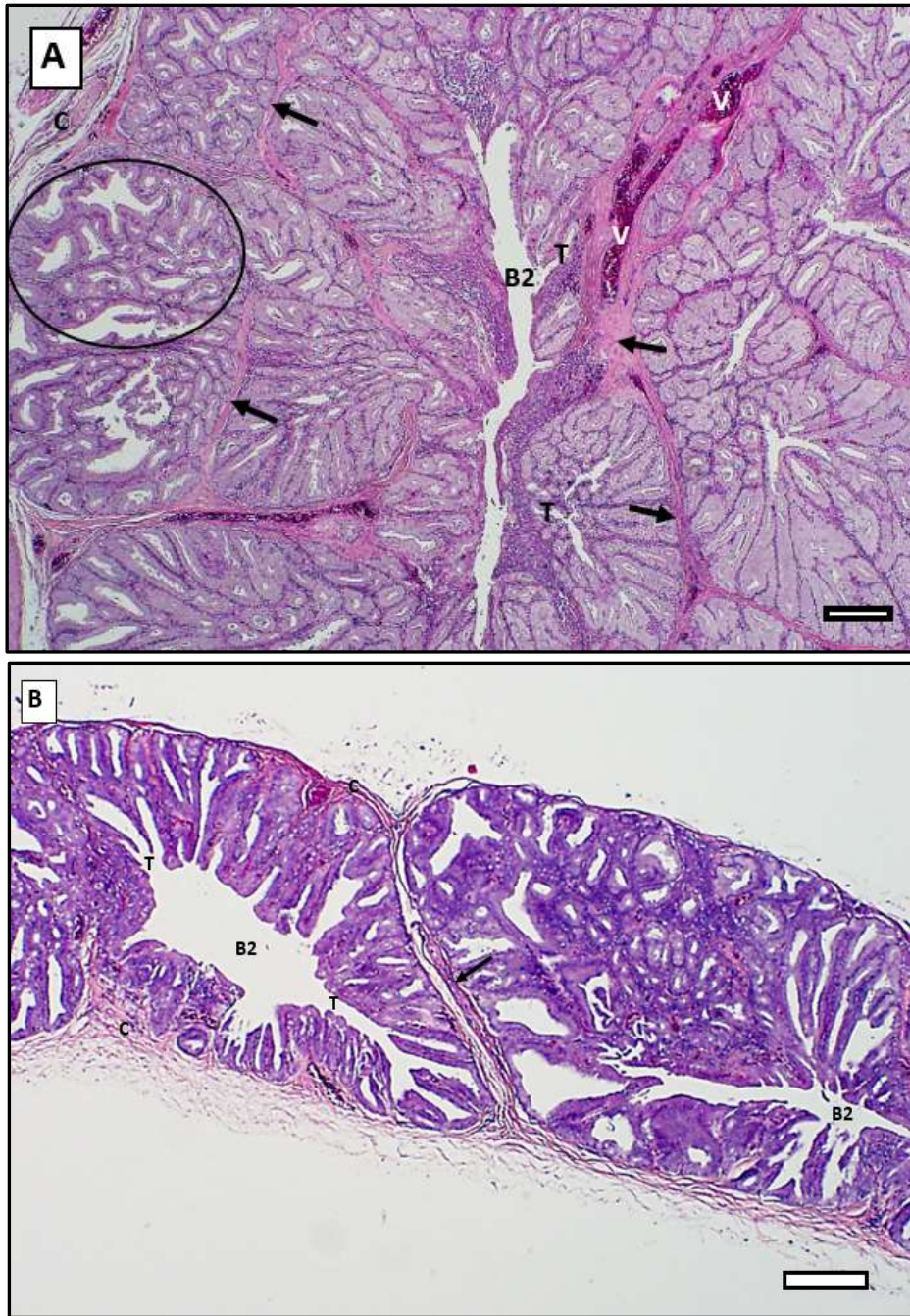


Figure 5.10: A transverse section of the mid-body of the lacrimal gland in the ostrich (A) and emu (B), showing glandular lobation, as well as secondary divisions of the main secretory duct. Connective tissue trabeculae (arrows) carrying blood vessels (V), extend from the gland capsule (C) dividing the parenchyma into lobes. Each lobe is subdivided into lobules (demarcated), each lobule effectively representing a simple branched tubular gland. Each tubular gland opens via a tertiary duct (T) into one of the secondary branches (B2) of the main secretory duct. Scale bar = 200 μ m

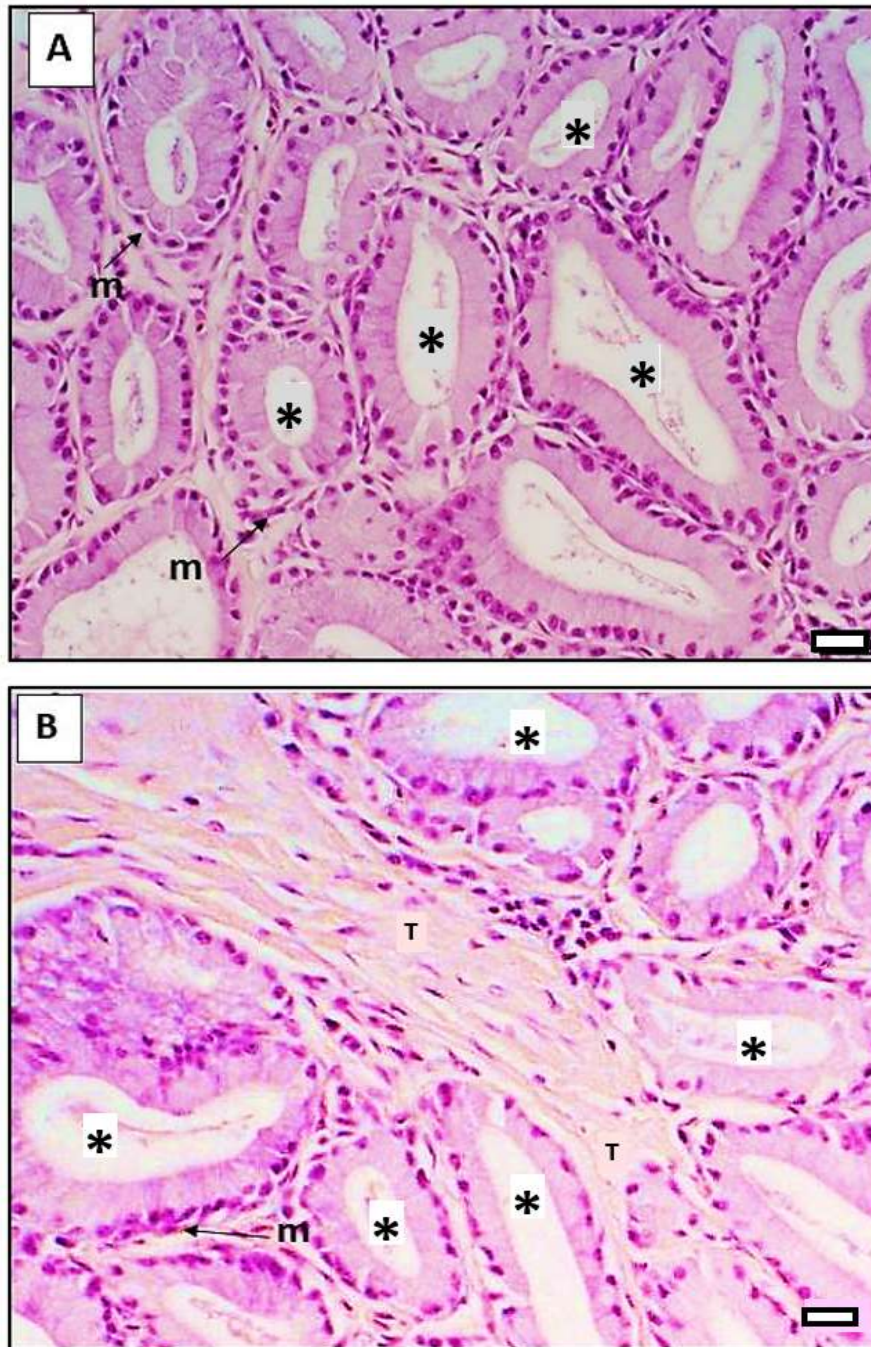


Figure 5.11: Lacrimal gland of the ostrich (A) and emu (B). Lobules display a concentration of secretory tubules (asterisks), lined by a single layer of columnar epithelium with basally positioned nuclei. The thin layer of interstitial tissue is cell poor. Connective tissue trabeculum (T) and myoepithelial cell (m). Scale bar = 20 μ m.

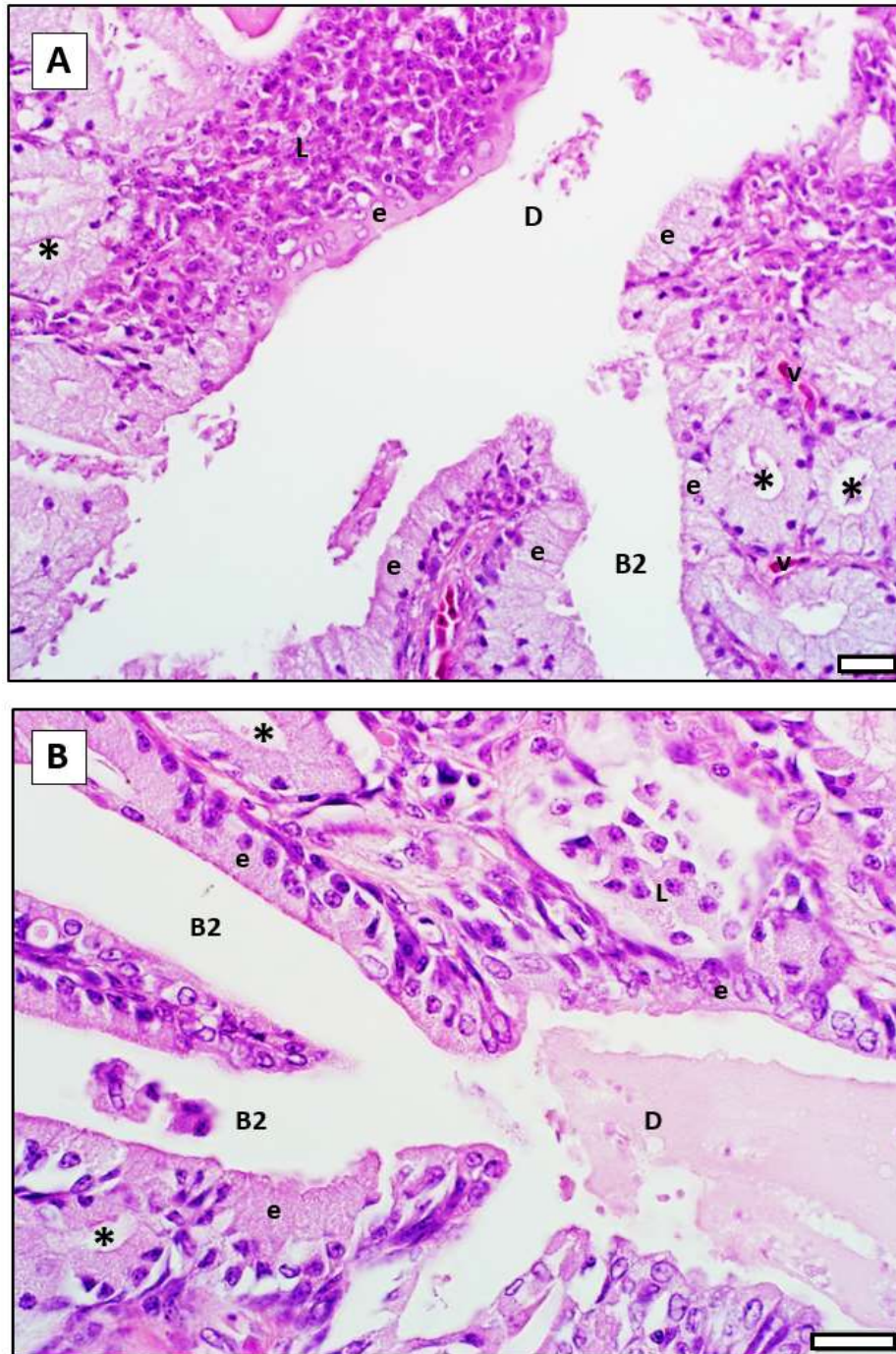


Figure 5.12: The body of the lacrimal gland of the ostrich (A) and emu (B) showing the division of the main secretory duct (D) into secondary branches (B2). Accumulated secretions are evident in the main secretory duct lumen of the emu. The ducts (D and B2) are lined by a single layer of tall cuboidal to columnar cells (e). Lymphoid tissue (L), tertiary ducts and secretory tubules (asterisks) as well as blood vessels (V), are evident in the connective tissue adjacent to the lumen of the main secretory duct and its secondary branches. Scale bar = 20 μ m.

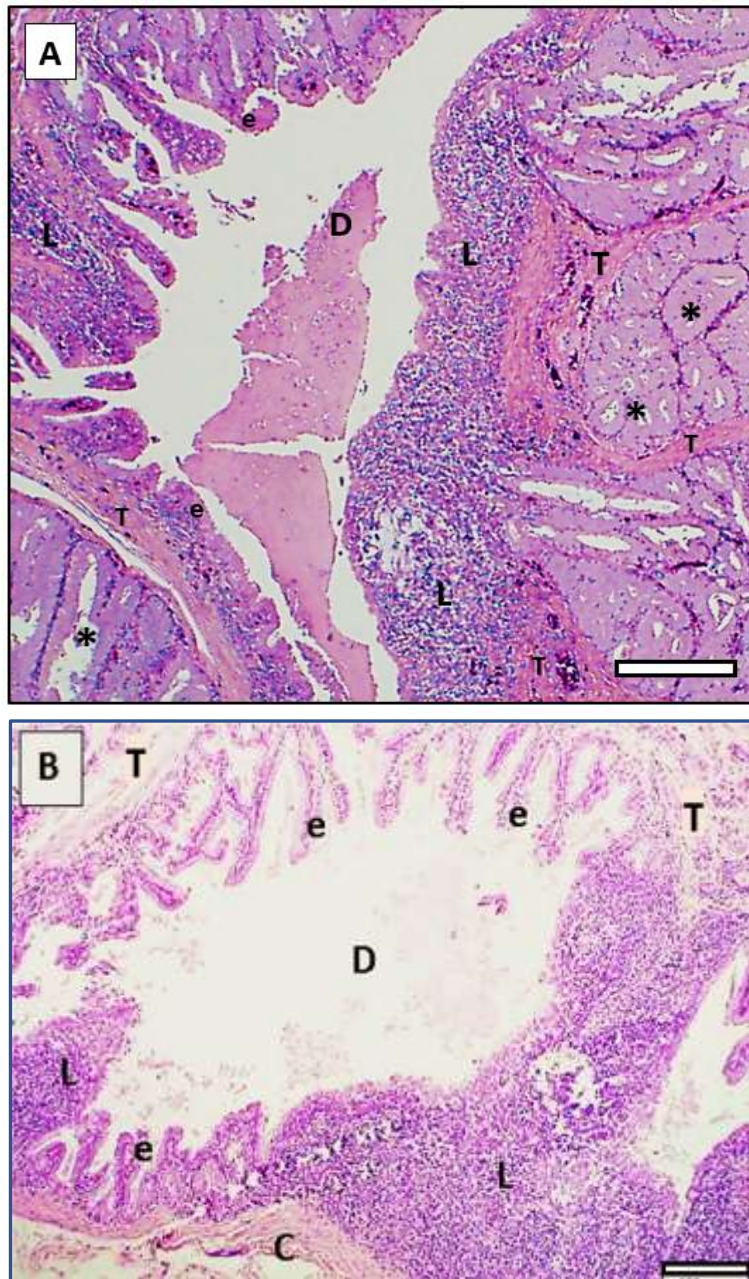


Figure 5.13: The lacrimal gland in the ostrich (A) and emu (B) showing aggregates of lymphoid tissue (L) adjacent to the main secretory duct (D). The main secretory duct is in parts lined by a single epithelial layer. (A). The proximal part of the main secretory duct showing adjacent simple branched tubular glands (asterisks) which empty into the lumen of the main secretory duct (D). Connective tissue trabeculae (T) extend into the glandular tissue. Note the secretion evident in the lumen of the main secretory duct (D) in the ostrich. (B). The mid to distal part of the main secretory duct showing the lumen of the duct (D). Note the connective tissue capsule (C) covering the main secretory duct and the connective tissue trabeculae (T) originating from the capsule and extending towards the duct lumen. Scale bar = 200 μ m (Fig. A), 100 μ m (Fig.B).

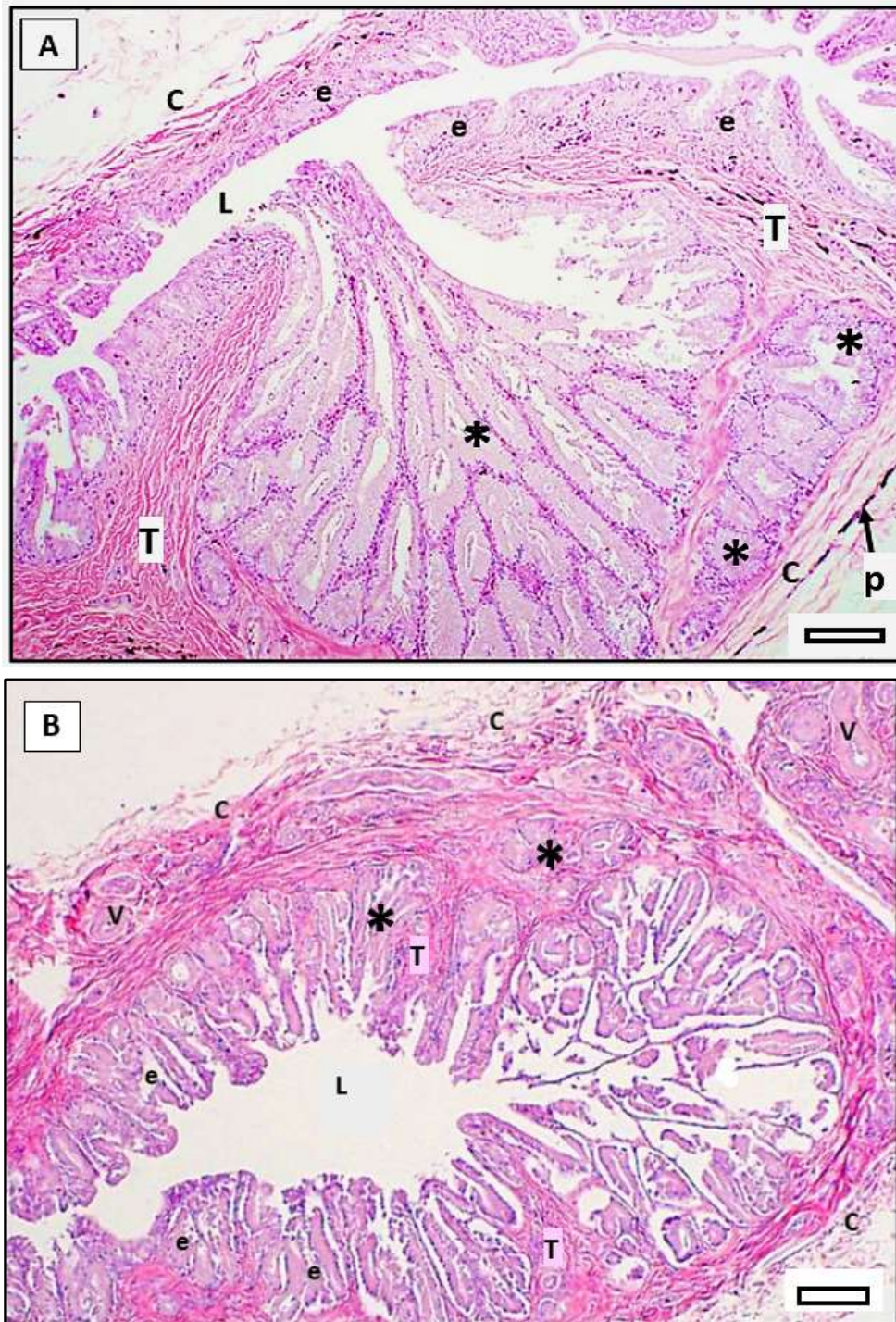


Figure 5.14: The main secretory duct of the lacrimal gland in the ostrich (A) and emu (B), showing well-developed trabeculae (T) extending into the glandular tissue adjacent to the lumen (L). The layer of glandular tissue is composed of simple branched tubular glands (asterisks) which opened directly into the main secretory duct. In parts, it appears as if the single layer of epithelium (e) lining the duct is thrown into folds. The duct is covered by a connective tissue capsule (C) carrying blood vessels (v). Note the capsular pigment (p) evident in the ostrich. Scale bar = 100 μ m.

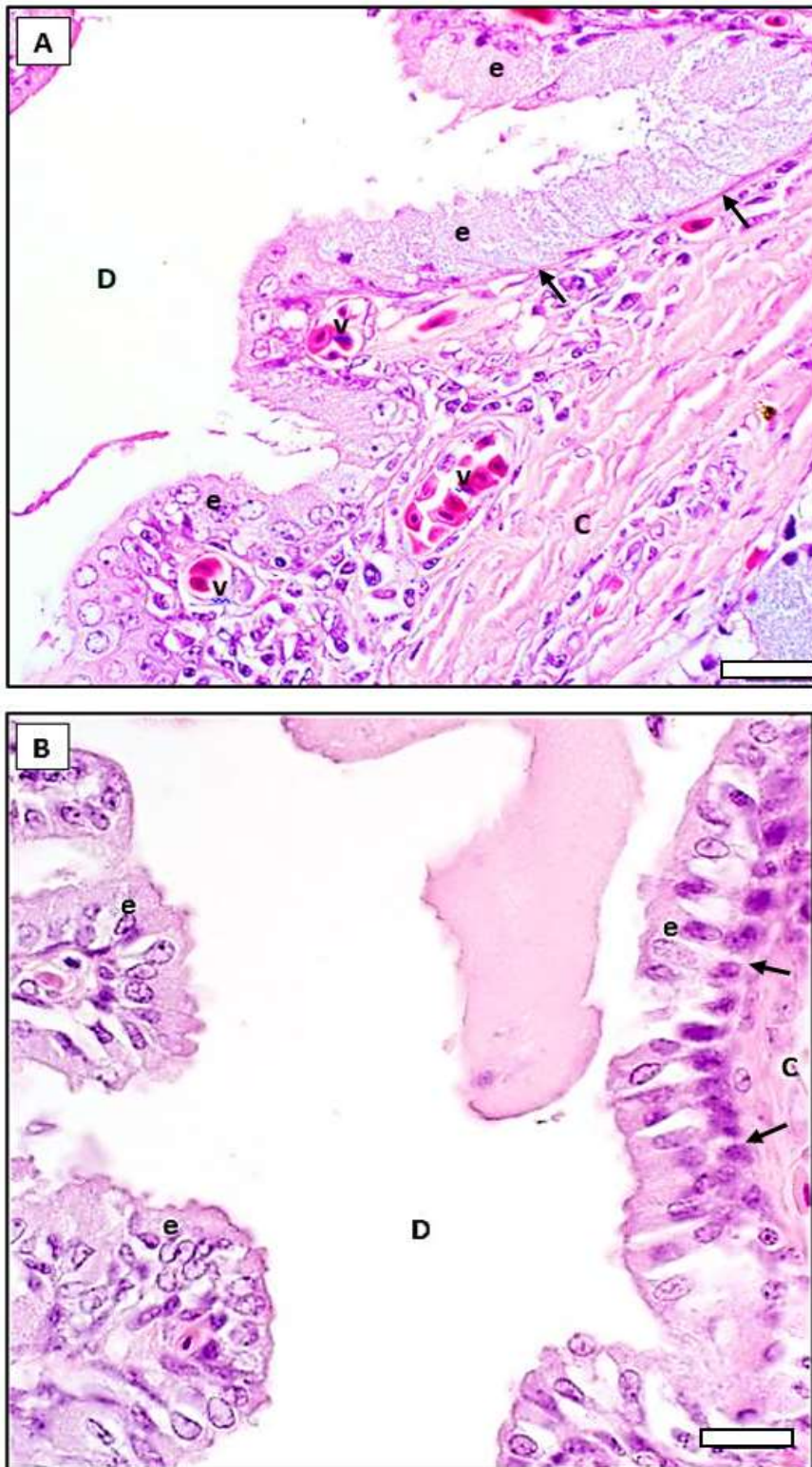


Figure 5.15: The main secretory duct of the lacrimal gland in the ostrich (A) and emu (B). The lumen of the main secretory duct (D) is lined by a single layer of columnar cells (e). Note the densely vacuolated cytoplasm and basally positioned nuclei. Blood vessels (v) are present in the underlying connective tissue (c). Note the secretion evident in the lumen of the main secretory duct in the emu. Basement membrane (arrows). Scale bar = 20 μ m.

5.7 References

- AITKEN, I. D. & SURVASHE, B. D. (1977) Lymphoid cells in avian paraocular glands and paranasal tissues. *Comparative Biochemistry and Physiology Part A: Physiology*, 58, 3, 235-44.
- ALTUNAY, H. & KOZLU, T. (2004) The fine structure of the Harderian gland in the ostrich (*Struthio camelus*). *Anatomia, histologia, embryologia*, 33, 3, 141-145.
- BANG, B. G. & BANG, F.B. (1968) Localized lymphoid tissues and plasma cells in paraocular and paranasal organ systems in chickens. *The American journal of pathology*, 53, 5, 735.
- BURNS, R. B. (1975) Plasma cells in the avian Harderian gland and the morphology of the gland in the rook. *Canadian journal of zoology*, 53, 9, 1258-1269.
- BURNS, R. B. (1976) The structure of the Lachrymal glands of the domestic fowl and of the duck. *Res Vet Sci*. 21, 292-299.
- BURNS, R. B., & MAXWELL, M. H. (1979) The structure of the Harderian and lacrimal gland ducts of the turkey, fowl and duck. A light microscope study. *Journal of Anatomy*, 128, 2, 285.
- BURNS, R. B. (1992) *Harderian Glands: Porphyrin Metabolism, Behavioral and Endocrine Effects*. The Harderian gland in birds, histology and immunology. Berlin, Heidelberg: Springer, 155-163.
- CHIEFFI, G., BACCARI, G. C., DI MATTEO, L., D'ISTRIA, M., MINUCCI, S., & VARRIALE, B. (1996) Cell biology of the Harderian gland. *International review of cytology*, 168, 1-80.
- DAVELAAR, F. G. & KOUWENHOVEN, B. (1980) Effect of the removal of the Harderian gland in 1-day-old chicks on immunity following IB vaccination. *Avian Pathology*, 9, 4, 489-497.
- Davelaar, F.G., Noordzij, A., & Van der Donk, J.A.(1982) A study on the synthesis and secretion of immunoglobulins by the Harderian gland of the fowl after eyedrop vaccination against infectious bronchitis at 1 day old. *Avian Pathology*, 11, 63-79.

DIMITROV, D. S. & NIKIFOROV, I. P. (2005) Histological and histochemical studies of Harderian gland, lacrimal gland and bursa of Fabricius in mulard ducks (*Anas sterilis*) with chlamydial infection. *Bulgarian Journal of Veterinary Medicine*, 8, 2, 119-27.

Fix, AS. (1990) The structure and function of conjunctiva-associated lymphoid tissue in chickens and turkeys. *Retrospective Theses and Dissertations*. Paper 9496.

KLEĆKOWSKA-NAWROT, J., GOŹDZIEWSKA-HARLAJCZUK, K., BARSZCZ, K., & Kowalczyk, A. (2015a) Morphological Studies on the Harderian Gland in the Ostrich (*Struthio camelus domesticus*) on the Embryonic and Post-natal Period. *Anatomia histologia embryologia*, 44, 2, 146-156.

KLEĆKOWSKA-NAWROT, J., GOŹDZIEWSKA-HARLAJCZUK, K., NOWACZYK, R., & KRASUCKI, K. (2015b) Functional anatomy of the lacrimal gland in African black ostrich *Struthio camelus domesticus* in the embryonic and postnatal period. *Onderstepoort Journal of Veterinary Research*. 82, 1, 01-12.

MAXWELL, M. H., ROTHWELL, B., & BURNS, R.B. (1986) A fine structural study of the turkey harderian gland. *Journal of Anatomy*, 148, 147 -157.

MONTGOMERY, R. D., & MASLIN, W. R. (1992) A comparison of the gland of Harder response and head-associated lymphoid tissue (HALT) morphology in chickens and turkeys. *Avian diseases*, 1, 755-759.

MUELLER, A. P., SATO, K. & GLICK, B. (1971) The chicken lacrimal gland, gland of Harder, caecal tonsil, and accessory spleens as sources of antibody-producing cells. *Cellular immunology*, 2, 2, 140-152.

OLIVEIRA, C. A., TELLES, L. F., OLIVEIRA, A. G., KALAPOTHAKIS, E, GONÇALVES-DORNELAS, H, & MAHECHA, G.A. (2006) Expression of different classes of immunoglobulin in intraepithelial plasma cells of the Harderian gland of domestic ducks *Anas platyrhynchos*. *Veterinary immunology and immunopathology*, 113, 3-4, 257-266.

PARRY, S. H., & AITKEN, I. D. (1977) Local immunity in the respiratory tract of the chicken. II. The secretory immune response to Newcastle disease virus and the role of IgA. *Veterinary Microbiology*, 2, 2, 143-65.

PAYNE, A. P. (1994) The harderian gland: a tercentennial review. *Journal of Anatomy*. 185, 1-49.

ROTHWELL, B., WIGHT, P. A. L., BURNS, R. B. & MACKENZIE, G. M. (1972) Harderian Glands of Domestic Fowl .3. Ultrastructure. *Journal of Anatomy*, 112, 233.

SAKAI, T. & VAN LENNEP, E. W. (1984) The Harderian Gland in Australian Marsupials. *Journal of Mammalogy*, 65, 1, 159.

SCHAT, K. A., KASPERS, B. & KAISER, P. (2014) *Avian Immunology*. 2nd ed. Academic Press.

SHIRAMA, K., KIKUYAMA, S., TAKEO, Y., SHIMIZU, K. & MAEKAWA, K. (1982) Development of Harderian gland during metamorphosis in anurans. *The Anatomical Record*, 202, 3, 371-378.

SHIRAMA, K. & HOKANO, M. (1992) *Harderian Glands: Porphyrin Metabolism, Behavioral and Endocrine Effects*. Harderian glands and their development in laboratory rats and mice. Berlin, Heidelberg: Springer, 25-51.

WIGHT, P. A. L., BURNS, R. B., ROTHWELL, B. & MACKENZIE, G. M. (1971) Harderian Gland of Domestic Fowl .1. Histology, with Reference to Genesis of Plasma Cells and Russell Bodies. *Journal of Anatomy*, 110, Nov, 307.

CHAPTER 6

General Conclusions

6.1 General

The ostrich and emu are palaeognathous ratites that are commercially important in that oil, feathers, meat and skin are utilized in various industries. Emu oil has important medicinal properties and is thus used for cosmetic purposes. Whereas Ostrich meat and feathers are utilized in the fashion and culinary industries. These avian species inhabit hot, arid regions and are omnivorous. A narrow frontal field of vision is relied on to forage and ocular movements play an important role in this regard. Extrinsic ocular muscles move the voluminous globe as to ensure accurate pecking. Secretions from the lacrimal apparatus are necessary to maintain optimal health of the local anatomical structures.

The avian Harderian gland and to a lesser extent the lacrimal gland, plays an important role in local ocular immunity, ensuring that the *Organum visum* and associated structures, as well as the upper airways are protected against environmental and microbial insult. The morphology of and innervation to the *M. bulbi* and lacrimal apparatus are similar in the ostrich and emu, with minor differences being evident.

6.2 *Musculi bulbi oculi*

In the ostrich and emu, the morphology of the eight extrinsic ocular muscles (excluding attachments) as well as the respective innervation to these muscles, follow the general avian pattern, with minor differences being evident. The morphology differs from the other palaeognathous species such as the Tinamous, in that the extrinsic ocular muscles in both species have a comparatively greater muscular element compared to tendon. A greater muscle element in comparison to tendon, may be related to the large globe size in both ostrich and emu requiring muscles of greater volume, exerting a greater force on the globe as to rotate it. In the ostrich and emu, the insertion of the quadrate muscle is collagenous in nature, which differs from other avian species and the significance of which remains to be determined. However, the histological structure of the insertion of the latter muscle, would be indicative of the robust, lever and sling-like action of the quadrate muscle.

This study confirmed that the morphometric qualities of the *M. bulbi* in the ostrich and emu are small when compared to other avian muscles and does relate to the restricted range of motion of the globe previously described in avian species. The *M. bulbi* in the ostrich is however significantly more powerful (except the ventral oblique and pyramidal muscles) compared to that in the emu and each extrinsic ocular muscle possesses a significantly greater cross-sectional area and isometric force generation. The significance of these morphometric values in relation to ocular motion and foraging behaviour in the ostrich and emu, remains to be determined. Further investigation is required into the microstructure and fibre type present in extrinsic ocular muscles of the ostrich and emu.

In both species, the majority of extrinsic ocular muscles insert posterior to the equator of the globe. The insertions of the *M. bulbi* differed to a greater extent compared to the respective origins, between the ostrich and emu. This study concluded that the morphology of the *M. bulbi* and associated nerves are comparable between the ostrich and emu, with minor differences being evident. This implies that similar surgical techniques could be performed during enucleation or other ocular surgeries in these two ratites.

6.3 Apparatus lacrimalis

In the ostrich and emu, the gross morphology of the lacrimal apparatus, as well as its innervation follow the general avian pattern. The Harderian gland is the larger of the lacrimal apparatus in both ostrich and emu and is morphologically distinct from the lacrimal gland. The gross morphology of the lacrimal apparatus differs markedly between the ostrich and emu. Despite the innervation and location of these glands within the orbit being comparable, the size, shape and morphometry differ notably between the ostrich and emu. The lacrimal apparatus in the ostrich is more robust, distinctly lobulated and pigmented compared the emu. When surgical and diagnostic procedures are performed on the lacrimal apparatus in these ratites, the morphometric and morphological variations between these species have to be taken into consideration.

The general histological structure of the ostrich and emu lacrimal apparatus is similar to other avian species, however there are notable differences. In both species, the glands are compound tubular in nature, whereas in most other birds, the lacrimal apparatus is described as being compound tubulo-alveolar in nature. It is evident that the Harderian gland in the ostrich and emu is categorised as a type II gland, due to its compound tubular structure. To what extent habitat has influenced the appearance of the structural peculiarities may require additional studies on other ratite species. Further investigation is required into the types of

lymphocytes evident within the Harderian gland. The significance of capsular melanin accumulations, also remains to be determined.

In the ostrich and emu, the interstitial content as well as the structure of the lobes, capsule and ducts, are similar to other avian species. There is evidence from the present study that the histological structure of the lacrimal apparatus in the ostrich and emu allows for a greater secretory capacity, as well as optimal response to antigen stimulation in the case of the Harderian gland. These features may reflect a response to the harsh, dry climatic conditions these ratites are adapted to. Minor differences are evident when comparing the Harderian and lacrimal glands of the ostrich and emu. The nature of the lymphoid aggregations in Harderian of the ostrich and emu, is indicative of the primary role that this gland plays in local immunity compared the lacrimal gland, as described previously in other avian species. Thus, the lobular architecture in the lacrimal glands of the ostrich and emu is better defined than that of the Harderian gland. Some differences are, however, apparent between the two components of the lacrimal apparatus and between the two ratites studied, in that the lymphoid aggregations in the Harderian gland of the ostrich are more pronounced, the significance of which remains to be determined.

In conclusion, the morphology of the lacrimal apparatus and eight extrinsic ocular muscles (excluding attachments) as well as the respective innervation to these structures, follow the general avian pattern, with minor differences being evident. These variations need to be considered when performing diagnostic and surgical procedures on these ratites. The morphometric properties of the *M. bulbi* may reflect a response to foraging habits and the structural peculiarities evident in the microscopic structure of the lacrimal apparatus, may indicate the unique adaptation of these ratites to the harsh and dry climatic conditions. The significance of numerous findings recorded during this study, however, remains to be determined.

APPENDICES



UNIVERSITEIT VAN PRETORIA
UNIVERSITY OF PRETORIA
YUNIBESITHI YA PRETORIA

Animal Ethics Committee

PROJECT TITLE	A comparative morphological and morphometric study of the Musculi bulbi oculi and Apparatus lacrimalis in the ostrich and emu
PROJECT NUMBER	V051-16
RESEARCHER/PRINCIPAL INVESTIGATOR	Dr E Kleyn

STUDENT NUMBER (where applicable)	UP_04388968
DISSERTATION/THESES SUBMITTED FOR	MSc

(Used previously approved applications v031-15 and v081-14)

ANIMAL SPECIES	Ostrich	Emu
NUMBER OF ANIMALS	20	20
Approval period to use animals for research/testing purposes	May 2016 – May 2017	
SUPERVISOR	Prof H Groenewald	

KINDLY NOTE:

Should there be a change in the species or number of animal/s required, or the experimental procedure/s - please submit an amendment form to the UP Animal Ethics Committee for approval before commencing with the experiment

APPROVED	Date	30 May 2016
CHAIRMAN: UP Animal Ethics Committee	Signature	

54285-15